SAMPLING STRATEGIES, METHODOLOGIES, AND MODELING OF COMPLEX MIXTURES WITHIN GALVESTON BAY AND THE HOUSTON SHIP CHANNEL

A Dissertation

by

KRISA M. CAMARGO

Submitted to the Office of Graduate and Professional Studies of
Texas A&M University
in partial fulfillment of the requirements for the degree of

DOCTOR OF PHILOSOPHY

Co-Chairs of Committee,	Weihsueh A. Chiu
	Thomas J. McDonald
Committee Members,	Yina Liu
	Anthony H. Knap
Interdisciplinary Faculty Chair,	Ivan Rusyn

May 2021

Major Subject: Toxicology

ABSTRACT

With recent climate data indicating a likely increase in future heavy precipitation events, Galveston Bay and the Houston Ship Channel (GB/HSC) serve as a natural case-study for disaster response research. For example, the region is known to be affected by regular flooding events and hurricanes. GB/HSC is also an urban estuary where several chemical classes have historically been detected in the region (e.g., PCBs, dioxins/furans (Dx/F), pesticides, metals). One chemical class of interest for this research are polycyclic aromatic hydrocarbons (PAHs). PAHs are ubiquitous and a representative complex mixture due to variable origins and excessive levels in the environment may cause adverse health effects.

After Hurricane Harvey, sediment redistribution within the City of Houston and Galveston Bay was a concern for both disaster response research (DR2) and environmental health. This research uses several tools to identify a representative complex environmental mixture within GB/HSC. The first tool used is a systematic evidence map (SEM), where (Dx/F) and mercury (Hg) were identified as the most common chemicals detected in GB/HSC. However, chemical data were inconsistently recorded, which made it difficult to discern whether a baseline chemical dataset existed. The second tool used is a geospatial technique called kriging. This particular tool is used to estimate PAH concentrations within GB/HSC sediments after Hurricane Harvey. Our comparative analysis with historical data found a small, but detectable increase in

surface sediment PAH concentrations; however, the levels detected did not exceed sediment quality guideline levels.

The third tool applied in this research was a KinExA Inline Biosensor (biosensor) technology. This biosensor uses a monoclonal antibody to quantify available PAHs in porewater (C_{free}). By detecting C_{free} PAH concentrations, the goal was to prioritize environmental samples for targeted analysis, since traditional methods (e.g., gas chromatography-mass spectrometry) are resource and time intensive. Our results show the biosensor is a rapid and cost-effective field ready technology capable of detecting C_{free} in both soils and sediments. Collectively, the results of this dissertation share three tools capable of characterizing complex environmental mixtures. The findings from this dissertation will be useful for exposure science, DR2, public health, and environmental risk assessment.

DEDICATION

To my mum for her continued support, L. for finding ways to remain in my life, and Mrs. R who taught me the beauty of writing.

ACKNOWLEDGEMENTS

I would like to thank my committee co-chairs, Dr. Chiu and Dr. McDonald for their guidance in understanding my results and their support in navigating the publication process. I would also like to thank my committee members, Dr. Liu and Dr. Knap, for their feedback, input, and analytical support provided throughout the course of this research.

Thanks goes to Dr. Sericano for his guidance in analytical chemistry techniques and instrumentation maintenance. I would also like to thank all of the Geochemical Environmental Research Group staff and research scientists since 2016 who have helped guide and aided me in learning sample extraction and analytical techniques.

I would like to thank Dr. Dellapenna and his students, H Hoelscher, N Wellbrock, and R Lewis, for their aid in sample collection, for lending me their expertise in sedimentary processes, and for allocating lab space throughout the course of this research.

Thank you also goes to Dr. Horney and her students GA Casillas, KR Kirsch, and KW Stone who aided in sample collection as well as imparted valuable insights regarding community engagement.

I would also like to thank Dr. Unger and his student K Prosser as well as his lab associates G Vadas and MA Vogelbein for training me when I worked at the Virginia Institute of Marine Science (VIMS) and for offering valuable insights regarding the biosensor.

Thanks goes to Dr. Gastel and S. Martin for sharing their expertise in science writing and aiding me in my manuscript edits. Your inciteful and thoughtful feedback has been invaluable.

I would also like to thank my friends and colleagues in College Station as well as the department faculty and staff at CVM, SPH, and GERG for making my time at Texas A&M University a memorable experience.

Thank you to The Association of Former Students and the Aggie Network Student Ambassadors, for without this dynamic group of people I would not have a greater appreciation of the Aggie Network and Texas A&M University.

Finally, thanks to my mum and dad for supporting me in my doctoral journey and for imparting the core values I used to help me succeed. I also want to thank BC and LC for their patience and lessons in living in the moment.

CONTRIBUTORS AND FUNDING SOURCES

Contributors

This work was supervised by a dissertation committee consisting of Professor Chiu of the Interdisciplinary Faculty of Toxicology Faculty, Professor McDonald of the Interdisciplinary Faculty of Toxicology and the School of Public Health, Professor Liu of the Department of Oceanography, and Dr. Knap of the Interdisciplinary Faculty of Toxicology and the Department of Oceanography.

All work for the dissertation was completed by the student. “Characterizing Baseline Legacy Chemical Contamination in Urban Estuaries for Disaster-Research through Systematic Evidence Mapping: Galveston Bay Case Study” was completed in collaboration with Mr. Brian Buckingham and Ms. Margaret Foster who contributed to the scoping development and data extraction portions of this research project. The data illustrated in Figure 2-3 was provided by Professor Chiu. Editorial feedback was provided by Professor Gastel and Ms. September Martin.

Dr. Shamila Bhandari provided the ArcGIS map in Figure 3-1 and Ms. Christena Hoelscher provided Figure 3-5 for “Polycyclic Aromatic Hydrocarbon Status in Post-Hurricane Harvey Sediments: Consideration for Environmental Sampling in the Galveston Bay/Houston Ship Channel Region.”

The biosensor technology utilized in “Biosensor Applications in Galveston Bay: Implications for Disaster Research” was provided by Dr. Michael Unger of the Virginia Institute of Marine Science (VIMS) with additional analytical support provided by Ms.

Mary Ann Vogelbein, Ms. Kristen Prossner, Mr. George Vardas, Professor Thomas J. McDonald, and Professor Liu. The Elizabeth River data incorporated into this article provided by Dr. Unger. Ms. Amanda Brewster and Mr. Mike Gaskins of TDI-Brooks International, Inc. completed the TOC analysis completed for this article.

All other work conducted for the dissertation was completed by the student independently.

Funding Sources

Graduate study was supported the Texas A&M University Regulatory Science in Environmental Health and Toxicology Grant (T32 ES026568 (2016 - 2018)), the National Institutes of Environmental Health Sciences (NIEHS) Superfund Research Program Grant P42 ES027704 (2018-2019), and the NIEHS KC Donnelly Supplement Award for 2018. This work was also made possible in part by the Department of Defense (DOD) Science Mathematics and Research for Transformation (SMART) Program (2019 – Present). This works' contents are solely the responsibility of the contributing authors and do not necessarily represent the official views of the DOD, NIH, or the NIEHS Superfund Research Program. The third manuscript's work was also supported by the Virginia Institute of Marine Sciences NIEHS Superfund Program Grant R01ES024245 with analysis and collection of Elizabeth River samples included in this work supported by the Virginia General Assembly.

NOMENCLATURE

A	Anthracene
An	Anthracene
AE	Acenaphthene
ANOVA	Analysis of Variance
ATSDR	Agency for Toxic Substances & Disease Registry
AY	Acenaphthylene
BaA	Benzo[a]anthracene
BaP	Benzo[a]pyrene
BbF	Benzo[b]fluoranthene
Bghi	Benzo[g,h,i]perylene
Biosensor	KinExA Inline Biosensor
BkF	Bezno[k]fluoranthene
C	Chrysene
CERCLA	Comprehensive Environmental Response, Compensation, and Liability Act of 1980
CHR	Chrysene
Co	Condition
Co	Context
CoCoPop	Condition, Context, Population
DA	Dibenzo[a,h]anthracene

Dx/F	Dioxin/Furans
DR2	Disaster Research Response
ERL	Effects Range Low
ERM	Effects Range Median
ESV	USEPA Region 4 Ecological Screening Value
F	Fluorene
Fl	Fluoranthene
GB	Galveston Bay
ghi	Benzo[g,h,i]pyrene
Hg	Mercury
HSC	Houston Ship Channel
IP	Ideno[1,2,3,c-d]pyrene
Nap	Naphthalene
NOAA	National Oceanic Atmospheric Administration
NPL	National Priority List
NTP	National Toxicology Program
PAHs	Polycyclic Aromatic Hydrocarbons
P	Population
P	Phenanthrene
PCBs	Polychlorinated Biphenyls
PER	Perylene
PY	Pyrene

PPB	Parts Per Billion or µg/L
ROSES	RepOrting standards for Systematic Evidence Syntheses
RSV	USEPA Region 4 Refinement Screening Value
SEM	Systematic Evidence Map
SJWP	San Jacinto Waste Pits
SR	Systematic Review
TCEQ	Texas Commission on Environmental Quality
USACE	United States Army Corps of Engineers
USEPA	United States Environmental Protection Agency

TABLE OF CONTENTS

Page

LIST OF FIGURES

Page

LIST OF TABLES

Page

1. INTRODUCTION

1.1. Legacy Chemicals, Natural Disasters, and Galveston Bay

Recent extreme events, such as the 2020 hurricane season, varied in frequency and magnitude (National Centers for Environmental Information, 2021). One particular extreme event, heavy rainfall, has notably increased since 1901 with occurrences expected to increase in both North America and across the globe (Wuebbles et al., 2017). Current data does not clearly indicate how rainfall and other extremes will impact future storms; however, recent trend analyses consider compound flood events, or a combination of oceanic storm surge and massive precipitation to be more likely in the future (Valle-Levinson et al., 2020; Wuebbles et al., 2017). Historically at least one extreme hurricane tends to occur nearly every fifty years (Roth, n.d.). The most recent Atlantic hurricane season has shifted in this trend as six major hurricanes were recorded in 2020 (National Oceanic & Atmospheric Administration, 2020b).

Areas with known contamination issues, such as historical waste and active industrial facilities, are of interest for disaster response research (DR2) as well as public and environmental health (Knap & Rusyn, 2016; Pardue et al., 2005; Romanok et al., 2016). For example, a few studies consider contaminant fate and transport as it relates to the disaster research response (DR2) or exposure risk (Horney et al., 2019; Knap & Rusyn, 2016; Pardue et al., 2005; Romanok et al., 2016). DR2 is also a research interest in Texas (Aly et al., 2020; Bera et al., 2019; Horney et al., 2019; Karaye et al., 2019), while urban contaminant characterization has been of interest in other global cities

(Huang et al., 2014; Hussar et al., 2012; Hwang & Foster, 2006; Kanzari et al., 2014; Kim et al., 2019; Rabodonirina et al., 2015; Suarez et al., 2006; Valentyne et al., 2018; Vane et al., 2014).

As the world's second largest petrochemical seaport, Galveston Bay and the Houston Ship Channel (GB/HSC) serves as a key economic and industrial resource for Houston, Texas (US Army Corps of Engineers, 2017). The amount of vessel activity seen in GB/HSC is comparable to other US seaports, such as Los Angeles, California (Campo, 2020); therefore, regular maintenance through dredging is necessary. Due to its historical and current industrial activity, several legacy contaminants, such as polycyclic aromatic hydrocarbons (PAHs), polycyclic biphenyls (PCBs), organochlorine pesticides, dioxin/furans (Dx/F), and heavy metals, have been detected in environmental media (Al Mukaimi, Kaiser, et al., 2018; Bera et al., 2019; Camargo et al., 2020; HARC & Galveston Bay Foundation, 2020; Hieke et al., 2016; Howell et al., 2011b; Lakshmanan et al., 2010; Louchouarn et al., 2018; Qian et al., 2001; Santschi et al., 2001; Sappington et al., 2015; Yeager et al., 2007).

GB/HSC estuary also functions as a natural filter for urban outputs and as a wildlife biodiversity hotspot (Al Mukaimi, Kaiser, et al., 2018; HARC & Galveston Bay Foundation, 2020). Despite the historical pollution, some local benthic marine populations have evolutionarily adapted to high concentrations of contaminants like PAHs and PCBs in sediments (M. Oziolor et al., 2016; E. M. Oziolor et al., 2014b, 2018a). However, under similar conditions, the question remains how local human

population health can be impacted from exposure to this same sediment and contaminant load after a flood or hurricane.

With Houston being the home of over 2 million people (Houston, 2021), local environmental exposures from industry and the atmosphere implicate public health. Since Hurricane Harvey left sediment deposits in the City of Houston (Karaye et al., 2019), the role of flooding and contaminant mobility remains in the region a research interest. In order to understand how natural disasters, such as Hurricane Harvey, influence contaminant exposure, several variables are required. These variables include spatial and temporal data as well as contaminant data so relevant exposure pathways are identified (Hanrahan, 2012; Oswer, 2002; Romanok et al., 2016). When spatial data is available, sampling strategies can be readily developed. If there is temporal data, then this information can identify any expected or unexpected trends in contamination loads. When both spatial and temporal data are combined, both datasets will be useful for DR2 and pre-disaster assessments.

An estimated 26-47 inches of rain (Harris County Flood Control District, 2018), or an estimated 9.3×10^{10} m^3 of water (Valle-Levinson et al., 2020), fell in Houston. Two physical bottlenecks combined with the compounded flooding exacerbated Hurricane Harvey's severity. The first bottleneck was due to poor overflow balance between Buffalo Bayou and the San Jacinto River confluence. This is noteworthy as the National Oceanic and Atmospheric Administration's (NOAA) Manchester station recorded a maximum surge of around 3.5 m during the fourth day of massive precipitation (Valle-Levinson et al., 2020). The second bottleneck originated from the

limited the outflow between Burnett Bay and Tabbs Bay; the latter of which discharges into Galveston Bay (Valle-Levinson et al., 2020). Additional overflows from Houston's bayou and waterway systems (Dellapenna et al., 2020; Harris County Flood Control District, 2018; Kiaghadi & Rifai, 2019) also contributed to the level of flooding.

The outflows described in the previous paragraph consequently contributed to a sediment flood deposit of 9.86×10^7 metric tons into Galveston Bay, with the flood layer averaging 14 cm (Dellapenna et al. in review, Du et al., 2019b, 2019a). Some of the damages associated with this flood event included spills and overflow from local industrial facilities (Kiaghadi & Rifai, 2019). Both of these spill types suggest chemical and physical contaminant redistribution occurred. An additional concern included the role of subsidence rates that could lead to the potential uncovering and redistribution of deeper sediments that contain historical contaminants (Dellapenna, et al., 2018; Al Mukaimi et al., 2018b).

Spatial data and comparable baseline data are ideal datasets to have for characterizing the extent of flood or hurricane impacts in a region (Romanok et al., 2016). However, the availability of such data is dependent upon regional data collections made by academic, private, and state or federal agencies. To identify and prioritize marine environmental quality, the historical program called the United States Environmental Protection Agency (USEPA) Mussel Watch was established in 1976 (Farrington et al., 2016). The resulting monitoring data generated from this program would in turn characterize chemical exposures of concern both humans and organisms (Farrington et al., 2016). This program eventually transitioned to NOAA's National

Status and Trends (NS&T) Program in 1985-1986, with regular monitoring occurring from 1985-1986 until 2011-2012 (Farrington et al., 2016). Therefore, a goal of Mussel Watch was to assess for legacy contaminants as well as emerging contaminants, while also considering the consequent impacts on the local ecosystem.

Within the state of Texas, the Texas Commission on Environmental Quality (TCEQ) established a program called the Texas Clean Rivers Program (CRP). Through this program, water quality issues are monitored and managed (Texas Commission on Environmental Quality, 2020c). As a result, both Mussel Watch and the CRP programs, supply monitoring data that have been collected across time for both biotic (e.g., tissues) and abiotic (e.g., surface sediments, nutrients, and water) factors. Since samples may not have been taken within an impacted disaster area, the applicability of either program's data will vary. Therefore, there is a data gap for rapid site identification and contaminant distribution after natural disasters.

1.2. Complex Mixtures: Polycyclic Aromatic Hydrocarbons (PAHs)

Of the historical chemicals detected in GB/HSC, PAHs are of interest for this dissertation due to their prevalence in environmental media as well as their common occurrence at Comprehensive Environmental Response, Compensation, and Liability Act (CERCLA) or 'Superfund' sites and National Priority List (NPL) sites (Agency for Toxic Substances and Disease Registry, 1995; Barron & Wharton, 2005). There are sixteen Superfund sites listed in Harris County Texas alone (United States Environmental Protection Agency, 2020). While the USEPA has a designated list of sixteen PAHs, known as the USEPA Priority 16 PAHs, these parent compounds are only

a few of the 100+ known PAHs detected in environmental media. PAHs also occur as complex mixtures with improved analytical technologies detecting emerging PAHs (Baird et al., 2007; Betts, 2014; Gao et al., 2019). The fate and transport of PAHs within the environment is also diverse. For instance, these compounds can originate from point discharge sources (e.g., industrial sites), evaporate into the atmosphere or a body of water, or more commonly sorb to solid particulate matter (e.g., organic matter, soot, skeet, and nanoparticles) (de Zwart et al., 2018; Ghosh et al., 2001; Xia et al., 2016). As urban environments become prevalent, there is an increasing need to understand the complex mixtures for water quality, environmental risk assessment (ERA), and human health purposes (de Zwart et al., 2018). Recent evidence also highlights a knowledge gap regarding how multiple stressors, such as contaminant and nutrients, impact urban estuaries (O'Brien et al., 2019).

PAHs are also relevant to study due to the available and detailed chemical and toxicological data for several parent PAHs, such as the EPA 16 (Agency for Toxic Substances and Disease Registry, 1995; de Zwart et al., 2018). Exposure to this compound class is also relevant as PAH exposure can occur within both rural and urban environments. Several examples of PAH exposure include cigarette smoke, car emissions, agricultural burning, industrial waste incineration, coal facilities, creosote-treated wood, or even hazardous waste sites (Agency for Toxic Substances and Disease Registry, 1995). Therefore, relevant exposure pathways for PAHs under pre- and post-natural disaster conditions include inhalation, dermal, and ingestion.

PAHs have historically been detected in GB/HSC sediments (E. M. Oziolor et al., 2014a; Qian et al., 2001; Santschi et al., 2001). Consequently, there was an interest in the extent of PAH distribution after Hurricane Harvey. There are other chemicals of interest since Patrick Bayou and the San Jacinto Waste Pits, two Superfund sites, are known point sources for mercury (Hg) or dioxin/furans (Dx/F) (Al Mukaimi, Kaiser, et al., 2018; Louchouarn et al., 2018). Given the complexity of PAHs, as well as known sources of Hg and Dx/F, complex environmental mixtures become a concern for DR2.

By understanding which individual chemicals are more commonly detected, future studies that seek to understand both the toxicity of environmental mixtures and the long-term fate and transport of these mixture can be developed. Several tools were implemented in this dissertation to characterize such an environmental mixture in GB/HSC. The first tool, a systematic evidence map (SEM), was used to help identify which legacy chemicals were of historical significance within GB/HSC. To understand the extent of PAH redistribution from Hurricane Harvey and identify regions of future sampling interest, a geostatistical technique called kriging was used through ArcGIS software. A third tool, called the KinExA Inline Biosensor, was also used to help prioritize soil and sediment PAH analysis for traditional gas-chromatography-mass spectrometry (GC/MS). Each of these tools signify relevant applications of technology for DR2 and exposure science.

1.3. Systematic Evidence Maps: Tools for Environmental Sciences and Environmental Health

With research needs shifting, systematic evidence maps (SEMs), scoping reviews, and systematic reviews (SRs) are beginning to frequent environmental health and environmental science journals (Neal R. Haddaway, 2018; Neal Robert Haddaway & Macura, 2018; Kohl et al., 2018; Macura et al., 2019; Miake-Lye et al., 2016; Munn, Peters, et al., 2018; Wikoff & Miller, 2018; Wolffe et al., 2020). These tools began emerging in the early 2000s, but there have been no standardized methods universally adopted for environmental sciences (Neal Robert Haddaway & Macura, 2018; Miake-Lye et al., 2016; Saran & White, 2018). One organization, the Collaboration for Environmental Evidence (CEE), has developed useful guidance documents with a particular focus on SEMs and systematic reviews within environmental sciences (Evidence, 2018). In contrast, the Cochran Library and PRISMA were the first organizations to provide guidance for systematic reviews addressing human medical research questions (Cochrane Library, 2020; PRISMA, 2015). There are additional organizations (e.g., Campbell Collaboration and the Veterans Affairs Evidence Synthesis Program) that also aim to share common practices and guidance related to systematic evidence maps (SEMs), scoping reviews, and systematic reviews (Miake-Lye et al., 2016; Saran & White, 2018).

However, SEMs and systematic reviews are not to be confused with traditional narrative reviews, which are subjective and expert-based (Golash-Boza, 2015; Munn, Peters, et al., 2018). SEMs commonly address broad research questions to help identify

research gaps. They therefore, reports on knowledge gaps through tabular or visual maps. SEMs also consider both peer-reviewed articles identified in databases (e.g. Medline, Ebsco, etc.) and grey literature (James et al., 2016; Miake-Lye et al., 2016; Munn, Peters, et al., 2018; Munn, Stern, et al., 2018b; Saran & White, 2018). A SEM is commonly used to share an overview of the literature by guiding audiences to relevant literature through visuals that highlight relevant data gaps. Scoping reviews in contrast, comprehensively evaluate the literature that is often identified by SEMs to yield deliverables for policy-makers. If enough literature is identified by a scoping review, a systematic review may follow. Although when there is limited literature for a meta-analysis to occur, only a SEM or scoping review will be conducted.

When considered collectively, all three of these tools follow an a priori protocol that ensures there will be a comprehensive literature search. This search occurs through a well-defined study scope where there are clear and definitive inclusion/exclusion criteria. To limit bias, each tool uses a minimum of two reviewers to independently screen and evaluate the literature during the title/abstract, full-text screening, and data extraction stages. Should any conflicts arise over a decision, both reviewers discuss their findings so they can agree upon a final decision.

Each tool also includes multiple stakeholders, as their perspectives are key to developing a relevant scope and inclusion/exclusion criteria (Neal R. Haddaway & Crowe, 2018). As mentioned earlier, the CEE continues to shape both SEM and systematic review applications in environmental sciences by providing reporting methodologies and formatting guidance (Neal R. Haddaway et al., 2018; Neal Robert

Haddaway & Macura, 2018; James et al., 2016). Other scientific disciplines, such as exposure science and toxicology, have also adopted at least one of the three tools at varying capacities (Cohen Hubal et al., 2020; Macura et al., 2019; Munn, Peters, et al., 2018; Munn, Stern, et al., 2018b; Sheehan & Lam, 2015; Wikoff & Miller, 2018; Wolffe et al., 2020).

The availability of SEM and systematic review tools continues to evolve with time. Consequently, articles such as the one by Kohl et al. (2018), are extremely valuable as they provide summaries of available online platforms used for SEMs, scoping reviews, and SRs. A caveat to consider for SEMs, scoping reviews, and SRs is the length of time required. For instance, SEMs can be completed faster than scoping reviews and SRs, since they identify and discuss knowledge gaps. In contrast, scoping reviews and SRs are more time intensive due to data quality review as well as detailed meta-analyses. Each tool is therefore unique and unfortunately some scientific disciplines have limited literature; however, the applications all three of these tools will continue to adapt to meet current environmental research data gaps (Karlsson & Gilek, 2020).

1.4. Kriging and its Applications in Environmental Sciences

Collectively, geospatial statistics seeks to quantify something (e.g., chemicals, precipitation) within an given spatial area. Kriging is a specific geostatistical method that interpolates a given dataset to estimate a given quantity within a specified geographical area using a level of uncertainty for the estimations (Chiles & Delfiner, 2012; McLeod et al., 2017; Schabenberger & Gotway, 2005). For environmental sciences, kriging has

been used to estimate contamination in drinking water and stream sediments (S. M. Kim et al., 2017; McLeod et al., 2017), while also considering the spatial dependence for multipollutant data (Jun & Park, 2013) and human activity (Ver Hoef, 2018). Consequently, kriging for DR2 questions could aid in sample design by identifying regions of concern and use limited sample sizes to provide estimates of contaminant loads. For this dissertation, ordinary kriging is utilized, where the assumption is that an unknown mean is held constant across a specified area (Chiles & Delfiner, 2012). Since traditional environmental chemistry methods are both time and resource intensive, kriging helps prioritize areas of interest.

1.5. Rapid PAH Identification: KinExA Biosensor Technology

Traditional analytical methods for PAH detection include GC-MS as well as high performance liquid chromatography (HPLC) paired with ultraviolet absorption or ultraviolet fluorescent detection. Both methods are highly sensitive, but they are time and resource intensive. If a technology could streamline PAH identification as well as prioritize samples for traditional analytical methods, this alternative would be both cost-effective and time efficient. In this case, the KinExA Inline BioSensor (biosensor), has been developed to detect PAHs using a mouse derived anti-pyrene-butyric acid monocolonal antibody (mAb), 2G8. This mAb is highly specific for 3-5 ring PAHs and results are obtained within at least 10 minutes (Li et al., 2016a; Spier et al., 2009).

The biosensor has consequently been deployed to quantify PAHs in real-time (Hartzell et al., 2017, 2018; Spier et al., 2011). Aside from providing rapid results, the biosensor also provides the opportunity to understand the amount of freely dissolved

(C_{free}) PAHs in the sediment porewater. By including this value with the bulk-sediment analysis, provided by either GC-MS or HPLC, the bioavailable or bioaccessible PAH concentration can be estimated to further aid sediment management (Ghosh et al., 2011; McGrath et al., 2019; Muz et al., 2020). This technology is another alternative to passive sampling, which also quantifies C_{free} in both soils and sediments (Cui et al., 2013; Riding et al., 2013). The utility of the biosensor in this dissertation demonstrates its utility for DR2 and shows how this technology is a rapid, flexible, and cost-effect alternative to traditional analytical methods and passive samplers.

1.6. Research Aims

Throughout this dissertation, public health exposures and risk will be considered. This project will utilize an evidence-based SEM to evaluate the contamination status of GB/HSC sediments (Aim 1) and produce a comprehensive PAH distribution map of sediments in GB/HSC (Aim 2). To aid in the rapid characterization of PAHs in GB/HSC, a fluorescent biosensor technology will be applied to GB/HSC soils and sediments (Aim 3).

Given these research aims, this dissertation will characterize environmental mixtures within GB/HSC by utilizing historic and current contaminant data. We aim to establish environmental monitoring parameters, a reference baseline geospatial map, and facilitate the rapid screening of environmental samples for targeted chemical analysis. This dissertation research will be significant because each aim modifies established exposure frameworks through outcomes that can be translated for policy and decision making in DR2, public health, and environmental risk assessment.

2. CHARACTERIZING BASELINE LEGACY CHEMICAL CONTAMINATION IN URBAN ESTUARIES FOR DISASTER-RESEARCH THROUGH SYSTEMATIC EVIDENCE MAPPING: GALVESTON BAY CASE STUDY

2.1. Overview

Natural disasters such as floods and hurricanes impact urbanized estuarine environments. Some impacts pose potential environmental and public health risks because of legacy or emerging chemical contamination. However, characterizing the baseline spatial and temporal distribution of environmental chemical contamination before disasters remains a challenge. To address this gap, we propose using systematic evidence mapping in order to comprehensively integrate available data from diverse sources. We also demonstrate this approach is useful for tracking and clarifying legacy chemical contamination reporting in an urban estuary system. We conducted a systematic search of peer-reviewed studies, government monitoring data, and grey literature. Inclusion/exclusion criteria are used as defined by a Condition, Context, Population (CoCoPop) statement. The study design searches literature from 1990-2019 using the following CoCoPop categories: chemicals of interest (condition), an environmental descriptor and the geographic region of Galveston Bay/Houston Ship Channel (GB/HSC) (context) as well as sediments (population). Most of the peer-reviewed studies reported dioxins/furans or mercury within the Houston Ship Channel (HSC); there was limited reporting of other organics and metals. In contrast, monitoring data from two agencies included 89-280 individual chemicals on a near-annual basis. Of the identified grey

literature, 18 reported metals, 31 reported organics, and 24 reported both. Regionally, peer-reviewed articles tended to record metals in Lower GB but organics in the HSC, while the agency databases spanned a wider spatial range in GB/HSC. Peer-reviewed articles' sampling frequency and was inconsistent since 1994. This systematic evidence map of GB/HSC has shown that chemical data from peer-reviewed and grey literature articles are sparse and inconsistent. Even with inclusion of government monitoring data, full spatial and temporal distributions of baseline levels of legacy chemicals are difficult to determine. There is thus a need to improve keyword indexing, geocoordinate inclusion, and uniformity of environmental data reporting methods for both peer-reviewed articles and grey literature.

2.2. Introduction

With a history of hurricanes and flooding, Texas coasts and inland cities face numerous natural hazards that can affect the fate and transport of contaminants. However, within the field of disaster research, pre-existing conditions research and long-term fate and transport research are largely lacking (Knap & Rusyn, 2016). In 2017 Hurricane Harvey struck the Texas Coast, resulting in extreme flooding over the span of four days. The resulting damages were estimated as being approximately $125 billion with more than 270,000 residences flooded (Blake & Zelinsky, 2018; Harris County Flood Control District, 2018; Texas Commission on Environmental Quality, 2018). However, it has been difficult to characterize the degree to which Harvey changed or redistributed chemical contaminants in the Houston area. This region has a long history of legacy contamination, such as contamination with polycyclic aromatic hydrocarbons

(PAHs), polycyclic biphenyls (PCBs), organochlorine pesticides, dioxin/furans (Dx/F), and heavy metals, from intensive industrial activity over the past 100 years (Al Mukaimi, Kaiser, et al., 2018; HARC and Galveston Bay Foundation, 2018; HARC & Foundation, 2019; HARC & Galveston Bay Foundation, 2020; Hieke et al., 2016; Howell et al., 2011a; Lakshmanan et al., 2010; Louchouarn et al., 2018; E. M. Oziolor et al., 2018a; Qian et al., 2001; Santschi et al., 2001; Sappington et al., 2015; Yeager et al., 2007). Therefore, these contaminant classes collectively are of interest because of their legacy presence and prevalence within GB/HSC environmental matrices (e.g., sediments, water) and biota (e.g., fish).

As an active port, the Houston Ship Channel (HSC) sees vessel activity comparable to the ports in Long Beach, California and New York/New Jersey (Campo, 2020). In turn, regular maintenance is required to deepen and widen the channel through dredging. The earliest dredging efforts date back to the mid-1850s when the navigational channel from the Gulf of Mexico to Houston was not readily accessible (Mark Vincent et al., 2015). Because of these regular maintenance activities, the region's sediment composition can vary since some marsh areas and private lands have been filled in with the dredge materials; Atkinson Island for example, served as a man-made dredge island (Mark Vincent et al., 2015).

Given the regular maintenance and historical contamination, both the dredged sediments and non-dredged sediments are of interest for public health as the public may be exposed to these sediments after a natural disaster or may be indirectly affected through environmental exposures. For example, sediment deposits were documented in

local parks after Hurricane Harvey (Karaye et al., 2019). This particular example highlights the role floods can play in the redistribution of sediments and thus implicate the potential of chemical redistribution. Hydraulic flood controls were also documented to influence water quality parameters (e.g., pH, microbial concentrations, chemical concentrations) after Hurricane Harvey (Kiaghadi & Rifai, 2019). With severe flooding events, hurricanes, tsunamis, and cyclones common in other parts of the world, understanding relevant exposures in global coastal and estuarine environments is timely for disaster-research. However, data on contaminant concentrations over space and time are necessary in order to understand the impact of disaster events, such as hurricanes, on contaminant exposure for residents in these areas. It is also important to have information on relevant contamination sources and identifying relevant exposure pathways (Hanrahan & Hanrahan, 2012; Oswer, 2002). If spatial information is available, future plans for environmental matrix sampling can be improved or expanded upon to address regional exposure risk or monitoring studies.

As transparency needs and regulatory reform pertaining to data requirements increase in the scientific community, both scoping reviews and systematic evidence maps (SEMs) are being implemented in environmental sciences and environmental health. These tools' methodologies and applications have grown since they first appeared in early 2000s literature (Neal R. Haddaway et al., 2018; Neal Robert Haddaway & Macura, 2018; Kohl et al., 2018; Macura et al., 2019; Miake-Lye et al., 2016; Munn et al., 2015; Munn, Peters, et al., 2018; Munn, Stern, et al., 2018a; Wolffe et al., 2020). However, methods for SEMs have not been standardized (Miake-Lye et al.,

2016; Saran & White, 2018). Nonetheless, SEMs are recognized as useful for identifying research gaps, summarizing findings, and sharing relevant resources for further investigation (Miake-Lye et al., 2016; Saran & White, 2018). Scoping reviews on the other hand, are considered the precursors to systematic reviews as they provide a comprehensive search of the literature through an a priori protocol that aids in reproducible searches and additional data extraction (Munn, Peters, et al., 2018). However, SEMs and scoping reviews, which are structured summaries, are not to be confused with traditional narrative reviews, which are often subjective and expert-based (Golash-Boza, 2015; Munn, Peters, et al., 2018). As many aspects of a scoping review are incorporated into an SEM, there is sometimes confusion as to when a scoping review becomes a SEM (Munn, Peters, et al., 2018).

Overall, SEMs can serve as a query tool to identify and characterize evidence for broad or specific research questions, thereby supporting greater objectivity and transparency (Neal R. Haddaway, 2018; James et al., 2016; Munn, Peters, et al., 2018; Rooney et al., 2014; Saran & White, 2018; Wolffe et al., 2020).

In this work, we apply a systematic evidence mapping approach to comprehensively integrate available data addressing the prevalence and occurrence of legacy chemical contaminants (PAHs, PCBs, pesticides, Dx/F, and metals). We consider the Galveston Bay (GB)/HSC estuary system since the region has well-known legacy contamination. Our goals are to determine whether a baseline chemical dataset exists, and whether any spatial or temporal patterns regarding the chemical distribution are discernible, and to share user-friendly visuals to aid in future SEMs both within this

region and other estuarine systems. To our knowledge, there have been no other systematic evidence maps of a similar scope or ones interested in estuarine environments. This project provides an overview of relevant regions of concern, as well as identify gaps within environmental data reporting in GB/HSC.

2.3. Methods

After Hurricane Harvey in 2017, this systematic map project was undertaken to understand available chemical data in GB/HSC. One possible outcome was to develop a representative map that can aid in future environmental sampling designs, thereby directing researchers to areas of vulnerability or areas with a chemical class of interest. A similar approach is relevant to other estuarine environments both in the United States and elsewhere in the world. Because of limited resources and time, the primary question, described in the next section, captures a broad and unique scope within the GB/HSC. Several experts from library sciences, oceanography, risk assessment, toxicology, environmental chemistry, and occupational health were engaged in developing the project scope.

2.3.1. Objectives & Scope Development

Baseline reference data are needed to understand the impacts of Hurricane Harvey on chemical redistribution. To address this interest, a SEM approach will help identify available evidence from a variety of literature sources (e.g., peer-reviewed articles, grey literature, government databases) (James et al., 2016). This SEM's objective was to determine whether there is a baseline reference dataset for GB/HSC legacy contaminants in sediment. Therefore, the following primary question was

developed: What is the historical spatial/temporal distribution of legacy contaminants in GB/HSC? Any secondary questions that may have arisen would have addressed any trends within the specific chemical classes. The following section details the components of the primary question and the relevant mini scoping review conducted before the SEM.

2.3.1.1. Components of the Primary Question

For this study, the aim was to detect prevalence and incidence of available chemical data in GB/HSC. To best capture such geographical distributions, areas of interest, and trend, we used the Condition, Context, and Population (CoCoPop) framework (Munn et al., 2015; Munn, Stern, et al., 2018b). Although other methods papers help prospective reviewers determine whether an SEM or systematic review should be conducted (Aiassa et al., 2015; James et al., 2016; Miake-Lye et al., 2016; Munn, Peters, et al., 2018; Munn, Stern, et al., 2018b), the CoCoPop methodology guidance developed in 2013 (Munn et al., 2015) fit the scope of this project because this approach frames relevant prevalence and occurrence questions. For this project, the type of environment/region, the GB/HSC estuarine system, served as the context. The chemicals served as the condition. Table 2-1 expands on the elements comprising the elements of this project's CoCoPop statement.

Primary Question Elements	Inclusion	Exclusion
Populations (P): ***Environmental Matrix***	***Environmental Matrix:*** Sediments are primarily analyzed, sediments are analyzed with other environmental matrices (water, air, fish tissue)	Label to use for Environmental Matrix: **no sediment** Study does not analyze any sediments
Condition (Co) ***Chemicals of Interest***	***Chemicals of Interest:*** *PAHs (polycyclic aromatic hydrocarbons):* Naphthalene; Phenanthrene; Anthracene; Fluoranthene; Chrysene; Benzo(b)fluoranthene; Pyrene; Perylene; EPA Priority 16 PAHs *PCBs (polychlorinated biphenyls):* Specific Individual Conegers (e.g. PCB 1-209); Specific Arochlor mixtures *OC Pesticides (organochlorine pesticides):* DDT p,p; DDT o,p; DDE p,p; DDD p,p; Heptachlor; Aldrin; Chlordane; Lindane; Mirex *Heavy Metals:* Arsenic (As); Copper (Cu); Mercury (Hg); Lead (Pb); Chromium (Cr); Copper (Cu); Nickel (Ni); Cadmium (Cd); Antimony (Sb); Iron (Fe); Trace elements; Zinc (Zn); Manganese (Mn) *Dioxins:* TCDD; 2,3,7,8-tetrachlorodibenzo para-dioxin; 2,3,4,7,8-PeCDF	Label to use: **no chemicals of interest** Any other chemicals analyzed or other factors analyzed
Context (Co): ***Type of Environment*** ***Region***	***Type of Environment:*** Studies must report estuary or wetland as a descriptor of the study region. Inner coastal tidal zones and bay descriptors may be considered as Galveston Bay may not always be labeled as an estuary ***Geographically relevant region:*** Texas; regions of Gulf of Mexico near Texas; Galveston Bay; Matador Bay; Houston Ship Channel; San Jacinto Estuary; Morgan's Point; Trinity Bay; Upper/Lower Galveston Bay These descriptors may be used in the abstracts and are specific areas of interest - general names of Galveston Bay and the Houston Ship Channel may be more frequently used.	Label to use for Type of Environment: **wrong environment** No estuary or wetland study environments describe the study region (e.g. coastline, ocean, rivers, streams, lakes) For example, a study in the Gulf of Mexico investigates sediments, but they were from an oil spill Label to use: **wrong region** Not geographically relevant region within Texas or if the study is within the Gulf of Mexico it is not near Texas coast(s)
Study Design Status	Primary Data point(s) reported or trends analyzed	Label to use: **review** Review Articles

Table 2-1 CoCoPop Statement elements with specific descriptions of the eligibility criteria used for inclusion and exclusion of articles during the screening and data extraction processes.

2.3.2. **Literature Search Methodology**

Both peer-reviewed literature and grey literature were searched in the English language, with the primary searches occurring between June 2018 and July 2019. Additionally, several national and regional monitoring programs (e.g., from the Texas Commission on Environmental Quality (TCEQ) and National Oceanic and Atmospheric Administration (NOAA)) were identified in a search conducted from November to December 2020. The organics (PAHs, PCBs, Dx/F, and pesticides) and metals data reported in sediments were extracted in December 2020 from the following databases: NOAA Data Integration Visualization Exploration and Reporting (DIVER) (National Oceanic & Atmospheric Administration, 2020a); NOAA National Centers for Coastal Ocean Science (NCCOS) (National Oceanic & Atmospheric Administration, 2017); Texas Commission on Environmental Quality (TCEQ) Surface Water Quality Web Reporting Tool (Texas Commission on Environmental Quality, 2020b); and the Texas Clean Rivers Program (CRP) (The Texas Clean Rivers Program, 2020).

The TCEQ data included in this project came from 18 TCEQ segments within the GB/HSC (1001D, 2428, 2430, 2425, 2430A, 2423OW, 1006, 1007, 1005, 2439, 1001, 2427, 2429, 2426, 2425A, 2422, 2421, 2424OW). These segments can be found using the two web tools cited in the previous paragraph, or they can be readily viewed using the TCEQ Surface Water Quality Viewer (Texas Commission on Environmental Quality, 2020a). Of the 18 TCEQ segments identified, only 15 were used, as 1001D, 2423OW, and 2424OW contained no data. The data extracted from these two TCEQ

programs were for individual metals and organics (e.g. PAHs, PCBs, and pesticides) reported in sediments.

Furthermore, the Texas A&M University OAKTrust, which is the digital repository for Texas A&M, and the ProQuest Dissertation & Theses Global, which is a global repository, were separately searched in December 2020. The theses/dissertations title/abstracts, publication year, and whether metals, organics, or both metals and organics were recorded. Data were extracted from documents that were no longer embargoed.

The scope and eligibility criteria for the initial search (Table 2-1) and corresponding data coding form via Google forms were established between November 2017 and June 2018. During this iterative process, article identification was limited if detailed search terms such as individual chemical names or a specific bay were used. In contrast, irrelevant articles were identified when broad search terms only considered ‘estuary’ or ‘sediment.’ The online software tool Rayyan aided in finalizing the scope and eligibility criteria (Figure A 1).

In addition to searches of the peer-reviewed literature searches, general searches of the grey literature were conducted both in Google and through Carrot2.org. The purpose of this search was to identify additional articles or documents not readily found through bibliographic or library database searches (Evidence, 2018). The grey literature was screened using the same eligibility criteria as database articles, with the first 100 searches set as the cutoff. Documents after the first 100 diminished in relevance.

To diminish bias, two reviewers independently screened title/abstracts identified for both the peer-reviewed articles and grey literature. Disagreements were settled through discussions between the reviewers. After title/abstract screening, data was extracted from the peer-reviewed articles and grey literature by utilizing a predesigned Google form. The purpose of this form was to code all extracted data. To verify relevant data would be extracted, the Google form was tested using the following articles: Almukaimi (2016), Louchouarn (2018), Santschi (2001), Suarez (2005), and Yeager (2007). All identified literature were fully screened using this Google form.

Upon completion of the screening, the coded information was then imported to Microsoft Excel for further data visualization and analysis. There was one central spreadsheet summarizing the findings of initial search, and a secondary spreadsheet compiling both the NOAA and TCEQ data. The data used to identify possible trends were publication and sampling years, metal concentrations, organic concentrations, sampling site descriptors, and geocoordinates (if available). The following sections provide additional details on the search strategies, eligibility criteria, and article screening process used for the project's data coding strategy.

2.3.2.1. Search Strategy & Terms – Databases

Initial test searches focused on the general area of Houston, TX, sediments, and several chemical names. As the scope developed, the following databases were searched: MEDLINE (OVID), Agricola (EBSCO); Environmental Complete (EBSCO), Wildlife & Ecology Studies Worldwide (EBSCO), GreenFILE (EBSCO), and Academic Search Ultimate (EBSCO). The search strings used for the MEDLINE database are outlined

based on the population, conditions, and contexts to help structure and enable quick amendments to the search (Evidence, 2018) and are detailed in Table 2-2. Similar search strings were used to search the EBSCO databases; however, to address alternative search string terms for the population (environmental matrix), we used the following phrases:

> (DE "SEDIMENTS" OR DE "ALLUVIUM" OR DE "CLAY" OR DE "CONTAMINATED sediments" OR DE "DETRITUS" OR DE "ESTUARINE sediments" OR DE "LAKE sediments" OR DE "LATERITE" OR DE "MUD" OR DE "RIVER sediments" OR DE "SAND" OR DE "SEDIMENT control" OR DE "SILT" OR DE "SUSPENDED sediments") OR TI sediment* OR AB sediment*

Database Search		# Hits
Search string: Population - Environmental Matrix	1. exp Geologic Sediments/ 2. sediment*.ti.ab 3. 1 or 2	Medline OVID: 183 retrieved EBSCO: 70 retrieved; 39 unique • Agricola (27) • Environmental Complete (15) • Wildlife & Ecology Studies Worldwide (15) • GreenFile (10) • Academic Search Ultimate (8)
Search string: Condition – Chemicals of Interest	4. exp Polycyclic Aromatic Hydrocarbons/ 5. exp DIOXINS/ 6. exp Metals, Heavy/ 7. aldrin/ or ddt/ or dieldrin/ or endrin/ or exp heptachlor/ or lindane/ or mirex/ 8. Polycyclic Aromatic Hydrocarbon*.ti,ab. 9. (dioxin* or aldrin or ddt or dieldrin or endrin or heptachlor or lindane or mirex).ti,ab. 10. (heavy metal* or lead or cadmium or mercury).ti,ab. 11. (Naphthalene or Phenanthrene or Anthracene or Fluoranthene or Chrysene or Benzofluoranthene or Pyrene or Perylene or DDD or DDE or TCDD or tetrachlorodibenzo or PeCDF or (Organochlorine adj1 pesticide*) or (Chlorinated adj1 hydrocarbon*) or Chlordane or (Trace adj1 (element* or metal*)) or USEPA priority polycyclic aromatic hydrocarbons or Copper or Nickle or Lead or Cadmium or Aresnic or Antimony or Mercury or Iron or Zinc or Manganese).ti,ab. 12. or/4-11	
Search string: Context – Type of Environment/Region	14. 3 and 12 15. exp Texas/ 16. exp "Gulf of Mexico"/ 17. (texas or galveston or houston or gulf of mexico or gulf coast).ti,ab. (southeast* adj1 ("united states" or america or states)).ti,ab. 18. or/14-17 19. 13 and 18	

Table 2-2 The search strings used for the three components of the CoCoPop (Condition, Context, Population) statement are summarized along with the corresponding total hits retrieved from both Medline OVID and EBSCO. The hits associated with the specific databases within EBSCO are also included in the parentheses.

To address alternative search string terms for condition (chemicals of interest) and context (region) the following phrases were used:

AB ((dioxin* or aldrin or ddt or dieldrin or endrin or heptachlor or lindane or mirex)) OR AB ((heavy metal* or lead or cadmium or mercury)) OR AB Polycyclic Aromatic Hydrocarbon* OR TI ((dioxin* or aldrin or ddt or dieldrin or endrin or heptachlor or lindane or mirex)) OR TI ((heavy metal* or lead or cadmium or mercury)) OR TI Polycyclic Aromatic Hydrocarbon* OR ((DE "POLYCYCLIC aromatic hydrocarbons") OR (DE "HEAVY metals" OR DE "ALUMINUM" OR DE "ANTIMONY" OR DE "BARIUM" OR DE "BERYLLIUM" OR DE "CADMIUM" OR DE "HEAVY metal content of forest soils" OR DE "HEAVY metal content of sediments" OR DE "LEAD" OR DE "MERCURY" OR DE "THALLIUM")) OR (DE "DIOXINS")

AND

TI ((Texas or Galveston or Houston or “Gulf of Mexico”) or "gulf coast" or (southeast* n1 ("United States" or America or states))) OR AB ((Texas or Galveston or Houston or “Gulf of Mexico”) or "gulf coast" or (southeast* n1 ("United states" or America or states)))

2.3.2.2. Search Strategy & Terms – Grey Literature

The first 100 hits from Google and Carrot2.org were screened first by title/abstract, then as full text. The following search terms and formatting were used to identify online materials to include: (1) +sediment houston galveston file:pdf; (2) +sediment +heavy metals houston galveston file:pdf; (3) +sediment +PAHs houston

galveston file:pdf. Figure A 2 in the supplementary materials summarizes the results for each of these internet searches.

2.3.2.3. Search Strategy in NOAA & TCEQ databases

Outside of the database and grey literature search, publicly available organics and metal data published by NOAA and TCEQ are referenced here. The search in NOAA's DIVER database located all available PCB congeners, PAHs (EPA 16 PAHs and the corresponding alkylated-PAHs), dioxin/furans, pesticides, and metals. This information was downloaded as a zip file and then imported into Microsoft Excel. The specific chemicals are listed in Table A 3. The NOAA NCCOS data were downloaded as text files, one for organics and one for trace elements, which were then imported into Excel. Once in Excel, the NCCOS data were sorted based chemical class PAHs (EPA 16 PAHs and their corresponding alkylated PAHs), PCBs, and pesticides. Only data from 1990-2019 were included.

Overlapping data was observed in the two TCEQ monitoring programs, since the TCEQ was the primary submitter for the Texas Clean River Project, while the Surface Water Quality Web (SWQW) Reporting Tool included data from TCEQ, the University of Houston, Patrick Bayou Total Maximum Daily Load (TMDL) Lead Organization, Parsons Engineering Science, and another agency (Texas Commission on Environmental Quality, 2020b). Only the TCEQ SWQW data are included because the Texas Clean River Project data duplicated a portion of the TCEQ SWQW data.

The TCEQ data were first downloaded as text files and then imported into Excel for further sorting. The available PAH, PCB, pesticide, and metal data were extracted

and sorted based on chemical class in a format similar to that for the NOAA data; however, there were no alkylated PAHs reported in the TECQ data. Additionally, TCEQ reported concentrations values as either "greater than" or "less than;" therefore, values were halved to standardize the dataset. In turn, all TCEQ values were extracted so they could be combined with the extracted NOAA and peer-reviewed data. The specific chemicals extracted for both NOAA and TCEQ are summarized in Table A 1.

2.3.2.4. Search Strategy in Texas A&M University OAKTrust and ProQuest Dissertation & Theses Global

To ensure relevant dissertations and theses were also considered, both the Texas A&M University and ProQuest Dissertation & Theses Global databases were searched. The terms "Galveston Bay" and/or "Houston Ship Channel" were used to identify titles and abstracts, which were further screened for relevant chemicals of interest and sediments. Only dissertations and theses published from 1990 through 2019 were considered. In the case of embargoed dissertations/theses, only the title/abstract were considered for inclusion; otherwise, documents' full-text were downloaded. All dissertations/theses were coded by reference, reference type (e.g., peer-reviewed article, masters, Ph.D.), publication year, and whether metals and/or organics were reported, and the reported outcomes.

2.3.2.5. Eligibility Criteria

The CoCoPop framework guided how the eligibility criteria were defined in this project. Because the primary question focused on historically contaminated sediments, the three elements of the CoCoPop framework were divided into five additional

categories: (1) Environmental Matrix, (2) Chemicals of Interest, (3) Type of Environment, (4) Region, and (5) Study Design Status. By utilizing each of these categories, we aimed to identify relevant information while also ensuring that multiple studies could be considered during the screening processes. If the articles did not meet the inclusion criteria as defined in Table 2-1, they received an exclusion label (Table 2-1). Of the five categories, the 'chemicals of interest' possessed an additional five categories of chemical classes as listed in Table 2-1. Each of these chemical classes have had historical relevance in the GB/HSC.

Since authors often did not describe an estuary or explicitly describe the geographical region, both of which were listed under Context, alternative descriptors such as "inner coastal tidal zone", "bay", "regions of the Gulf of Mexico near Texas" or "Upper/Lower Galveston Bay" were used. When the title and abstract did not identify the geographic region, this information was obtained from the full text. As reviews can be biased and may not adequately consider historical references, this project excluded all reviews.

2.3.2.6. Article Screening

All peer-reviewed articles and grey literature were screened for relevance using the eligibility criteria defined in the previous paragraph. To facilitate the screening process, the free and accessible software tool Rayyan is utilized (Collaboration for Environmental Evidence, 2019). Rayyan includes a "blind-mode," which ensures that each reviewer independently screens articles, thereby avoiding biases. Through machine learning, Rayyan also utilizes a user's inclusion and exclusion decisions to make the

screening process faster (Kohl et al., 2018). Based on the eligibility criteria established for this systematic map, Rayyan also enabled both reviewers to use and reference the same set of labels (Table 2-1) to identify which articles they planned to include, planned to exclude, or were uncertain to whether to include. If the reviewers were uncertain whether to classify an article as included or excluded, they shared their reasoning in order to reach a consensus. Figure A 1 of the supplementary materials summarizes the screening process.

2.3.2.7. Coding Strategy

The data for this systematic map was coded via a Google form, the results were saved in Microsoft Excel spreadsheets, and the spreadsheets were organized to be searchable and user friendly (James et al., 2016). During scoping development, the Google form was verified by testing the previously listed test articles. Additional commentary or observations made by the reviewer were annotated in paragraph format at the end of the Google form. Each reviewer verified the other's coding by looking over their Google forms and re-reading the included articles. Once the coded data were agreed upon, it was then extracted into Microsoft Excel to help assess for general trends. A list of the coding descriptors used can be found in Table A 1.

2.3.3. Statistical Analyses

All coded data extracted were inputted into Microsoft Excel where the concentration units were verified and then imported to GraphPad Prism 9.0.0. for further data analysis. Tableau 2020.3.3 was also used to visualize and map the prevalence of organics versus metals reported in GB/HSC. Analysis of variance (ANOVA) was used to

determine variability between temporal and regional groups once all the raw concentration data were normalized through log-transformation. The statistical software, R (version 3.6.1), was used to create a graphic that compared publication year and sampling year for reported chemicals. The summary values from both the NOAA and TCEQ databases are contrasted with NOAA's Screening Quick Reference Tables (SQuiRT) effects range low (ERL) and effects range median (ERM) for sediment quality guideline (SQG) references. Since each compound varied in detection values, the ERL and ERM values provide a reference value for potential exposure risk at the benthic level within the GB/HSC ecosystem.

2.4. Results

2.4.1. Number and Types of Articles, Contaminants, and Spatial Data

After duplicate removal, a total of 487 articles and documents were searched; 423 were excluded using the eligibility criteria defined in Table 2-1. There were 55 included articles included for full text screening, where an additional 15 articles were added after separate secondary searches (Figure 2-1). After critical appraisal, 36 articles were included for data visualizations and concentration analyses; detailed summaries of appear in Table 2-3. Figure 2-1 further details all stages of the screening process and indicates why given studies were included and excluded with their reasons (Haddaway et al., 2018).

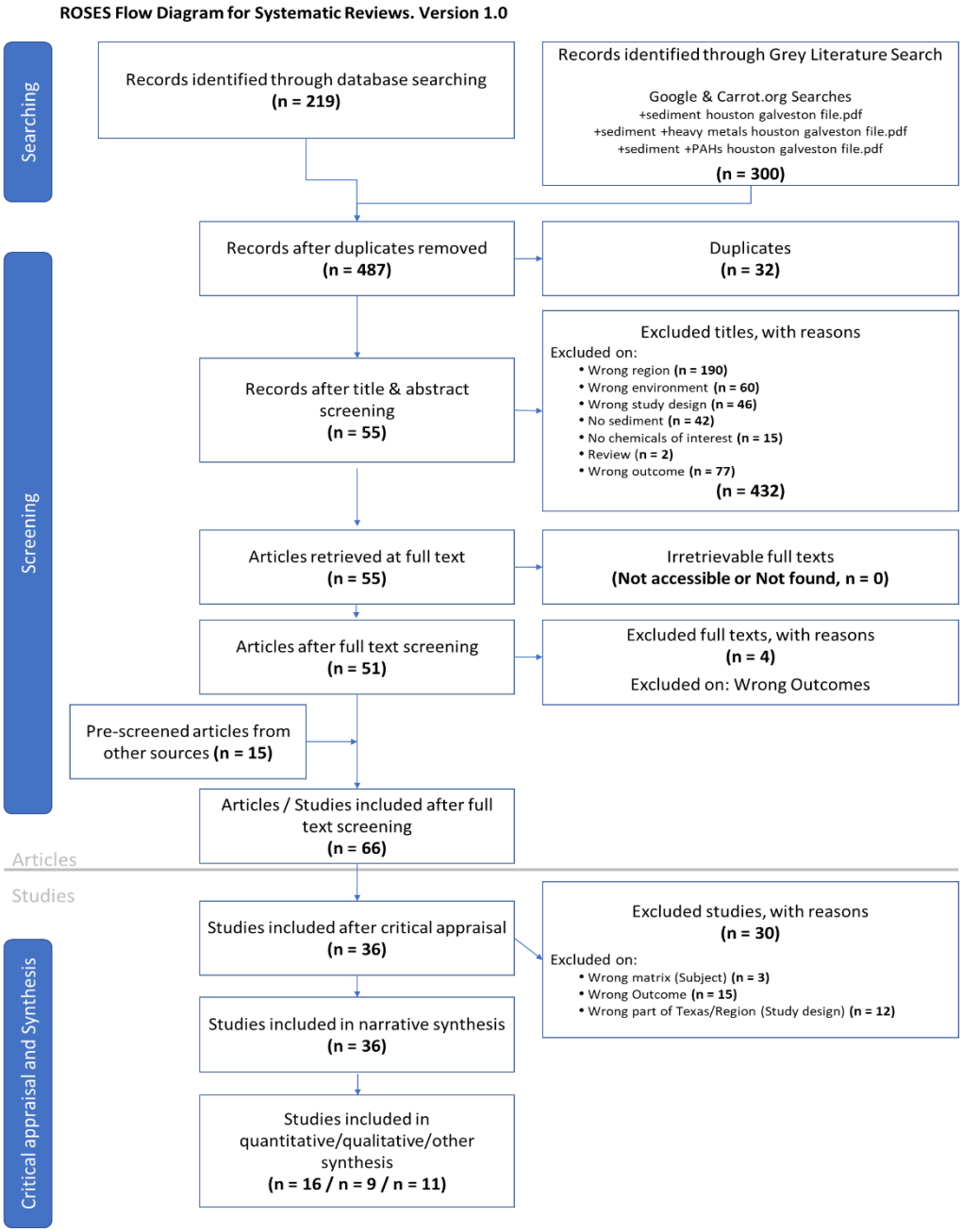

Figure 2-1 ROSES flow diagram (Haddaway NR, Macura B, Whaley P, and Pullin AS. 2017. ROSES flow diagram for systematic reviews. Version 1.0. DOI: 10.6084/m9.figshare.5897389) shows the process in which all articles considered for the narrative analysis were selected for inclusion/exclusion during the screening and data extraction processes.

Ref.	Ref. Type	Mx	Samp Year	General Sampling Location	Metals	Organics	Concen.	Reported Outcome
Aguilar et al. 2014	Peer-Rev	Surf Sed. (<5 cm)	2010	San Jacinto Waste Pits/ Channelview	-	**PCBs** (PCB-77; PCB-81; PCB-105; PCB-114; PCB-118; PCB-123; PCB-126; PCB-156; PCB-157; PCB-167; PCB-169; PCB-189)	Av. in pg/g dry wt	Improving Dx/F extraction method using the San Jacinto Waste Pit samples
Al Mukaimi et al. 2018	Peer-Rev	Sed. Core	2012; 2014	West Bay; East Bay; Texas City; Trinity Bay; Upper Bay; Clear Lake; Taylor Lake; Houston Ship Channel	Hg; Pb; Al; Ni; Zn	-	Av.; Bkg; Max. in ng/g	SQ Check; Environmental Policy; Focus on Hg
AlMukaimi 2018	D/T (PhD)	Sed. Core	2012; 2014	West Bay; East Bay; Texas City; Trinity Bay; Upper Bay; Clear Lake; Taylor Lake; Houston Ship Channel	Hg; select cores with Pb, Al, Ni, and Zn	-	Av.; Bkg; Max. in ng/g	Subsidence; Sedimentation; Hg Detection
Apeti et al. 2012	Peer-Rev	Surf Sed. (<3 cm)	2006-2007	Confederate Reef; Offatts Bayou; Ship Channel; Todd's Dump; Yacht Club	Total Hg	-	Av in ug/g dry wt	Potential of Bioaccumulation; Monitoring Efforts

Table 2-3 Summary of all studies included for the systematic evidence map. Each row describes the relevant categories for each individual reference used. References (Ref); Reference Type (Ref Type); Peer-Reviewed Article (Peer-Rev.); Dissertation/Theses (D/T); Grey Literature (Grey Lit.); Undergraduate Research Scholars Thesis (Undergrad); Matrix (Mx); Surface Sediment (Surf Sed); Sediment Core (Sed Core); Sediments (Sed.); Sampling Year (Samp Year); Concentrations Reported (Concen.); Averages (Av.); Background (Bkg); Descriptive Statistics (Descrip. Stat); Individual Chemicals Reported (ICR); Maximum (Max); Organics (Orgo); Sediment Quality (SQ); Not Reported (NR); Supplemental Table (Suppl Table).

Table 2-3 Continued

Ref.	Ref. Type	Mx	Samp Year	General Sampling Location	Metals	Organics	Concen.	Reported Outcome
Carr et al. 1996	Peer-Rev	Surf Sed.	1992	Morgan Point; Jack's Pocket; Eagle Point; East Bay; West Bay; Burnett Bay; Cedar Bayou; Trinity Bay; Kemah Flats; Texas City; Jones Bay; Chocolate Bay; Alexander Island; Black Duck Bay; Atkinson island; Swan Lake; Dollar Bay	Al, Ba, Be, Cr, Cu, Fe, Mg, Mn, Ni, Sr, V, Zn	Pesticides (aldrin, dieldrin, endrin, mirex, chlordanes, BHCs, DDTs) PCBs PAHs	Analysis NR	Sediment Quality; Risk Assessment; Exposure Assessment
Davis 2018	D/T (MS)	Surf Sed.	1992-2017	TCEQ Segments: 1005 (HSC); 1006 (HSC); 1007 (HSC); San Jacinto Bay (2427); Burnett Bay (2430); Upper GB (2421); Bayport Channel (2438)	-	EPA 16 PAHs: Nap; A; AE; AY; F; FL; P; PY; C; BaA; BaF; BkF; BaP; ghi; IP; DA	Descrip. Stat for 1992-1997; 1999-2002; 2004-2008; 2009-2013; 2014-2017 all in ug/kg	Temporal & Spatial Distribution of PAHs; Sourcing of PAHs; SQGs
Dean et al. 2009	Peer-Rev	Surf Sed. (<5 cm)	2002-2004	Houston Ship Channel (HSC)	-	Individual 18 Dx/F	Median & Ranges in pg/g	Understand the Bioaccumulation of Dx/F

Table 2-3 Continued

Ref.	Ref. Type	Mx	Samp Year	General Sampling Location	Metals	Organics	Concen.	Reported Outcome
Dobberstine 2007	D/T (MS)	Sed. Core	2004; 2005	lower Garpenter Bayou; lower Cedar Bayou; East Fork of Double Bayou; Robinson Bayou; Little Cedar Bayou	As; Cd; Cu; Pb; Ni; Sn; Hg; Zn	Organo-chlorine/ phosphorus pesticides; PAHs	ICR in mg/kg (metals) & ug/kg (orgo)	Identify a reference site within upper GB via evaluation of Sediment Quality Triad
Galveston Bay Estuary Program; TCEQ, USEPA, HARC 2019	Grey Lit.	NR	1973-2009	Houston Ship Channel, Trinity Bay, Upper & Lower Galveston Bay, East Bay, West Bay, Christmas Bay Complex	As; Ca; Cr; Cu; Pb; Hg; Ni; Ag; Zn	-	General Trends	Trends
Gardinali 1996	D/T (PhD)	Surf Sed.	1993	West Bay; East Bay; Lower GB; Upper GB; Trinity Bay; along the HSC	-	17 Dx/F; Total PCBs (a focus on PCBs: 77; 81; 126; 169; 105; 114; 118; 123; 156; 157; 167; 189; 128; 138; 158; 166; 170);	ICR (pg/g); Total PCDD/Fs in pg/g; Total PCBs in ng/g	Bioaccumulation & distribution of halogenated aromatic hydrocarbons
HARC and Galveston Bay Foundation 2017	Grey Lit.	Sed.	2002-2016	Galveston Bay, Houston Ship Channel	Hg; Zn; Ni; Pb; As; Ag; Cu; Cr; Ca	Pesticides (DDT; Lindane; Dieldrin, Chlordane) PAHs (PY; AY; FL; AE; P; A; F; DA; BaP; C; Nap) PCBs (in general)	NR	Comparisons to Prior TECQ data

Table 2-3 Continued

Ref.	Ref. Type	Mx	Samp Year	General Sampling Location	Metals	Organics	Concen.	Reported Outcome
Hieke et al. 2016	Peer-Rev	Sed. Core (1-5 cm)	2006	inlet off Burnett Bay; Lower San Jacinto Bay; Negrohead Lake, San Jacinto Waste Pits; Beak Lake; Anahuac Channel; inlet by Kirby Inland Marine Oper Center; inlet south of Greens/ Baffalo Bayou split; inlet off entry to Buffalo Bayou; near Bay Shore Park; inlet off Tabbs Bay; Atkinson Island; transcect in GB	-	Sum of 18 Dx/F = PCDD/F	Av. in ng/g dry wt	SQ; Remedial Actions; Microbial Management & Trends
Howell et al. 2011	Peer-Rev	Surf Sed.	2002-2003	mouth of Patrick Bayou; near Patrick Bayou; main channel; near tributary; near Patrick Bayou/main channel	-	Sum of 209 PCBs	Av. in ug/g OC or ng/g OC	Sediment/Water Quality; Exposure Assessment; Bioaccumulation Factor

Table 2-3 Continued

Ref.	Ref. Type	Mx	Samp Year	General Sampling Location	Metals	Organics	Concen.	Reported Outcome
Kennicutt MC 2017	Peer-Rev	Sed.	1980s, 1991-1995, 1990-1997, 2000, 2001-2002, 2003-2006	-	Cr; Cu; Ni; As	Pesticides PAHs PCBs (general)	NR	SQ
Lakshmanan et al. 2010	Peer-Rev	Surf Sed. (<5 cm)	2002-2003; 2008	General HSC	-	209 PCBs 43 PCBs 18 PCBs	Av. in ng/g dry wt	Bioaccumulation; SQ; Risk Assessment; Environmental Monitoring
Leonard 2018	D/T (Undergrad)	Soils	2017	SJWP, Lynchburg Ferry landing, Burrnet Bay, Highland Acid Pit, French Limited, Sikes Superfund Site	T-Hg	Nap; A; AE; AY; F; FL; P; PY; C; BaA; BaF; BkF; BaP; ghi; IP; DA	ICR & Totals in ug/kg	Release & Remobilization after a natural disaster
Louchouarn et al. 2018	Peer-Rev	Sed. Core	2006	inlet off Burnett Bay; Lower San Jacinto Bay; Negrohead Lake; S. of I10 Bridge; San Jacinto Waste Pits; Beak Lake; Anahuac Channel	-	Individual 18 Dx/F	Av. in pg/g	Fate & Transport (Dx/F)

Table 2-3 Continued

Ref.	Ref. Type	Mx	Samp Year	General Sampling Location	Metals	Organics	Concen.	Reported Outcome
NOAA 2020/2017	Data-base	Sed.	1993, 1994, 1996, 2000-2006, 2010	Upper Galveston Bay; Lower Galveston Bay; HSC	See Supplemental Table 2	See Suppl.Table 2	mg/kg; ng/g; ug/g	Monitoring Data
Oziolor et al. 2014	Peer-Rev	Sed.	-	Houston Ship Channel (Vince Bayou, Patrick Bayou)	-	PCDD/F PCBs PAHs	NR	Microevolutionary Outcomes from Exposure
Oziolor 2017 (Embargo)	D/T (PhD)	-	-	-	-	-	-	-
Qian et al 2001	Peer-Rev	Sed.	1990, 1994	Ship Channel, Hanna Reef, Yacht Club, Todd's Dump, Offatts Bayou, Confederate Reef	-	PAHs	Ranges and Mean in ng/g	NOAA Status & Trends (NS&T) Mussel Watch Program; Biota-Sediment Accumulation Factor (BASF)
Chatterjee R. 2007 (summary of Yeager et al. 2007)	Grey-Lit	NR	-	Upper HSC	-	Dx/F (general)	NR	Commentary for Dioxin Contribution Sources
Santschi et al. 2001	Peer-Rev	Sed.	1995	Trinity Bay	Pb; Ba; Hg; Cd	Sum 24 PAHs Sum 18 PCBs Sum DDTs	ug/g	Comparison to Natural Background Levels
Seward 2012	D/T (MS)	Sed. Core	2004	Galveston Bay; HSC; lower San Jacinto River; lower Trinity River floodplain	-	Individual 17 Dx/F; Total PAHs	Dx/F in pg/g Total PAHs in ng/g	Historical contamination; fate & sourcing; redistribution; sorption & bioavailability
Simons et al. 2009	Peer-Rev	Sed	2000-2004	Galveston Bay	Pb; Hg; Zn; As	PAHs	Averages in ug/g	Resource for Ecological Conditions

Table 2-3 Continued

Ref.	Ref. Type	Mx	Samp Year	General Sampling Location	Metals	Organics	Concen.	Reported Outcome
Suarez et al. 2005	Peer-Rev	Surf Sed. (<5 cm)	2002-2003	Upper Galveston Bay/HSC	-	Individual 18 Dx/F	TEQs per kg dry wt;	Trends & Status of Dx/F
Suarez et al. 2006	Peer-Rev	Surf Sed. (<5 cm)	2002-2003	Upper Galveston Bay/HSC	-	Individual 18 Dx/F	-	Sediment Flux
TCEQ 1994	Grey Lit	Sed.	1992, 1993	-	Cu; Zn; Hg; Pb; Cr	DDT Av. PCBs	Ranges in ug/kg	Trends; Sediment Quality
TCEQ SWQW 2020	Data-base	Sed.	1990-2019	Upper Galveston Bay; Lower Galveston Bay; HSC	See Suppl Table 2	See Suppl. Table 2	ug/kg; ng/g; mg/kg	Monitoring Data
University of Houston-Clear Lake and the University of Houston Houston, Texas 2003	Grey Lit	NR	-	-	-	PAHs	Zhang et al. paper highlighted	Reports & Trends
Wei 2016	D/T (PhD)	Surf Sed.	2001-2010	TCEQ Segments 1005 (HSC); 1006 (HSC); 1007 (HSC)	Pb; Cu; Hg; Zn	-	Av. in mg/kg (unclear if this value was per year or by station)	Spatio-temporal water & sediment distributions; seasonal variation of air pollutants; pollutants & health outcomes

Table 2-3 Continued

Ref.	Ref. Type	Mx	Samp Year	General Sampling Location	Metals	Organics	Concen.	Reported Outcome
Yeager et al. 2007	Peer-Rev	Sed. Core	2006-2007	inlet off entry to Buffalo Bayou; near Bay Shore Park; inlet by Kirby Inland Marine Oper Center; inlet off Buffalo Bayou near BB Toll Bridge; inlet south of Greens/Baffalo Bayou split; terrestrial control off of Trinity River; inlet off Upper San Jacinto Bay; inlet off Tabbs Bay	-	PCDD/F	Av. in ng/kg dry wt	Sedimentary Processes & Flux
Yeager et al. 2010	Peer-Rev	Surf Sed. (3-4 cm)	2007	Hog Island, Alexander Island	-	PCDD/F	Av. in pg/g	Remedial Actions
Yuill 1991	D/T (PhD)	Sed.	1987; 1988	-	-	-	-	Not included for analysis due to sampling occurring prior to 1990 and no focus on metals
Zhang et al. 2003	Grey Lit.	NR	-	-	-	PAHs	NR; Flux Rates Calculat-ed	Sediment Flux; Risk Management Strategies

In total, 18 articles reported metals, 31 reported organics, and 24 reported both. Of the studies reporting quantitative data, seven were peer-reviewed articles that included latitudes and longitudes; NOAA and TCEQ databases also included latitudes and longitudes. The remaining eight quantitative studies/reports used general location descriptors (e.g., Bear Lake, Lower San Jacinto Bay, etc.). Given the mix of exact geocoordinates and general location descriptors, the three general regions of HSC, Upper GB, and Lower GB were used to discern any spatial patters in the chemical data (Figure 2-2). In the peer-reviewed articles, there was a distinct difference between the frequency of metal reporting versus organic reporting. For example, most metals data were spread throughout each of the three regions, but there was more diversity in Lower GB than the HSC and Upper GB (Figure 2-2a). Sample numbers also varied for each research agency. The samples analyzed for organics for instance, were mainly in the Upper HSC with a cluster noted in the San Jacinto Waste Pits (SJWP) (Figure 2-2b). Both NOAA and TCEQ monitoring programs reported throughout GB/HSC (Figure 2-2c-e).

The peer-reviewed articles contained data with numerous metals (Ag, Al, As, Ba, Be, Cd, Cr, Cu, Fe, Hg, Mg, Mn, Ni, Pb, Sb, Sn, Zn), with Hg being the most commonly reported metal, and Dx/F the most common organic reported. Averages or ranges were sometimes included for individual metals (Al Mukaimi et al., 2018b; Almukaimi, 2016; Apeti et al., 2012; Leonard, 2018; Santschi et al., 2001; Simons & Smith, 2009; Texas Commission on Environmental Quality, 1994; Wei, 2016), while other articles described observed trends (Galveston Bay Estuary Program; TCEQ, USEPA, 2019; HARC and Galveston Bay Foundation, 2017b; Kennicutt II, 2017b).

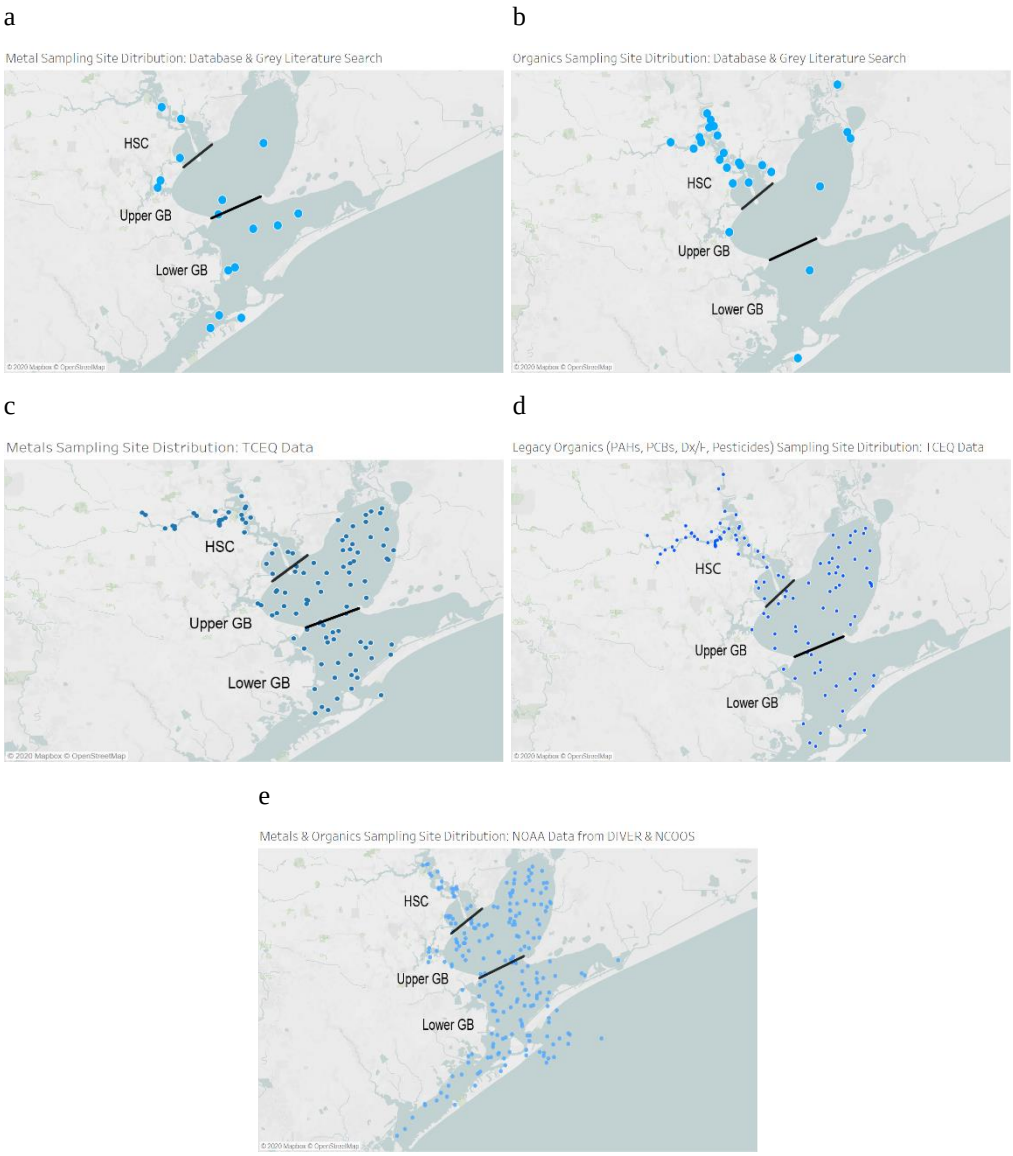

Figure 2-2 The maps summarize the general regional locations for metal (a) and organic (b) concentrations reported in the peer-reviewed literature and grey literature. The TCEQ samples analyzed for metals (c) and for organics (d) show additional sites to those illustrated in (a) and (b). The NOAA metals and organics data shared the same geocoordinates are therefore are all on the same map (e). All circles designate either general sampling site (a, b) or specific sampling sites as not all publications shared detailed geocoordinates (c,d,e).

In contrast, both NOAA and TCEQ published extensive metal and organic analytes (Table A 3). Additionally, we noted two of the eight dissertations/theses included in this study, used the same TCEQ database described earlier in the methods section (F. R. Davis, 2018; Wei, 2016). Therefore, the raw TCEQ data was included for these two studies rather than their averages or descriptive statistics. All other dissertations/theses contained original data.

The PAHs or PCBs are reported in the peer-reviewed articles/reports, they appeared either as general totals or specific groupings. For PAHs, the peer-reviewed articles commonly reported total levels of PAHs as averages or summed certain PAH analytes (F. R. Davis, 2018; Gardinali, 1996; Leonard, 2018; Qian et al., 2001; Santschi et al., 2001; Seward, 2010; Simons & Smith, 2009), whereas individual PAHs or general PAH trends were described but not numerically represented (Carr et al., 1996; HARC and Galveston Bay Foundation, 2017a; Kennicutt II, 2017a; E. M. Oziolor et al., 2014b; University of Houston-Clear Lake and the University of Houston Houston, 2003; Zhang et al., 2003). Shorthand abbreviations for PAHs used throughout this manuscript appear in Table A 2.

Data on PCBs also were reported; however, peer-reviewed articles commonly reported the sum of all 209 PCB congeners (Howell et al., 2011a; Lakshmanan et al., 2010), 18 PCBs (Lakshmanan et al., 2010; Santschi et al., 2001), and 43 PCBs (Lakshmanan et al., 2010), or included the general discussion of the presence of PCBs (Carr et al., 1996; HARC and Galveston Bay Foundation, 2017b; Kennicutt II, 2017a; E.

M. Oziolor et al., 2014b; Texas Commission on Environmental Quality, 1994). Only one study included data on several individual PCBs (Aguilar et al., 2014).

The only pesticide found to be quantitatively reported in the peer-reviewed literature was DDT (Texas Commission on Environmental Quality, 1994) or the sum of DDTs (Santschi et al., 2001). Four peer-reviewed articles included information about completed analyses or qualitative descriptions of detecting the following pesticides: aldrin, dieldrin, endrin, mirex, chlordanes, BHCs, DDTs, or lindane) (Carr et al., 1996; HARC and Galveston Bay Foundation, 2017b; Kennicutt II, 2017a).

As Dx/F were the most common organics, most peer-reviewed articles contained data for 18 individual Dx/F (Dean et al., 2009; Louchouarn et al., 2018; Suarez et al., 2005; Suarez, Rifai, Palachek, et al., 2006) or the sum of all 18 individual Dx/F, which is also denoted as PCDD/F (Hieke et al., 2016; Yeager et al., 2007, 2010). Only one article included qualitative descriptions of Dx/F trends within GB/HSC (Rhitu, 2007), which also referenced Yeager et al.'s (2007) findings. For articles containing data on Dx/F in GB/HSC, the outcomes were often related to sediment quality, bioaccumulation, fate, transport, and trends within a given time period. Sediment quality outcomes were common for both metals and organics data, but ecological monitoring was often included for metals data discussion. Additional summary statistics for the peer-reviewed articles and reports are summarized in Tables A 4 and A 5.

In contrast to the peer-reviewed articles and reports, the two national and regional agencies, NOAA and TCEQ, reported between 89 to 280 individual chemicals. For some chemical classes additional totals were included. For example, some PCB

congeners were grouped together (e.g., PCB 13/12, PCB 59/62/79, PCB 61/70/74/75) versus a summative total of all 209 congeners. To understand the diversity of the individuals detected and their corresponding concentration ranges, the summary statistics for both NOAA and TCEQ are summarized in Tables A 6-12.

The search of published dissertations/theses showed that research on chemical contamination of both metals and organics exists in undergraduate (Leonard, 2018), master's (F. R. Davis, 2018; Dobberstine, 2007; Seward, 2010), and doctoral research (Almukaimi, 2016; Gardinali, 1996; E. Oziolor, 2017; Wei, 2016; Yuill, 1991). Of these dissertations/theses, four contained data on metals (Almukaimi, 2016; Leonard, 2018; Wei, 2016; Yuill, 1991), five contained data on organics (F. R. Davis, 2018; Gardinali, 1996; Leonard, 2018; E. Oziolor, 2017; Seward, 2010), and one contained research on both select metals and organics (Dobberstine, 2007).

Of the nine dissertations/theses included, one had an embargo; therefore, only this document's title/abstract were only considered for inclusion (E. Oziolor, 2017). Another dissertation/thesis was excluded based on the full-text screening, as the sampling years occurred before 1990 (Yuill, 1991), although, this study did provide an interesting historical timeline for significant events within GB/HSC (e.g., 1900 hurricane, formation of petroleum companies in the HSC, dredging).

Two of the remaining eight included dissertations/theses contained data from publications already considered within this project (Almukaimi, 2016; Seward, 2010). For example, in Seward (2010), the data included in this thesis had been previously published by Yeager et al. (2007). Thus, the data included within these

dissertations/theses were not re-extracted. For the other dissertations/theses included in this study, data containing totals or individual chemical data for Dx/F and Hg were extracted. As two dissertations/theses did not provide Dx/F or g data, their summary statistics were reported in Tables A 13-15 (Dobberstine, 2007; Gardinali, 1996).

To capture reporting trends for both metals and organics reporting trends, the heatmap in Figure 2-3 compares sampling years and publication years based on whether metals, organics, or both were sampled. Two hurricanes, Hurricane Ike and Hurricane Harvey, mark two significant environmental events within Galveston Bay. Therefore, samples collected before either event are useful to consider for potential chemical spatial and temporal trends. In many instances data came from samples collected 2-5 years before the article was published (Figure 2-3). For instance, Agular et al.'s (2014) sample collection occurred in 2010, while their results were published in 2014. In contrast to this collection versus publication difference, Yeager et al. (2007) collected samples in 2006 and 2007, with multiple publications utilize these same samples (Louchouran et al. 2018 and Heike et al. 2016). Conversely, some dissertation/theses also confirmed the peer-reviewed data they had published or utilized (Almukaimi, 2016; Seward, 2010), while other dissertation/theses contained data from the same databases identified in this project (F. R. Davis, 2018; Wei, 2016).

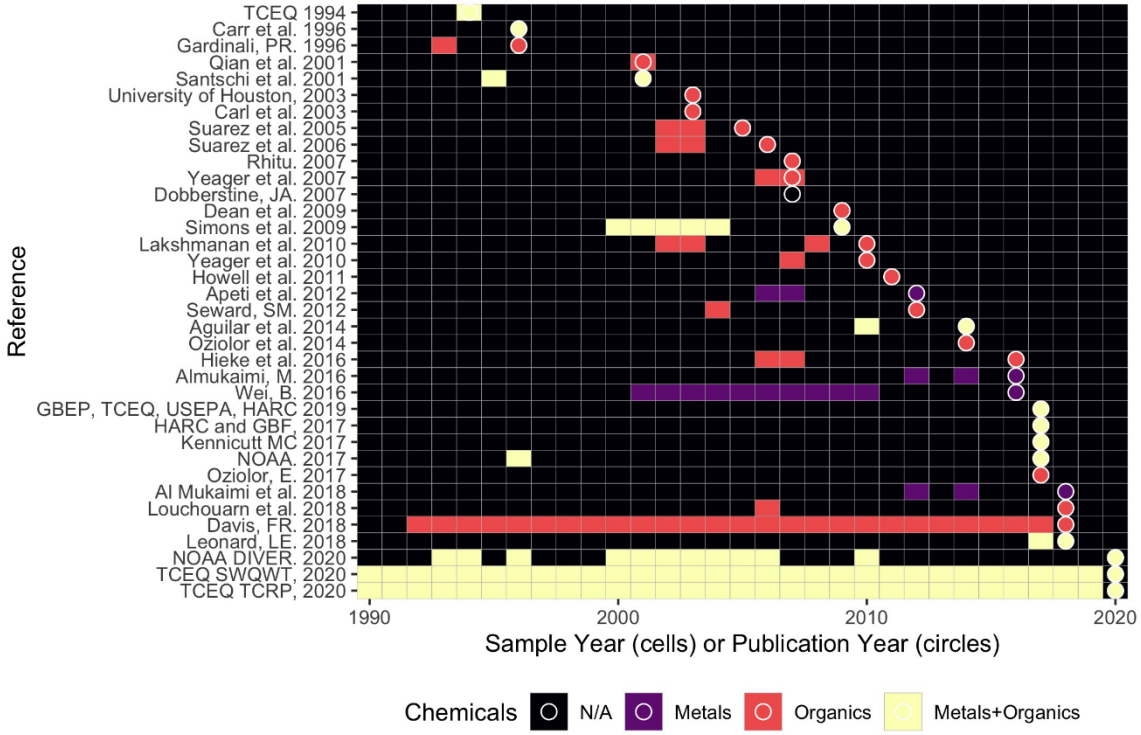

Figure 2-3 Heatmap illustrates the sparsity of reported sampling times in comparison to the publication year. The colored boxes and the colored circles signify whether metals (purple), organics (red), both metals and organics (yellow) or no chemicals were reported (black). All references shown in this figure are from the database and grey literature search with most of the publication originating from peer-reviewed journals.

The results discussed in this section indicate that, although there are historical sediment sample data are available, the timeframes in which they were collected are inconsistent and data on metals and organics is sparse. However, there appears to be more GB/HSC organics data available through NOAA and TCEQ, while there is limited organics data contained in peer-reviewed articles. A similar trend is observed for the

metals data. Considering the sample general locations (Figure 2-2) and the heatmap (Figure 2-3) together indicates that data for any individual chemical or chemical class are sparse both spatially and temporally.

2.4.2. **Trends for Chemical Concentrations**

Chemical data differed between the peer-reviewed articles and the NOAA and TCEQ databases. The former more often contained data on either Hg or Dx/F. For concentration specific analysis, these two chemicals were investigated for their variability across time and within the HSC, Upper GB, and Lower GB regions (Figure 2-4). Hg levels reported in the Upper GB varied compared to Hg levels in Lower GB. However, a nested one-way ANOVA indicates that no true variability in Hg levels exists between time groups ($p=0.63$), although it did reveal variability between each regional group ($p<0.0001$; Chi-square, df: 104.6,1). To confirm this test, sampling time was ignored, and the Hg data was grouped based on the region (HSC n=260; Upper GB n=334; Lower GB n=161); a one-way ANOVA verified the nested one-way ANOVA regional variability ($p<0.0001$; $R^2=0.1474$).

Of the articles containing Hg data, four were peer-reviewed (Al Mukaimi, Kaiser, et al., 2018; Apeti et al., 2012; Santschi et al., 2001; Simons & Smith, 2009) the rest of the Hg data came from NOAA and TCEQ. For Hg, the most common sampling year in the peer-reviewed literature for Hg was in 2012, but data from NOAA and TCEQ spanned several years (NOAA: 1993-96; 2000-06; 2010 and TCEQ: 1990-2019). Patrick Bayou, a known point source for Hg in the HSC, had been sampled both by researchers from the peer-reviewed literature (Al Mukaimia et al. 2018) and TCEQ, but not NOAA.

This particular site is located in an industrialized section of the HSC and is also a Superfund site, which is a hazardous waste site listed under the Comprehensive Environmental Response, Compensation and Liability Act (CERCLA).

a b

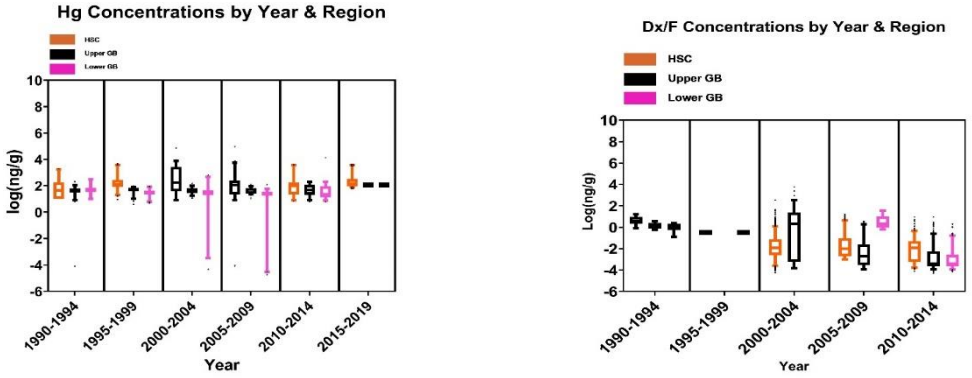

Figure 2-4 Boxplots contrast sampling year versus the concentration of Hg (a) and Dx/F (b) from all data extracted from peer-reviewed literature, grey literature, and databases. Sampling year groups were further grouped by general region (HSC, Upper GB, Lower GB) where results were analyzed by t-test or ANOVA.

In comparison to the Hg reported within GB/HSC, the Dx/F appeared to vary in distribution throughout the region and across time (Figure 2-4b). However, a nested one-way ANOVA indicated variability between each time group (p=0.0348; F, Dfn, Dfd =

4.445, 4, 8) and each regional group ($p<0.0001$; Chi-square, df: 346.5, 1). To confirm the regional variability, sampling time was ignored and the Dx/F data were grouped based on region (HSC n=4,606; Upper GB n=873; Lower GB n=1784). A one-way ANOVA verified the nested-one-way ANOVA regional variability ($p<0.0001$; $R^2=0.03459$) indicating trends over time.

In contrast to the Hg data, most of the Dx/F data originated from TCEQ, with nine peer-reviewed articles (Aguilar et al. 2014, Hieke et al. 2016, Lakshmanan et al. 2010, Louchourarn et al 2018, Santschi et al. 2001, Simons and Smith 2009, Suarez et al 2006, Yeager et al 2010, Yeager et al. 2007) containing data from 1995, 2000-2003, 2005-2006, and 2010. NOAA only contained data from 2006 and Gardinali (1996) contained data from 1993. Give the San Jacinto Waste Pits (SJWP) are a known point-source of dioxins, most of the peer-reviewed articles research this site. In contrast the two monitoring programs assessed the general GB/HSC region.

Because the HSC and the Upper GB were the regions for which data most commonly appeared in both peer-reviewed literature and monitoring programs databases, additional temporal comparisons were made within these two regions for both Hg and Dx/F. The Hg data were divided based on the following two timeframes to assess for variability between two distinct time periods: 2005-2009 HSC and 2010-2014 HSC. A two-tailed t-test indicated these time groups did not differed ($p=0.23$), which implies that from 2005-2014 most Hg concentrations detected in both regions may have remained the same across time. The same temporal grouping was applied for Hg in Upper GB, but neither group differed ($p=0.8693$). The Dx/F data was also divided into

the same temporal and regional groups. The HSC and Upper GB regional grouping means differed ((HSC: $p<0.0001$; $t=5.989$, $df=1121$); (Upper GB: $p<0.0001$; $t=4.839$, $df=649$), implying that the Dx/F concentrations from 2005 to 2014 were not consistent. In this case, Dx/F appeared to be in a state of flux, with the concentrations varying between regions and across time.

Both Hg and Dx/F remained the most prevalent chemicals studied, despite diverse chemicals analyzed through monitoring programs and peer-reviewed articles. Santschi et al. (2001) and Simons and Smith (2009) reported on both PAH totals, and varying PCBs (e.g., 209 PCBs, 43 PCBs, 18 PCBs, or certain individual PCBs) being reported by Aguilar Lakshmanan et al. (2010), Santschi et al. (2001), and Simmons and Smith (2009). Only Santschi et al. (2001) reported on total DDTs, and both NOAA and TCEQ reported additional pesticides (Table A 3).

Additional descriptive statistics for metals and organics contained in peer-reviewed articles appear in Tables A 4 and 5. The NOAA and TCEQ data for individual metals appear in Tables A 6 and 7, and data for individual PAHs, pesticides, Dx/F, and PCBs are reported in Tables A 8-12.

Minimum and maximum values as well as the interquartile ranges (IQRs) were both compared with NOAA's SQuiRT chart ERL and ERM values for sediment quality guideline (SQG) references (National Oceanic & Atmospheric Administration, 2008). Overall trends for the GB/HSC region are difficult to discern for both metals and organics, despite diverse chemical profiles and multiple sampling years.

2.5. Discussion

2.5.1. Major Findings & Knowledge Gaps

As SEMs expand more into environmental sciences and environmental health, they will continue to provide unique insights to broad research questions. A few relevant research questions may consider the following topic areas: role of monitoring programs for chemical exposures, the likelihood of using an intervention to mitigate a particular exposure or address additional exposures relevant for disaster response research (DR2). By identifying relevant knowledge clusters, both historical data can be referenced and knowledge gaps can be identified for investment into additional research (Aiassa et al., 2015; Bilotta et al., 2014; James et al., 2016; Miake-Lye et al., 2016; Munn, Peters, et al., 2018; Munn, Stern, et al., 2018b; Saran & White, 2018; Wolffe et al., 2020). Therefore, SEMs can facilitate answers to research questions by addressing the fate, transport, biotransformation, and exposure of chemicals so a clean-up or reference value could be established.

Estuaries are only one common environment across the globe; thus, the CoCoPop methodology presented in this project can be applied to other environments, other pollution related questions, and DR2 questions. Two studies in which SEMs have been applied regard the polar environment (Mangano et al., 2017) and freshwater systems with microplastics (Yao et al., 2020). These two studies illustrate the utility of SEMs in uncovering relevant knowledge gaps while also improving reporting methods for environmental research. However, the current project showed that some regions, although historically contaminated, may lack consistent sampling data. With sparse

environmental background data, disaster research considering before/after effects or exposures within a given environment will be limited. One area that could therefore be affected is fate/transport modeling and pathway analysis. Consequently, the findings in this study establish baseline references as well as identify relevant historical articles on environmental conditions in GB/HSC.

The results of this systematic evidence mapping show that available legacy contaminant data in the GB/HSC region are limited in terms of spatial, temporal, and chemical coverage, particularly within peer-reviewed articles. Even after dividing the data into three broad geographical regions (HSC, Upper GB, Lower GB) and 5-year intervals, there was no chemical class consistently sampled; however, when the monitoring databases were considered, additional data on metals and organics were recorded for future reference. To help illustrate individual distributions of individual chemicals, Tables A 4-12 include both data from peer-reviewed articles and monitoring data from NOAA and TCEQ. The most common chemicals recorded are Dx/Fs and Hg; however, this observation was common for peer-reviewed articles. In contrast to the peer-reviewed articles, both NOAA and TCEQ regularly reported both organic and metals data in certain timeframes (e.g., early 2000s, late-2000s, or early 2010s).

Thus, there is a knowledge gap for reported legacy contaminants in GB and HSC and therefore limited knowledge regarding concentration distributions in this region. Although monitoring databases were not considered in the original search strategy, the data reported by NOAA and TCEQ provided temporal and spatial data comparable to data from the peer-reviewed articles. Thus, the data presented here only provides an

overview of regions within GB/HSC that may be of interest for additional studies. Our results also identify that inconsistent reporting methods of chemical data within GB/HSC remains a knowledge gap in the region.

Since environmental chemistry is an exhaustive process, both for sample collection and sample analysis are resource intensive. For example, Dx/F analysis roughly costs $525 per sample (Personal communication). As a result, the peer-reviewed articles considered in this SEM may have had finite resources, which limited the number of chemical analyses conducted. In contrast to the peer-reviewed articles, both NOAA and TCEQ considered extensive chemical lists. Perhaps due to differing resources and a specific interest in monitoring, both agencies were able to consider additional chemical analyses compared to academic researchers.

With baseline data often of interest for pre-/post- comparisons, datasets containing comprehensive physio-chemical values before a natural disaster or seasonal flood are highlight sought after. A recent example that sought to develop such a dataset occurred in Sydney, Australia's estuarine system (Birch & Lee, 2018). As there was already an interest in developing baseline data for Sydney, resources were readily available for the level of monitoring data required. However, in many environmental studies, researchers may face difficulties regarding site access, sampling trip costs, shifting environmental conditions, or even emerging contaminants. The limited analyses for the peer-reviewed articles also posed a problem for establishing any relevant baseline or reference database in this study. Similarly, if researchers focus on individual chemicals rather than how they interact as environmental mixtures or in combination

with other chemicals, a limited understanding remains for exposure risk. Therefore, with estuaries serving as the final sink for many anthropogenic inputs, there remains a need to characterize chemicals and their metabolites from a systems biology standpoint (e.g., adverse outcome pathways) (Cuevas et al., 2018) as well as from a mixtures standpoint.

2.5.2. **Implications for Research, Management, Policy, and Practice**

For biomedical sciences, guidelines on systematic reviews and evidence mapping have been developed over many decades (Cochrane Library, 2020; PRISMA, 2015). These guidelines encourage authors to provide as much information as possible related to the methods, materials and study design of the items reviewed. In contrast, no such protocols existed until the mid-2010s for environmental management and environmental sciences (Neal R. Haddaway et al., 2018; Neal Robert Haddaway & Macura, 2018; Macura et al., 2019). Through continued efforts by organizations such as the Collaboration for Environmental Evidence (CEE), use of systematic reviews and systematic maps as tools in environmental research continues.

The current systematic evidence map demonstrates the need to use more uniform environmental parameter reporting for sediments and other environmental media. Although chemical concentration data and geocoordinates are sometimes reported, these values were not consistently reported and there were data gaps for chemical classes. This inconsistent reporting and inadequate use of topic labels within environmental health sciences is a common problem (Behnke et al., 2020; Bernes et al., 2017; Mangano et al., 2017; Nevalainen et al., 2021; Randall et al., 2015; Yao et al., 2020). Therefore, in future environmental publications, specific key terms should be used in titles and abstracts to

promote database searchability. Use of CEE guidance documents for environmental science research will also continue to improve reporting methodology. Another tool that could improve SEMs are "knowledge graphs," which are interactive visual summaries of available research (Wolffe et al., 2020). These graphs in turn could improve reporting methods, the recording of data, and the visibility of SEMs for future research questions related to policy, management, and research practices.

2.5.3. **Limitations of the Search & Search Strengths**

Like any search strategy, ours may have missed some studies with relevant information. When developing the scope of this study, we found general terms such as "Gulf of Mexico" to be too broad, but if we specifically searched for "Houston Ship Channel," there were few studies. To ensure that we were broad yet specific enough, we search terms such as "Texas," "Galveston," "Gulf Coast," and "United States" to name a few. However, even with these search terms, we may have missed articles that did not contain any of these terms in their titles, abstracts, or lists of key words.

How authors described or listed the legacy contaminants in their titles and abstracts also limited our search. In most cases, the general classes of dioxin/furans and pesticides as well as acronyms of PAHs and PCBs were enough to identify articles. Yet, some articles may have listed the legacy contaminant differently or not at all within their titles, abstracts, or key words; this situation appeared to occur with earlier publications before 2006. In this instance, this difference in article searchability could potentially be attributed to shifting character counts for the title page and abstracts. If authors were to

used common terminology and specify regional and specific locations in their keywords, more studies and reports could be readily identified for future reference.

Another limitation in this SEM was the level of detail provided by included articles. For instance, articles often contained limited geospatial information related to their samples and only a few included relevant general regional descriptors (Aguilar et al., 2014; Apeti et al., 2012; Hieke et al., 2016; Louchouarn et al., 2018; Yeager et al., 2007). However, the monitoring programs data reported by NOAA and TCEQ included specific geocoordinates and relevant GB/HSC regional descriptors. As DR2 is likely to require spatial analysis for assessment of both pre- and post-disaster conditions, current researchers should consider how they report their sample geocoordinates. Although when environmental samples are taken near private lands or near commercial agricultural areas, general descriptors of the sampling area will be a useful substitute. This alternative geographical description would consequently protect any private property that may be implicated by a study's research findings. Overall, if one understands chemical distribution in urbanized estuaries aside from GB/HSC, then the effects of local natural disasters within these ecosystems could be studied further.

Another limitation of this study was the update made for the Carrot2.org search engine prior to this systematic evidence map report. When the search terms used for both Google and Carrot2.org were put into the newest Carrot2.org version, the search strings used yielded fewer hits than the search recorded in this study. Should this SEM be redone, a specific online search within the grey literature will be developed to identify relevant theses, reports, white papers, and other grey literature. However, this review

detailed and documented internet searches (Evidence, 2019), with all grey literature having a full text document retrieved. As additional SEM and systematic review tools become available (Kohl et al., 2018), this SEM could be updated in the future.

2.6. Conclusions

This systematic evidence map (SEM) presented a survey of available legacy contaminant data for Galveston Bay (GB) and the Houston Ship Channel (HSC) sediments. We identified relevant grey literature in addition to peer-reviewed articles from databases, as the former may have contained additional historical data. We categorized the data by location and time, as well as by types of contaminants and sample matrices, and aimed to identify relevant trends if present. The extracted data contained few trends to note, largely because of the inconsistent sample collection timeframes and lack of sample location diversity. Most of the literature reported on dioxins/furans (Dx/F) and mercury (Hg), but few data consistently recorded other organics and metals. This gap can be addressed by using the NOAA and TCEQ data, but specific chemicals may need to be examined separated to discern any trends.

Additionally, several peer-reviewed articles did not consistently record chemical data which resulted in data sparsity for certain regions of GB/HSC. In turn, this data sparsity makes it difficult to understand how environmental events, such as Hurricane Ike and Harvey, or activities such as dredging may have historically affected contaminant distribution in GB/HSC. Some of these data gaps may be addressed through monitoring data provided by regional and national agencies such as NOAA and TCEQ. Future researchers studying the GB/HSC should continue addressing the following

knowledge gaps: frequency of contaminant reporting, spatial data collection, and sample sizes.

Additionally, future SEMs and systematic reviews of environmental contaminants would benefit from more consistent use of key words with titles and abstracts. More uniform reporting of geolocations and chemical data would also be beneficial. This project also helps establish initial efforts to characterize and understand available historical data regarding estuaries, which are one of many environments that SEMs could be applied to. Therefore, this project shows not only where reporting methods can improve, but also how other researchers could use similar approaches as presented here to expand the global understanding of chemical contamination in marine and freshwater environments. With support from the scientific community, improving reporting methods can also expand the application of systematic review and systematic mapping protocols for environmental science and DR2.

3. POLYCYCLIC AROMATIC HYDROCARBON STATUS IN POST-HURRICANE HARVEY SEDIMENTS: CONSIDERATIONS FOR ENVIRONMENTAL SAMPLING IN THE GALVESTON BAY/HOUSTON SHIP CHANNEL REGION[1]

3.1. Overview

Hurricane Harvey led to a broad redistribution of sediment throughout Galveston Bay and the Houston Ship Channel (GB/HSC), but the resulting changes in chemical contaminant distributions have yet to be characterized. To address this question, we collected and analyzed post-Harvey sediment for concentrations of the EPA 16 Priority Pollutant polycyclic aromatic hydrocarbon (PAHs), determining the extent to which the spatial distribution and sourcing of contaminants may have changed in contrast to historical surface sediment data (<5cm) from the National Oceanic Atmospheric Administration (NOAA) available for the years 1996-2011. We found a small, but detectable increase from pre- to post-Harvey in PAH concentrations, with PAH diagnostic sourcing indicating combustion origins. Of the detected PAHs, none exceeded Sediment Quality Guideline values. Overall, we have added to the understanding of PAH spatial trends within the GB/HSC region, and developed a reference PAH baseline to inform future studies.

---

[1] Reprinted with permission from "Polycyclic Aromatic Hydrocarbon Status in Post-Hurricane Harvey Sediments: Considerations for Environmental Sampling in the Galveston Bay/Houston Ship Channel Region" by Camargo, K; Sericano, JL; Bhandari, S; Hoelscher C; McDonald, TJ; Chiu, WA; Wade, TL; Dellapenna, TM; Liu, Y; and Knap, AH. 2020. *Marine Pollution Bulletin*, 162, 111872, Copyright 2020 by Elsevier Ltd.

3.2. Introduction

Hurricane Harvey stalled over Houston, TX in August 2017, where concerns grew about the spread of legacy contaminants within in the Galveston Bay (GB) and the Houston Ship Channel (HSC) region Materials & Methods (Al Mukaimi, Kaiser, et al., 2018; Hieke et al., 2016; Howell et al., 2011c; Jackson et al., 1998; Kennicutt II, 2017a; Qian et al., 2001; Santschi et al., 2001; Yeager et al., 2007). The two main freshwater rivers that discharge into GB are the San Jacinto River and Trinity Rivers, with the Bolivar Roads as both the primary tidal inlet as well as serving the entry way for the HSC that extends 80 km into the city of Houston with a maintained depth of 14 m (National Oceanic & Atmospheric Administration Estuarine Programs Office, 1988; US Army Corps of Engineers, 2017). Economically, the HSC is a part of the Port of Houston, which sees over 200 million tons of cargo each year via 9,000 vessels and 200,000 barges and ship channel work provides around 1.2 million jobs (US Army Corps of Engineers, 2017). The Port of Houston serves a mixture of industries as well as domestic and international businesses (US Army Corps of Engineers, 2017).

The Galveston Bay Foundation's and HARC's 2017 and 2018 Galveston Bay Report cards grade the overall pollution events and sources as a "C", or in other words "Adequate for Now" (HARC and Galveston Bay Foundation, 2017b, 2018). Consequently, after strong winds and flooding from Hurricane Harvey, concerns emerged as to contaminant mobilization and consequent redistribution of present contaminants due to documented land subsidence (Al Mukaimi et al., 2018a; Du et al., 2019b, 2020). However, the quantitative impact of Harvey on the distribution of

contaminants has not yet been established. Although recognizing there are diverse classes of organic contaminants and heavy metals known to be present in GB/HSC, we selected PAHs for detailed investigation due to their ubiquitous presence in the environment, their historical detection in local oysters, and previously collected sediments (Al Mukaimi et al., 2018b; Jackson et al., 1998; Qian et al., 2001) and their listing in the Appendix A of 40 CRF Part 423 (Appendix A to 40 CFR, Part 423–126 Priority Pollutants, 2014). Of the EPA 16 Priority Pollutant PAHs, high molecular weight (HMW) PAHs have ring structures >3 rings, and several of these (e.g. benz[a]anthracene, benzo[a]pyrene, dibenz[a,h]anthracene, and benzo[k]fluoranthene) are considered "reasonably anticipated to be a human carcinogen" (National Toxicology Program, 2011). Our study objectives were to characterize concentrations of the EPA 16 Priority Pollutant PAHs present in post-Harvey sediments and determine whether there was a new baseline, in contrast to historically available PAH concentration data. We also aimed to determine the extent to which PAHs were spatially distributed and the consequent relative sourcing of the PAHs given both the historically available PAH concentration data and post-Harvey data.

3.3. Materials & Methods

3.3.1. Data Collection and Core Processing

A total of 32 sediment vibracores and pushcores (Figure 3-1) were collected on three cruises (October 2017, December 2017, January 2018). Vibracores were collected using an Oztec vibracoring head attached to a 7.6 cm diameter aluminum barrel, with core recovery ranging from 1-4 m. Push cores were collected using a repurposed Benthos®

checkvalve pushcoring head, which was attached to an aluminum conduit with stainless steel hose-clamps and electrical tape. The conduit was in 1.5 m long sections that screwed together, with a maximum length of 5m. The removable core barrels consist of 7.6 cm diameter polycarbonate tubes generally ranging in length from 0.3-0.6 m. During recovery, the pushcoring system was brought to the surface and the core barrels were capped while the end of the core was still in the water to prevent the loss of the cores from the check valve. While holding the core vertically, the bottom core cap was immediately sealed with electrical tape while still being kept vertical.

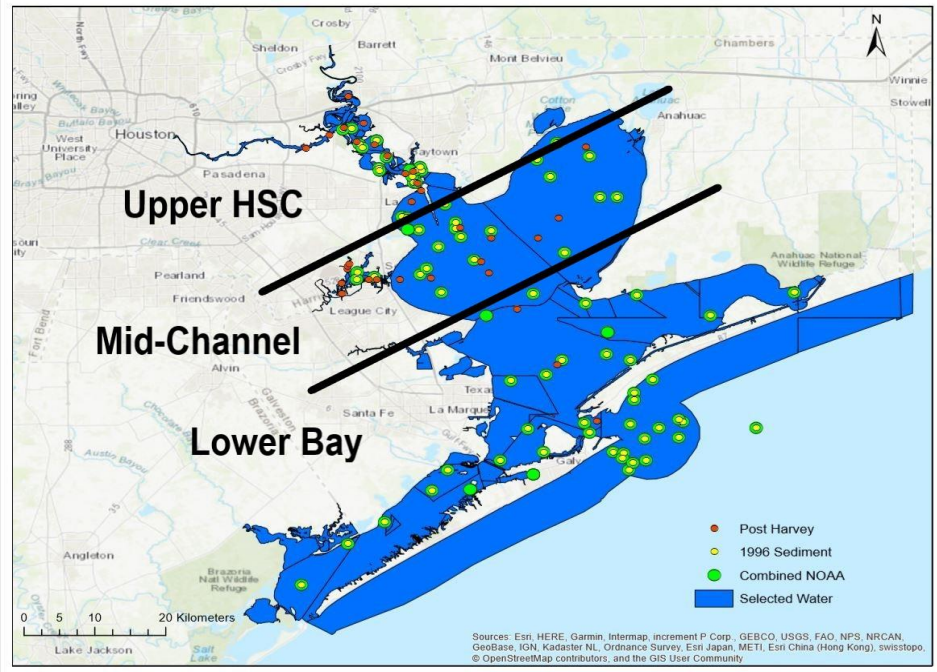

Figure 3-1 Base map of all sample sites for sediment data from 1996-2011 (NOAA) and 2017 (post-Harvey). The 1996 data comprised of 72 sample sites, the 1997-2011 data comprised of 6 monitoring sites, and the post-Harvey data comprised of 32 sampling sites.

Flourofoam was pushed into the core top so that it rested just above the sediment-water interface, the flourofoam was cut flush with the top of the core barrel and then the top of the core was sealed with a core cap and electrical tape and stored vertically for transport back to the lab. Box cores were collected using a GOMEX style boxcorer. For each box core, a 15.24 cm diameter sub-core as collected and sub-sectioned into 1 cm thick slices using an extruder. In addition, a 7.6 cm diameter polycarbonate sub-core was collected for x-radiography. All cores were stored in a cold room which is held at a constant temperature of 4°C.

Subsequent surface samples (< 5cm depth) were collected in 8oz combusted glass jars with Teflon cap liners and were subsequently stored at -20°C until further processing and analysis. As sample collection occurred after Hurricane Harvey, these sites were selected in the same regional areas as sample collected in prior sediment sampling programs (Al Mukaimi et al., 2018a & b).

In addition to the sediment collected in 2017, organic data in sediment from the National Oceanic & Atmospheric Administration (NOAA) and the National Centers for Coastal Ocean Science (NCCOS) were downloaded in their original text file format and then converted to an Excel spreadsheet. The NOAA data platform Data Integration Visualization Exploration and Reporting (DIVER) Explorer: Southeast (National Oceanic & Atmospheric Administration, 2020a) provided sediment data from 1997-2011, while the NCCOS's National Status and Trends More Data website supplied 1996

sediment data from Galveston Bay (National Oceanic & Atmospheric Administration (National Oceanic & Atmospheric Administration, 2017).

3.3.2. **Sampling Preparation and Analysis**

Surface sediment samples were stored at -20°C until further processing and analysis. NOAA National Status and Trends (NS&T) Methods were followed for trace organic analysis in sediments. All sediments were freeze-dried and solvent extracted with methylene chlorine using a Dionex 200 Automated Solvent Extractor (ASE). Prior to the solvent extraction, deuterated polycyclic aromatic hydrocarbons were added for quantification (d8-naphthalene, d10-acenaphthene, d10-phenanthrene, d12-chrysene, and d12-perylene, Absolute Std 98 + % pure). For QA/QC, duplicate samples, matrix spike samples, and a standard reference material (NIST SRM 1944) were run and analyzed with the sample sets. An average method detection limit (MDL) was 0.38 ng·g-1 d.w for 20 g of sediment with a range from 0.14-0.84 ng·g-1 d.w. Analytes detected below the MDL were included as a part of the total PAH concentrations.

PAHs were isolated from other organics via silica-alumina column chromatography (silica: Aldrich Grade 923 100-200 mesh; alumina: Aldrich, basic, Brockman I 150 mesh). Sulfur present in the sediments was removed with activated copper (Baker 20 to 30 mesh) that was added to the top of each silica-alumina column and a 1:1 mixture of pentane and methylene chloride (200 ml, Burdick and Jackson GC2 grade) was used for column elution. For the quantification of 18 parent and their corresponding alkyl homolog PAHs containing from 1 to 4 carbons substituted for hydrogen (C1-4 Naphthalenes; C1-3 Fluorenes; C1-4 Phenanthrenes/Anthracenes; C1-3

Dibenzothiophenes; C1-3 Fluoranthenes/Pyrenes; and C1-4 Chrysenes), gas chromatography and mass spectrometry detection was used (Agilent Technologies model 5890N-MSD) in selected ion mode (SIM). Standard solutions were injected at five different concentrations to calibrate the GC/MS where deuterated aromatic compounds served as internal standards (d10-Fluorene and d12-Benzo(a)pyrene). Injections were made in splitless mode and the fused silica capillary column used was 30 m x 0.25 mm i.d., DB-5MS (0.25 μm film) with the oven temperature heating at a rate of 12°min-1 from 60°C to 300°C. Concentrations reported are in ng/g on a dry weight basis (ng·g-1 d.w.) where analytes were identified based on confirmation ions and the retention time of the PAH quantification ion compared to certified standards. The 16 PAHs listed as priority pollutants (Appendix A of 40 CFR, Part 423-126) as well as low molecular weight (LMW) PAHs consisting of 2-3 ring PAHs, high molecular weight (HMW) PAHs consisting of 4-5 ring PAHs, and total PAHs consisting of all 16 Parent Priority Pollutant PAHs are reported in ng·g-1 d.w. Statistical Analysis

3.3.3. **Statistical Analysis**

All data collected were log-normalized as raw data concentrations were highly variable for each dataset. Data analysis was carried out using GraphPad Prism version 8.4.1. Historical data collected for years include 1996, 1997, 2007, 2010, and 2011 compared to the 2017 data we collected, and analyzed using one-way ANOVA followed by a trend test. Based on the ANOVA results, and because the comparisons of interest are pre- versus post-Harvey an unpaired t-test was conducted for the years 1996-2011 vs 2017 for 2-3 Ring PAHs, 4-5 Ring PAHs, and 6-Ring PAHs.

Galveston Bay can also be divided into several large sub-bay regions that include East Bay, West Bay, Upper GB, Lower GB, Trinity Bay and additional small sub-bays (Moffatt & Nichol, 2010) each varying in depth with a maximum of around 4 m (National Oceanic & Atmospheric Administration Estuarine Programs Office, 1988).

The following general location regions were used for the double-plot ratios in PAH relative sourcing: Upper HSC (comprised of samples taken above Morgan's Point), Mid-Ship Channel (samples within Clear Lake, Trinity Bay and Below Morgan's Point), and Lower Bay (samples below Smith's Point to Galveston Island). To understand the general sourcing for PAH inputs to GB/HSC, the following double-plot ratios were used: Fl/(Fl+ PY) vs. BaA/(BaA + CHR) and Fl/(Fl + PY) vs An/(An + PHE). To further distinguish between pyrogenic sources the following alkylated PAH homologs were totaled and compared to their respective parent compounds: C1-4 Naphthalenes; C1-3 Fluorenes; C1-4 Phenanthrenes/Anthracenes; C1-3 Fluoranthenes/Pyrenes; and C1-4 Chrysenes (Table 3-1).

Two additional ratios, one called a 'pyrogenic index' and the other called 'perylene index' were calculated. The first ratio, 'pyrogenic index,' is used to help differentiate between petrogenic and pyrogenic PAHs and is calculated by dividing the sum of the EPA parent PAHs with three to six rings by the sum of the alkylated series listed in the previous paragraph (Wang et al., 2014). The 'perylene index' on the other hand, has been used to distinguish whether detected perylene is either from biogenic and pyrogenic origins; it is calculated by dividing a sample's perylene concentration by a the sum of the five-ring PAH parent compounds (Wang et al., 2014).

	Sample ID	Total US EPA PAHs	Total Alkylated PAHs	Pyrogenic Index	Pyrogenic PAHs (ratios >0.05) or Petroleum PAHs (ratios <0.05)	Perylene Index (%)	Biogenic origins (>10%) or pyrogenic origins (<10%)
Lower GB	HARV 7A	87.9	62.8	1.9	pyrogenic PAHs	49	Biogenic origins
Lower GB	GB1	96.4	88.0	1.7	pyrogenic PAHs	62	Biogenic origins
Lower GB	C09	106.8	117.7	1.6	pyrogenic PAHs	66	Biogenic origins
Lower GB	HARV11	134.8	70.7	2.3	pyrogenic PAHs	20	Biogenic origins
Lower GB	GB2	75.6	62.5	1.7	pyrogenic PAHs	53	Biogenic origins
Lower GB	GB3	165.8	184.4	1.3	pyrogenic PAHs	56	Biogenic origins
Lower GB	GB4	189.3	174.0	1.5	pyrogenic PAHs	48	Biogenic origins
Lower GB	HARV05	157.6	128.5	1.6	pyrogenic PAHs	40	Biogenic origins
Mid-Channel	HARV 1	258.4	217.6	1.7	pyrogenic PAHs	49	Biogenic origins
Mid-Channel	HARV 17	457.7	334.9	1.7	pyrogenic PAHs	32	Biogenic origins
Mid-Channel	Harv 14	376.0	132.9	3.7	pyrogenic PAHs	35	Biogenic origins
Mid-Channel	C18	87.9	74.7	1.6	pyrogenic PAHs	42	Biogenic origins
Mid-Channel	C10	42.0	61.8	1.3	pyrogenic PAHs	73	Biogenic origins
Mid-Channel	GB5	124.5	126.1	1.3	pyrogenic PAHs	46	Biogenic origins
Mid-Channel	HARV10	244.0	175.2	1.7	pyrogenic PAHs	28	Biogenic origins
Mid-Channel	Harv15	3195.3	571.2	6.4	pyrogenic PAHs	12	Biogenic origins
Mid-Channel	ML1	785.4	263.7	4.1	pyrogenic PAHs	37	Biogenic origins
Mid-Channel	ML-2	702.7	226.0	3.7	pyrogenic PAHs	21	Biogenic origins
Mid-Channel	ML3	666.5	236.4	3.8	pyrogenic PAHs	37	Biogenic origins
Upper GB	BC-6	198.1	199.9	1.5	pyrogenic PAHs	63	Biogenic origins
Upper GB	BC-7	303.9	290.4	1.4	pyrogenic PAHs	52	Biogenic origins
Upper GB	BC-8	373.7	404.6	1.4	pyrogenic PAHs	56	Biogenic origins
Upper GB	BC-9	38.1	52.7	2.1	pyrogenic PAHs	88	Biogenic origins
Upper GB	BC-10	1396.7	705.1	2.4	pyrogenic PAHs	49	Biogenic origins
Upper GB	BC-11	593.4	578.3	1.4	pyrogenic PAHs	51	Biogenic origins

Table 3-1 Summary table comparing the total US EPA Priority 16 PAH concentrations, the total alkylated PAH concentrations, and two calculated indices: pyrogenic index and perylene index. Both indices are used to help further differentiate petrogenic and pyrogenic sourcing as illustrated by the double ratio plots in Figure 4. All samples listed in this table are post-Harvey sediments.

Table 3-1 Continued

	Sample ID	Total US EPA PAHs	Total Alkylated PAHs	Pyrogenic Index	Pyrogenic PAHs (ratios >0.05) or Petroleum PAHs (ratios <0.05)	Perylene Index (%)	Biogenic origins (>10%) or pyrogenic origins (<10%)
Upper GB	BC-12	1021.9	729.9	1.8	pyrogenic PAHs	33	Biogenic origins
Upper GB	BC-13	359.0	184.4	2.4	pyrogenic PAHs	39	Biogenic origins
Upper GB	C201, C202, C203	311.8	322.3	1.1	pyrogenic PAHs	46	Biogenic origins
Upper GB	C221, C222, C223	601.7	563.7	1.4	pyrogenic PAHs	55	Biogenic origins
Upper GB	VCPROP 4 1,2,3	337.2	304.2	1.7	pyrogenic PAHs	68	Biogenic origins
Upper GB	VCPROP 2 1,2,3	1635.0	1645.2	1.2	pyrogenic PAHs	50	Biogenic origins
Upper GB	HARV 12	297.7	145.1	2.5	pyrogenic PAHs	26	Biogenic origins

The corresponding 'perylene index' value is then converted to a percentage with 10% marking the cutoff value; above 10% implies the detected perylene has pyrogenic origins and below 10% implies biogenic origins (Wang et al., 2014).

For the 2016 sediment cores comparisons between the two sites VC-2 and VC-4, raw concentration data in ng-g-1 d.w were reported for depth comparisons. Comparisons were made at different depths, but because only a single sample was available at each site, no formal statistical analysis was performed.

ArcGIS mapping was performed on log-transformed concentration data for Low Molecular Weight (LMW) PAHs, High Molecular Weight (PAHs), and Total PAHs. This data was then Kriged using ArcGIS default geostatistical method: Kriging/Co-Kriging and the Semi-variogram/Covariance Modeling. To handle coincidental sample

points (two or more values for same locations), mean values were used. For this particular dataset, ordinary kriging type was used, and predication was selected as an output surface type.

3.4. Results

3.4.1. PAH Distributions in Sediments

As illustrated in Figures 3-2ad, each PAH category had a similar distribution from 1996-2017, with a minor elevation of each category for 2017. To further understand PAH distributions these categories were explored by year. A one-way ANOVA across all groups indicated significant difference by year (Table 3-2). Post-hoc pairwise tests indicated that 1996 and 2017 were statistically different, and the trend test were significant with all p-values all <0.0001 for all four PAH categories of (Total PAHs, 2-3 Ring PAHs, 4-5 Ring PAHs, and 6 Ring PAHs). Because our focus is on pre- versus post-Harvey, we then assessed whether all the pre-Harvey data could be grouped together. No differences were evident by one-way ANOVA across all pre-Harvey groups (p values between 0.5 and 0.9). After this re-grouping, we found significant differences pre- and post-Harvey by a two-tailed unpaired t-test (Table 3-2). Based on these results, the 1996-2011 pre-Harvey data were grouped together for mapping and kriging and compared to the 2017 post-Harvey data (discussed in PAH Distribution Maps section).

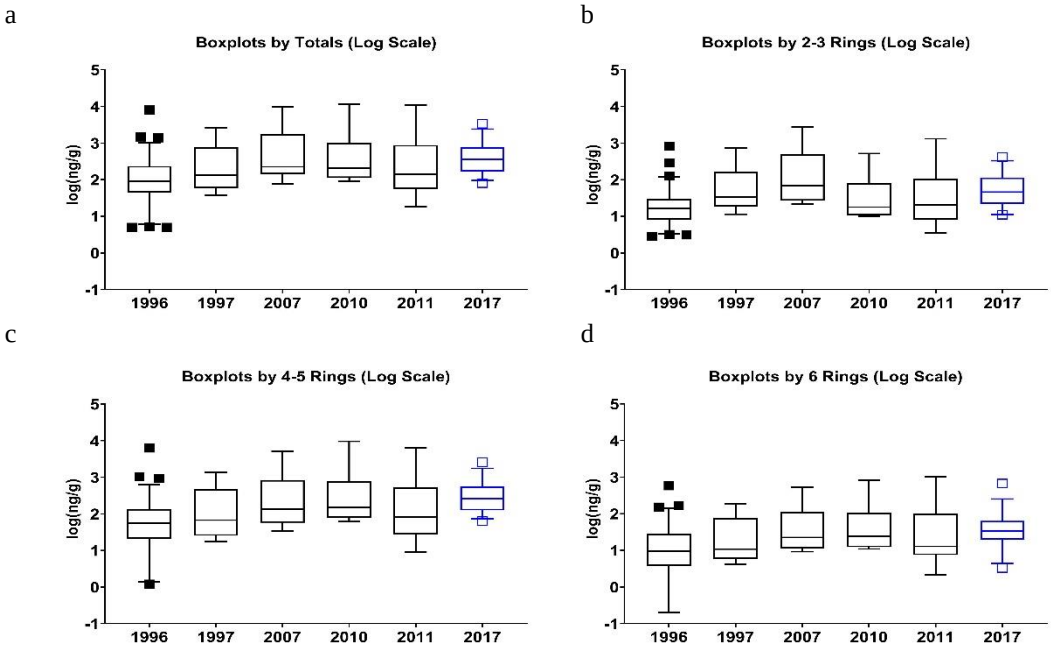

Figure 3-2 Boxplots for PAHs (a: Total, b: 2-3 Ring, c: 4-5 Ring, d: 6 Ring) for 1996-2017. Black boxplots signify the NOAA 1996-2011 data, while the blue boxplot signifies the 2017 post-Harvey data.

PAH Category	p-value	R^2
Total PAHs	0.0002	0.1766
2-3 Ring PAHs	<0.0001	0.2042
4-5 Ring PAHs	<0.0001	0.2038
6 Ring PAHs	0.0015	0.0613

Table 3-2 Summary Statistics for the one-way ANOVA analysis between each year of within data collection (1996, 1997, 2007, 2010, 2011, 2017).

PAH Category	p-value (1996-2011 vs 2017)	Difference Between Means (1996-2011 vs 2017)
Total PAHs	0.0003	0.4810±0.1293
2-3 Ring PAHs	0.0016	0.3475±0.1074
4-5 Ring PAHs	<0.0001	0.6134±0.1407
6 Ring PAHs	0.0013	0.4660±1422

Table 3-3 Summary statistics for the two-tailed unpaired t-test for years 1996-2011 PAH categories listed versus the 2017 PAH data.

The latest pre-Harvey surface sediment data from the NOAA database were from 2011, so to provide additional evidence that Harvey was a likely cause of any changes, we compared PAH concentrations in Scotts Bay (pre-Harvey) (Figure 3-3). Sample sizes are too small for statistical analysis, so are only presented qualitatively. Consistent with the surface sediment data above, the VC2 and C20 cores (post-Harvey) average concentrations in the top 15cm showed increases in 2017 from the 2016 levels in the two SB cores. The trends observed in the VC4 is the opposite for the first 15cm, which given the location of this core in the San Jacinto River estuary, they may be attributed to the new sediment deposits from Hurricane Harvey (Dellapenna et al., 2020; Du et al., 2019b). These results are consistent with prior top sediments data, which indicated top sediments had been eroded from the HSC (Al Mukaimi, Dellapenna, et al., 2018; Du et al., 2019a).

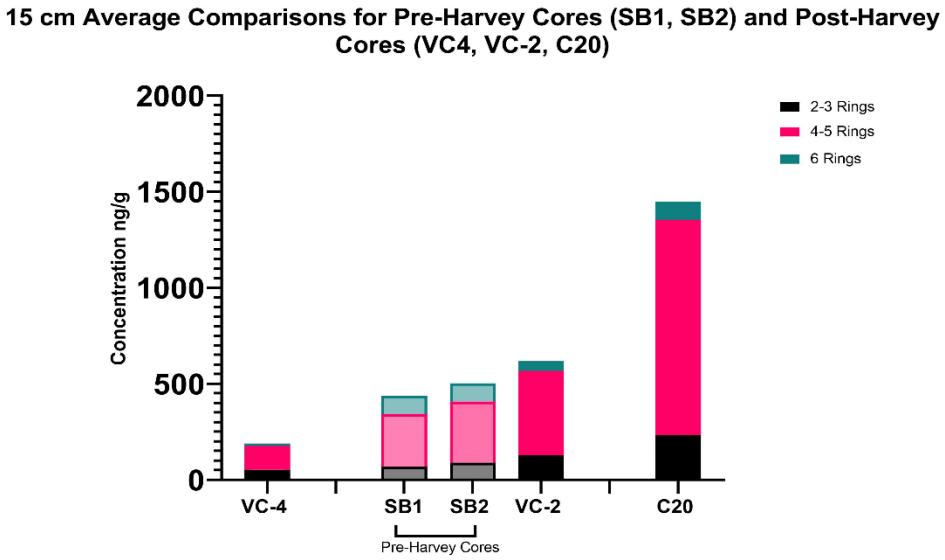

Figure 3-3 Comparison of sediment core PAH distributions (2-3 Ring, 4-5 Ring, and 6 Ring) collected pre-Harvey in 2016 (SB1 and SB2) and post-Harvey in 2017 (VC2, VC4, C20). Due to the small sample size, a qualitative comparison is made between each of pair of cores based on depth.

3.4.2. **PAH Diagnostic Ratios**

We divided the study area into three regionals: 1) Lower Bay, 2) Mid-Channel, and 3) Upper HSC (Figure 3-1). The Lower Bay encompasses samples taken below Smith's Point to Galveston Island, Mid-channel include samples taken within Clear Lake, Trinity Bay, and below Morgan's Point, and finally Upper HSC consists of samples taken above Morgan's Point. Figures 3-4a-d indicate consistent relative sourcing trends within each of three regions between the years 1996 (Figure 3-4a, 3-4c) and 2017 (Figure 3-4b, 3-4d).

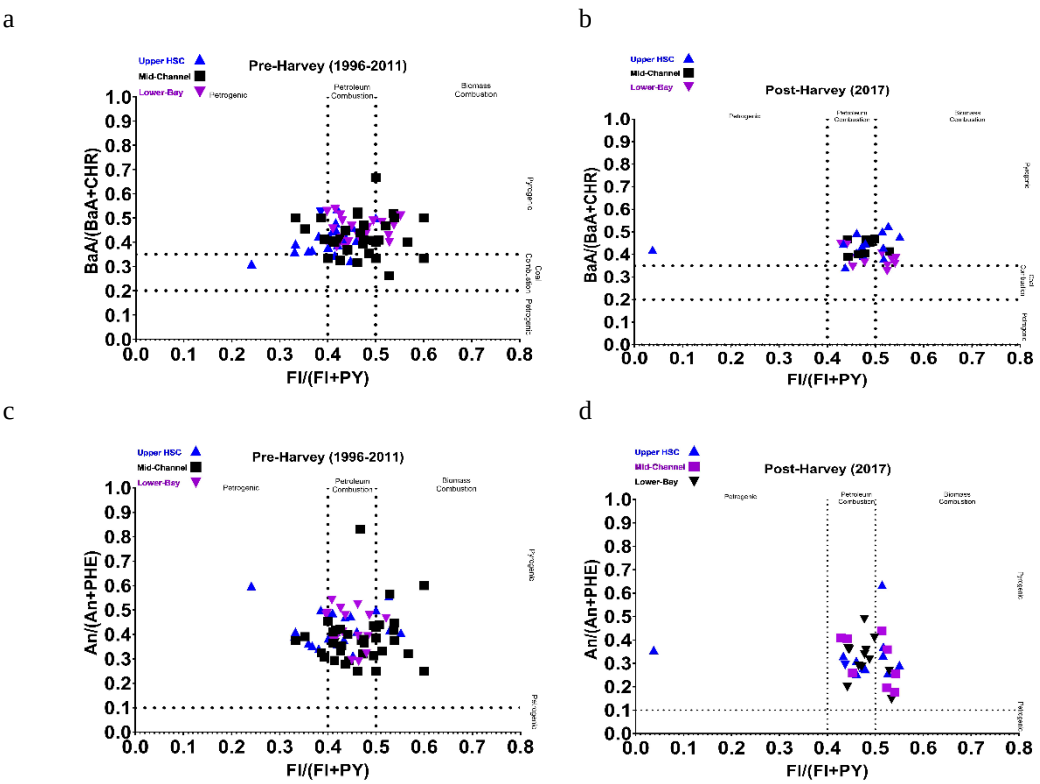

Figure 3-4 Double Ratio sourcing plots comparing 1996 NOAA data (a, c) and post-Harvey data (b, d). Panels a and b show BaA/(BaA+CHR) vs. Fl/(Fl+PY); panels c and d show An/(An+PHE) vs. Fl/(Fl+PY). The blue up-triangles show sites from the Upper HSC; purple squares show sites from the mid-channel (between Morgan's point to the beginning of Lower Galveston Bay; black down-triangles show sites from the Lower Bay to the entry point at Bolivar Peninsula.

To distinguish PAH sourcing in the 1996 and 2017 sediments, the following PAH diagnostic ratios were used: An/(An+PHE), BaA/(BaA+CHR), and Fl/(Fl + PY) diagnostic ratios were used (E. Davis et al., 2019; Soliman et al., 2019; Tobiszewski & Namieśnik, 2012; Valentyne et al., 2018; Yunker et al., 2002). As molecular masses of

202 (Fl, PY) and 276 (IP, Bghi) are the most stable parent compounds, they are good source indicators. In both the 1996-2011 and 2017 sediments, the median concentrations of fluoranthene (Fl) and pyrene (PY) suggest pyrogenic inputs are likely; especially since ideno(1,2,3-c,d)pyrene (IP) is also present (Stogiannidis & Laane, 2015). Since the BaA/(BaA+CHR) ratios are >0.35 and the corresponding Fl/(Fl+PY) are also >0.4 (Figure 3-4a, 3-4b), both the 1996-2011 and 2017 sediment had combustive sourcing inputs (E. Davis et al., 2019; Tobiszewski & Namieśnik, 2012; Yunker et al., 2002). This combustive sourcing is further supported by the A/(A+PHE) ratios, all of which are >0.1, and the Fl/(Fl+PY) ratios which are >0.4 (Figure 3-4c, 3-4d) (Yunker et al., 2002). However, the Fl/(Fl+PY) ratios for both the 1996-2011 and 2017 sediments are within the 0.4-0.5 range suggesting the combustive source is likely a petroleum-based origin (Yunker et al., 2002).

To determine whether petrogenic or pyrogenic inputs were more prevalent in the 2017 post-Harvey sediments, the EPA Priority 16 PAHs (unsubstituted parent compounds) and the following alkylated PAH homologs were tabulated: C1-4 Naphthalenes; C1-3 Fluorenes; C1-4 Phenanthrenes/Anthracenes; C1-3 Fluoranthenes/Pyrenes; and C1-4 Chrysenes in Table 3-1.

All samples except GB3, GB5, HARV 10, BC-9, C20, and VC Prop 2 had elevated parent compound totals compared to the total alkylated PAH totals indicating pyrogenic sources predominately influenced these sediments (Boehm, 2005; Stogiannidis & Laane, 2015; Yunker et al., 2002). The pyrogenic index calculated for all the post-Harvey sediments further suggests pyrogenic inputs as all of the ratios exceeded

the typical petroleum input range of 0-0.05 (Wang et al., 2014). The pyrogenic index is meant to quantitatively determine whether pyrogenic or petrogenic PAHs are the dominant compounds in the samples (Wang et al., 2014).

For the six sites listed previously, the alkylated PAHs exceeded the parent compound totals, indicating petrogenic sources were likely inputs (Boehm, 2005; Yunker et al., 2002). However, while pyrogenic sourcing was prevalent in most of the sediment samples, the perylene index (% PY within the five-ring PAH isomers) indicate the PAHs present in all the post-Harvey samples had diagenetic origins; or originated from organic matter under anoxic conditions (Rocha & Palma, 2019; Stogiannidis & Laane, 2015; Wang et al., 2014). Since all sediments discussed in this project were collected near and around the urban center of Houston, TX, this mixture of PAH sources is further influenced by roadway runoff, stormwater effluent, as well as atmospheric deposition. In this latter respect, Hurricane Harvey may have ultimately influenced the wet deposition of PAHs already present in the atmosphere.

3.5. Discussion

3.5.1. Benthic Organism Risk Assessment & Sediment Quality Evaluation

Considering the PAH classifications discussed in prior sections provided relative sourcing origins as well as overview distributional relationships, the associated risks for aquatic ecosystems exposed to these sediments are considered by comparing the effects range-low (ERL) and effects range median (ERM) values to the PAH concentrations quantified in this study (Table 3-4). This comparison references established screening values in NOAA's Screening Quick Reference Tables (National Oceanic & Atmospheric

Administration, 2008) whereby determining whether this study's PAH concentration values in post-Hurricane Harvey sediments pose a possible risk to benthic organisms. Routine National Sediment Quality surveys are conducted in accordance with Section 503 of the Water Resources Development Act of 1992 (Hou Aixin, DeLaune Ronald D, Tan MeiHuey, Reams Margaret, 2009).

	Pre-Harvey Median	Pre-Harvey IQR	Pre-Harvey Range	Post-Harvey Median	Post-Harvey IQR	Post-Harvey Range	ERL	ERM
Naphthalene	3.5	2.5, 5.5	0.5, 18.4	7.45	4.33, 12.15	2.57, 26.33	160	2100
Acenaphthylene	1.9	0.6, 4.2	0, 26.6	3.99	2.27, 8.07	0.71, 26.09	16	500
Acenaphthene	0.8	0.5, 1.4	0.2, 34.9	3.47	1.88, 8.01	0.59, 60.99	44	640
Fluorene	1.1	0.5, 2	0.2, 34.5	5.52	2.52, 11.09	1.39, 94.84	19	540
Phenanthrene	3.3	1.7, 6.8	0.2, 501.5	14.40	6.86, 25.53	3.2, 142.67	240	1500
Anthracene	2.2	0.9, 6	0.1, 228.3	5.68	3.46, 1.56	1.12, 138.25	85.3	1100
Fluoranthene	8.3	3.1, 18.3	0.1, 1473	33.07	12.68, 72.71	4.7, 462.63	600	5100
Pyrene	9.5	3.9, 25.3	0.2, 1502.7	39.13	14.68, 83.67	5.68, 403.6	665	2600
Benzo(a)anthracene	4.3	1.4, 10	0.1, 676.4	15.87	8.09, 35.50	1.83, 192.94	261	1600
Chrysene	5.7	2.1, 12.2	0.1, 711.6	20.42	9.98, 59.45	2.45, 319.09	384	2800
Benzo(b)fluoranthene	8.5	3.1, 18.8	0.1, 800.4	37.17	15.86, 73.55	4.37, 538.74	-	-
Benzo(k)fluoranthene	2.3	0.9, 5.1	0, 178.7	8.60	4.55 18.01	0.83, 196.21		
Benzo(a)pyrene	6.6	2.6, 16	0.1, 684.4	17.53	9.49, 32.69	2.05, 244.5	430	1600
Perylene	6.8	3, 16.2	0.2, 187.2	77.12	41.50, 161.95	14.88, 347.93	-	-
Indeno(1,2,3-c,d)pyrene	4.2	1.6, 12.1	0.1, 291.5	11.81	5.12, 27.14	0.91, 334.89	-	-
Dibenzo(a,h)anthracene	1.2	0.5, 2.9	0, 66.1	2.17	1.25, 4.11	0, 40.17	63.4	260
Benzo(g,h,i)perylene	5.5	2.3, 16.7	0.1, 289.5	20.40	10.49, 49.14	2.39, 333.32	-	-
2-Methylnaphthalene	2	1, 3.2	0.2, 11	4.37	2.55, 9.61	1.13, 21.26	70	670
Total LMW PAHs	29.8	12.3, 67.2	2.6, 2035.5	81.32	39.00, 184.55	16.92, 746.48	552	3160
Total HMW PAHs	51.4	19.5, 117.1	1.8, 5712	271.10	129.00 547.66	63.6, 2787.82	1700	9600
Total PAHs	89.2	35.8, 214.1	5, 8040.2	366.37	168.91, 779.89	80.52, 3384.41	4022	44792

Table 3-4 Modified NOAA SQuiRT Chart with individual PAHs, HMW PAHs, LMW PAHs, and Total PAHs listed in the first column; corresponding SQuiRT Chart for the effects range-low (ERL) and effects range median (ERM) values and study PAH values analyzed in this study are summarized here.

However, Sediment Quality Guidelines (SQGs), first applied by NOAA in 1989, serve to generally protect fisheries in addition to aquatic environment surface water

quality and health (Kwok et al., 2014). As such the NOAA ERM and ERL values have continued to guide whether corrective actions are required to clean or remove sediments within study areas even though they are limited by varying factors (e.g. temperature, salinity, biota, grain size) unique to aquatic ecosystems (Birch, 2018; Chapman, 2018; Kwok et al., 2014). As a result, these factors can impact environmental exposure to chemicals found in the sediments. For example, GB/HSC is an estuary, which is dynamically changing and has variable benthic conditions (e.g. variable salinity) SQGs are not necessarily translatable to this particular ecosystem as the SQGs were developed for either freshwater or saltwater environments (Chapman, 2002). Typically, SQGs are used in sediment management projects (e.g. disposal and relocation of dredging materials should the dredge materials be deemed harmful to aquatic ecosystems) and a preliminary screening process for assessing chemical levels in sediment (Kwok et al., 2014). For the purposes of this project, the SQGs outlined in Table 3-4 will provide an initial comparison to determining whether post-Harvey sediments redistributed after the hurricane pose a possible environmental risk to the local benthic ecosystem. Based on Table 3-4, of the detected PAH concentrations (reported in ng·g-1 d.w.), both the 1996 and 2017 medians were well below both the ERL and ERM values. However, there were a few individual Post-Harvey values for several PAHs that exceeded the ERL values (e.g. Acenaphthylene, Acenaphthene, Fluorene, Anthracene). As for low molecular weight (LMW), high molecular weight (HMW), and total PAHs, both the 1996 and 2017 sediment data had a site where the ERL values were exceed and the corresponding ERM was nearly met. While the post-Harvey samples do not necessarily require remediation

or corrective action, the detected PAH concentrations and the corresponding PAH ranges do suggest PAH analysis at later timeframes and in the same or similar sites would be of interest (Table 3-4).

3.5.2. **PAH Distribution Maps: 1996-2011 vs 2017 Post-Hurricane Harvey**

The PAH distribution maps (Figures 3-5a-f) map three categories of PAH concentrations in logscale: Low Molecular Weight (LMW) PAHs, High Molecular Weight (HMW) PAHs, and Total PAHs. Each of these figures utilize kriging where values were interpolated on a logscale. The pre-Harvey sediments indicate a relatively consistent LMW and HMW pattern (Figures 3-5a-d), while there is a notable difference in the post-Harvey sediments for LMW and HMW PAH distributions (Figure 3-5b, 3-5d).

As HMW PAHs (4-6 ring PAHs) predominately originate from combustion sources, one of which is black carbon or soot, these PAHs have been found to predominantly remain in the particulate phase either in the atmosphere (Park et al., 2001b) or in sediments (Kanzari et al., 2014; Rabodonirina et al., 2015). Consequently, the HMW PAHs are more likely to sorb and partition to organic matter (Chiou et al., 1998; Rabodonirina et al., 2015; Wang et al., 2014). and not readily biodegrade. As the post-Harvey layer was mostly mud dominant with a sand layer at the base, the likelihood of HMW PAHs to be present in the mud layer is likely due to the present organic matter. Thus, the post-Harvey deposit consists of sediment eroded, primarily from within the HSC/upper bay, which was then transported and dispersed around Galveston Bay (Dellapenna et al., 2020; Du et al., 2019b, 2020).

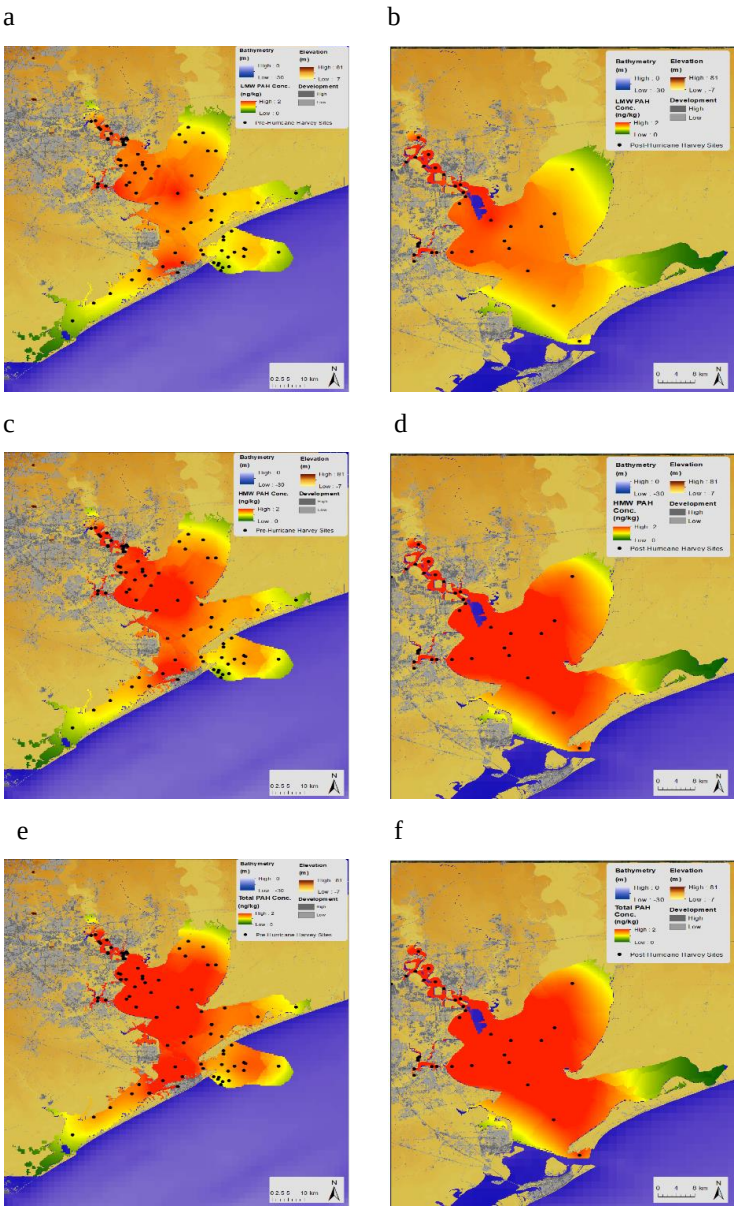

Figure 3-5 Geospatial distribution maps of kriged concentrations of PAHs pre-Harvey (a, c, e) and post-Harvey (b, d, and f) sediments. Each pair of maps compares different PAH categories (a and b: Low Molecular Weight; c and d: High Molecular Weight; e and f: Total). Shown on land are developed areas (evident in the Upper Houston Ship Channel and Houston, TX as well as near Texas City, TX) and land elevation (low throughout the region, with higher elevations above the San Jacinto River).

Figure 3-5d shows this pattern as the HMW PAHs have elevated distributions in the Upper HSC that then decrease towards Galveston Bay and Trinity Bay. However, it is important to note the values shown do not include the confidence intervals. As a result, some of the regions farther from the data point (e.g. coast line of Trinity Bay and Lower Galveston Bay) may have high uncertainties associated with the values due to the limited number of nearby sampling sites.

In relation to the PAH diagnostic ratios, PAH transportation and spatial distribution within the environment is influenced by variable environmental matrices (e.g. grain size, organic matter), atmospheric deposition, and anthropogenic sources such as emission mixing (E. Davis et al., 2019; Rocha & Palma, 2019; Tobiszewski & Namieśnik, 2012; Yunker et al., 2002). The distribution maps shown in Figure 5a-f illustrate three different categories of PAH distributions in GB/HSC: LMW PAHs (3-5 a-b), HMW PAHs (3-5 c-d), and Total PAHs (3-5 e-f). For the pre-Harvey conditions, there are zones of elevated LMW and HMW PAHs, which Figures 3-4a and 3-4c indicate originate from petroleum combustion. When the pre- and post-Harvey LMW and HMW PAH maps (Figure 3-5a-d) are compared, there are two consistent elevated zones of PAHs: one in the middle of GB/near Trinity Bay, and the other is near inner coastal Galveston Island and Interstate-45. This observation is seen through the shades of red-orange; although note the change in concertation for both pre- and post-Harvey sediments as evidenced in Figure 3-2 and the tabulated LMW and HMW PAH totals in Table 3-3. The total PAH maps (Figure 3-5 e-f) on the other hand, illustrate how all PAHs detected in GB/HSC for both pre- and post-Harvey sediments were distributed

over these two sampling time periods. However, there is a distinct increase in total PAHs detected in post-Harvey sediments (av. 366.37 ng/g) compared to the total PAHs detected in pre-Harvey sediments (av. 89.2 ng/g) (Table 3-3). Figure 5e shows under pre-Harvey conditions the Upper HSC, Clear Lake, inner Coastal Galveston Island (near I-45), and the middle of Galveston Bay have elevated PAH concentrations. Then, Figure 3-5f shows under post-Harvey conditions, the PAH concentrations are steadily distributed from the Upper HSC into the rest of Galveston Bay. However, note there are boundary differences Figure 3-5, as the post-Harvey maps exclude the Gulf of Mexico entry and West Bay since there were no sediment samples collected in these respective regions after Hurricane Harvey.

As HMW PAHs are predominantly present in both pre- and post-Harvey sediments, this difference could be attributed to the sorption properties of HMW PAHs to the post-Harvey mud. With HMW PAHs sorbed to mud or other particulate matter, they are not as readily degraded as petrogenic PAHs (E. Davis et al., 2019; Tobiszewski & Namieśnik, 2012). As such, these sorption properties suggest PAHs could partition into the available organic matter that is redistributed by severe rainfall and flooding events occurring in the GB/HSC area.

Since this study's PAH results suggest the presence of petrogenic PAHs both before and after Hurricane Harvey (Figure 3-5b and 3-5d), these PAHs presence could likely be attributed to local oil spills or from atmospheric deposition. Although, Thyng 2019 modeled how natural ocean currents could have brought Deepwater Horizon oil residues to the Texas coastline near Galveston Bay and the Bolivar Peninsula (Thyng,

2019). However, there was no indication in our post-Harvey results to suggest these oil residues had entered the GB/HSC estuary system.

When only the pre-Harvey data is considered (Figures 3-5a, 3-5c, 3-5e), the areas predicted to influence total PAH concentration distribution are within the Upper HSC, portions of Mid-Ship Channel (Clear Lake, central Galveston Bay) and urbanized areas near inner Galveston island. These areas demonstrate elevated HMW PAHs and partially elevated LMW PAHs, thereby indicating a possible point-source or event. Under post-Harvey conditions, the HMW PAHs and Total PAHs (Figures 3-5d, 3-5f) followed similar distribution patterns to the pre-Harvey data in that the Upper Ship Channel through Morgan' Point and into Trinity Bay and Lower Galveston Bay demonstrated a notable gradient. Therefore, when comparing PAH classes between pre- and post-Harvey conditions, the HMW PAHs tended to contribute more to the overall Total PAH distributions than LMW PAHs. This distribution can likely be explained by the prominent flood period and hydraulic trapping of suspended sediment in the mid bay during the Harvey flood (Dellapenna et al., 2020; Du et al., 2020). However, it is important to note that while the post-Harvey distribution appears dispersed within GB, the sediments sampled after Hurricane Harvey do not necessarily reflect proximal sourcing. In other words, the Harvey deposit illustrated in Figure 3-5b, 3-5d, and 3-5f are showing the sediments redeposited from the San Jacinto Estuary and Buffalo Bayou; two areas within the Upper HSC. Therefore, these maps also suggest several areas of interest for future sampling designs: Upper HSC – Morgan's Point, Morgan's Point to Trinity Bay, Morgan's Point to Lower Galveston Bay. Furthermore, as are a few relevant

oyster reefs (e.g. Redfish Oyster Reef and Hannah's Reef) in the last region (Morgan's Point to Lower Galveston Bay), there may be addition interest in monitoring these sediments for oyster exposures and in turn human and animal oyster consumption.

3.6. Conclusions

Overall, Hurricane Harvey appeared to result in a small, but detectable, increase in surface sediment PAH concentrations as compared to historical data. This small shift is consistent with studies of Harvey-induced sediment transport and dispersal (Dellapenna et al., 2020; Du et al., 2019b, 2020), which suggest that the newly deposited sediment was eroded largely from the HSC/upper bay, where contamination is typically greater. A separate study detected 2 to 4-ring PAHs (e.g. naphthalene, pyrene, and fluoranthene) more often than 5 to 6-ring PAHs in surface water samples collected after Hurricane Harvey (Bacosa et al., 2020). Interestingly, this study detected a similar trend in PAH origins whereby most of the source inputs were pyrogenic with other mixed and petrogenic sources seen. Additionally, this study detected a gradient trend in HMW and Total PAHs after Hurricane Harvey in three general regions of interest: Upper HSC, Mid-Channel, and Lower Bay. Overall sourcing patterns indicated combustive sourcing that are likely associated with anthropogenic sources from the highly urbanization within the region. Moreover, sourcing patterns were not noticeably different pre- and post-Harvey. Based on the gradient trend detected in the Post-Harvey samples, the Upper HSC and the area between Morgan's Point and Lower Galveston Bay may be of interest to focus sampling in future studies. However, given the San Jacinto Estuary and Buffalo Bayou sediments were deposited in GB, both the Upper HSC and Galveston Bay will

need to be sampled to determine whether the PAH distribution is more similar to pre-Harvey or post-Harvey. Then, even though the PAH concentrations detected were not close to any SQG levels (ERL or ERM), this does not mean future sediment samples from the Upper HSC or other areas in Galveston Bay will consistently reflect this trend; especially since the estuarine environment is dynamic. In light of future hurricane seasons, understanding PAH spatial trends and the potential environmental risks associated with sediments can help develop a working baseline for reference within the Galveston Bay and Houston Ship Channel region.

4. BIOSENSOR APPLICATIONS IN GALVESTON BAY: IMPLICATIONS FOR DISASTER RESEARCH

4.1. Overview

Given the time and monetary costs associated with traditional analytical chemistry, there remains a need to rapidly characterize environmental samples for priority analysis, especially within disaster research response (DR2). As PAHs are both ubiquitous and occur as complex mixtures at many National Priority List sites, these compounds are of interest for post-disaster exposures. This study tests the field application of the KinExA Inline Biosensor in Galveston Bay and the Houston Ship Channel (GC/HSC) and characterizes the PAH profiles of this region's soils and sediments. To our knowledge, this is the first application of the biosensor to include soils. The biosensor enables calculation of total free PAHs in porewater (C_{free}), which is confirmed through gas chromatography-mass spectrometry analysis. To determine potential risk of the collected soils the United States Environmental Protection (USEPA) Agency's Regional Screening Level (RSL) Calculator is used along with the USEPA Region 4 Ecological Screening Values (R4-ESV) and Refined Screening Values (R4-RSV). The biosensor's predictivity for total PAH concentration had a goodness of fit of R^2= 0.766, with C_{free} ranging from 0-1.94 μg/L in GB/HSC sediment cores, 0.25-27.37 μg/L in soils, 0-5.65 μg/L in GB/HSC surface sediments, and 0.25-129.06 μg/L in Elizabeth River sediments. The RSL results for the soil samples were all below a hazard quotient of 1 indicating low risk of PAH exposure. In contrast, several individual parent

PAH concentrations in both the GB/HSC and Elizabeth River sediments exceeded the R4-ESV and R4-RSV values, indicating a need for follow-up sediment studies. The resulting data support the utility of the biosensor for future DR2 efforts understanding PAH pollution. These results also offer preliminary PAH exposure risk considerations by aiding the prioritization of environmental sample analysis.

4.2. Introduction

Given the recent record-breaking frequency and magnitude of natural disasters within North America (National Centers for Environmental Information, 2021), the ability to conduct research efficiently following disasters continues to grow in importance. Within the state of Texas, an area of interest in natural disaster research has been the intersection between public health and the impacts of post-disaster impacts, especially for vulnerable human and ecological populations (Aly et al., 2020; Bera et al., 2019; Horney et al., 2019; Karaye et al., 2019; Knap & Rusyn, 2016; Sansom et al., 2018). Galveston Bay and the Houston Ship Channel (GB/HSC) serve as a unique economic and industrial marine navigation channel for the city of Houston, TX, which is the world's second-largest petrochemical complex and home to over 2 million people (Dellapenna et al., 2020; Houston, 2021; US Army Corps of Engineers, 2017). The region is an urban estuary, which serves as both a diverse ecological resource and a natural filter for nearby industrial and urban outputs (e.g. atmospheric deposition, agricultural runoff, roadway runoff, wastewater spills, oil spills, etc.) (Al Mukaimi et al., 2018b; Dellapenna et al., 2020; HARC & Galveston Bay Foundation, 2020; Oziolor et al., 2014, 2018; Park et al., 2001a, 2001b).

Hurricane Harvey made landfall along the Texas coast in August 2017, bringing between 26-47 inches of rainfall to the Houston area within 4 days (Harris County Flood Control District, 2018). Due to this extreme rainfall event, an estimated 1.31×10^8 metric tons of sediment were deposited into Galveston Bay, with an average of 14 cm of flood layer sediment deposited (Dellapenna et al. in review, Du et al., 2019b, 2019a). Additionally, the slow movement of Hurricane Harvey contributed to severe flooding that inundated both the City of Houston as well as its nearby bayous and waterways (Dellapenna et al., 2020; Harris County Flood Control District, 2018; Kiaghadi & Rifai, 2019). Some of the damages related to this flooding event included, but were not limited to, overflow from wastewater treatment plants and spills from local industrial facilities (Kiaghadi & Rifai, 2019), which coupled with the sediment flood layer (Dellapenna et al., 2020; Du et al., 2019b, 2019a) implicated the feasibility of chemical, biological and physiological contaminant redistribution. An additional factor that is influential in contaminant redistribution is the local subsidence rates (Al Mukaimi et al. 2018a, 2018b) since deeper sediments with historical anthropogenic inputs could be uncovered and thereby become available for redispersion under flood conditions.

Given GB/HSC is a highly industrial and urban estuary, chemical contaminants such as polychlorinated biphenyls (PCBs), polycyclic aromatic hydrocarbons (PAHs), organochlorine pesticides, heavy metals, and dioxin/furans have been historically documented within the region (Al Mukaimi et al., 2018b; Bera et al., 2019; Camargo et al., 2020; HARC & Galveston Bay Foundation, 2020; Hieke et al., 2016; Howell et al., 2011; Lakshmanan et al., 2010; Louchouarn et al., 2018; Qian et al., 2001; Santschi et

al., 2001; Yeager et al., 2007). Of these contaminants, PAHs are of interest due to their ubiquitous prevalence within environmental matrices (e.g., sediments, water), their occurrence as complex mixtures and the risk that exposure may pose to both ecological species and public health in urban environments (Agency for Toxic Substances and Disease Registry, 1995; Brown et al., 2017; Hussar et al., 2012; Hwang & Foster, 2006; Kim et al., 2019; Oziolor et al., 2014a; Vane et al., 2014).

Due to the severe flooding event resulting from Hurricane Harvey, PAH redistribution was a concern due to particulate matter availability in the floodwaters to which PAHs can sorb to as well as ample PAH inputs from the urban environment (e.g., crude oil, roofing tar, asphalt, creosote, industrial combustion, roadway dust, atmospheric deposition, etc.). Since PAHs occur as complex mixtures, a subset of sixteen PAH compounds has been established as the United States Environmental Protection Agency's (USEPA) Priority 16 PAHs due to their suspected carcinogenicity and toxicity as well as prevalence at National Priority List (NPL) sites (Agency for Toxic Substances and Disease Registry, 1995; Appendix A to 40 CFR, Part 423–126 Priority Pollutants, 2014). Traditional and highly sensitive detection methods for PAHs include high-performance liquid chromatography (HPLC) with either ultraviolet (UV) absorption or UV fluorescent detection; gas chromatography (GC) with either mass spectrometry (MS) or flame ionization detection (FID) (Li et al., 2016b). However, these methods are time and resource-intensive when used to detect PAHs.

To supplement and fast-track these traditional PAH detection methods, several immunoassays paired with biosensing platforms have been developed with each ranging

in their PAH detection sensitivity (Behera et al., 2018; United States Environmental Protection Agency, 1996a, 1996b). One biosensor technology, The KinExA Inline Biosensor (Sapidyne Instruments), employs a mouse-derived anti-pyrene-butyric acid monoclonal antibody, 2G8, capable of detecting all 3-5 ring PAHs (Li et al., 2016). With this level of specificity, the KinExA Inline Biosensor (biosensor) employs the 2G8 antibody to obtain real-time quantification of PAHs in environmental samples; in particular sediment porewater (Hartzell et al., 2017; Hartzell, et al., 2018). This particular biosensor also offers a cost-effective and rapid analysis of environmental samples with results per sample obtained within 10 minutes (Li et al., 2016b).

For sediment and risk management purposes, understanding both bulk-sediment PAH concentrations and freely available PAH (C_{free}) concentrations in sediment porewater aid in the estimation of PAH bioavailability and bioaccessibility (Ghosh et al., 2011; Hartzell et al., 2018; McGrath et al., 2019; Muz et al., 2020). As a result, passive sampling methods have emerged as common practice to rapidly and accurately predict and measure the bioavailable and bioaccessible chemical fractions within soils and sediments (Cui et al., 2013; Riding et al., 2013). When the biosensor was tested against a passive sampler, the C_{free} values measured were agreeable despite differences between each approach methodology for C_{free} (Conder et al., 2021)

The goal of this study was to determine the field application of the biosensor within GB/HSC as well as to characterize the PAH profile in soil and sediment porewater within this region. This project is also the first to our knowledge to apply the biosensor technology to soils obtained within a neighborhood setting. Several Elizabeth

River sediments served our known PAH contaminated samples, because our GB/HSC sediments and soils contained unknown PAH contamination levels. This project's applied-research approach supports the utility of a flexible and cost-effective technology capable of supporting both disaster research response (DR2) and longer-term sediment management of PAHs.

4.3. Materials & Methods

4.3.1. Sediment Collection and Study Sites

4.3.1.1. Galveston Bay/Houston Ship Channel/Clear Lake, TX

Two sediment cores (SB1 and SB2) were collected in 2016, where each core was sectioned at 5cm intervals for the first 45cm (Figure 4-1a), while surface sediments were collected during May 2019 (n=13) and December 2019 (n=30) (Figure 4-1c). Both surface sediment and sediment core collection methodologies are previously described (Camargo et al., 2020). The GB/HSC transect was selected to deploy and apply the biosensor for rapid characterization of the area with Clear Lake, Texas serving as a comparator site. Clear Lake (CL) is a recreational and sheltered system compared to the commercial shipping lane the GB/HSC transect serves. The geocoordinates for the sediment samples are reported in Table C 1.

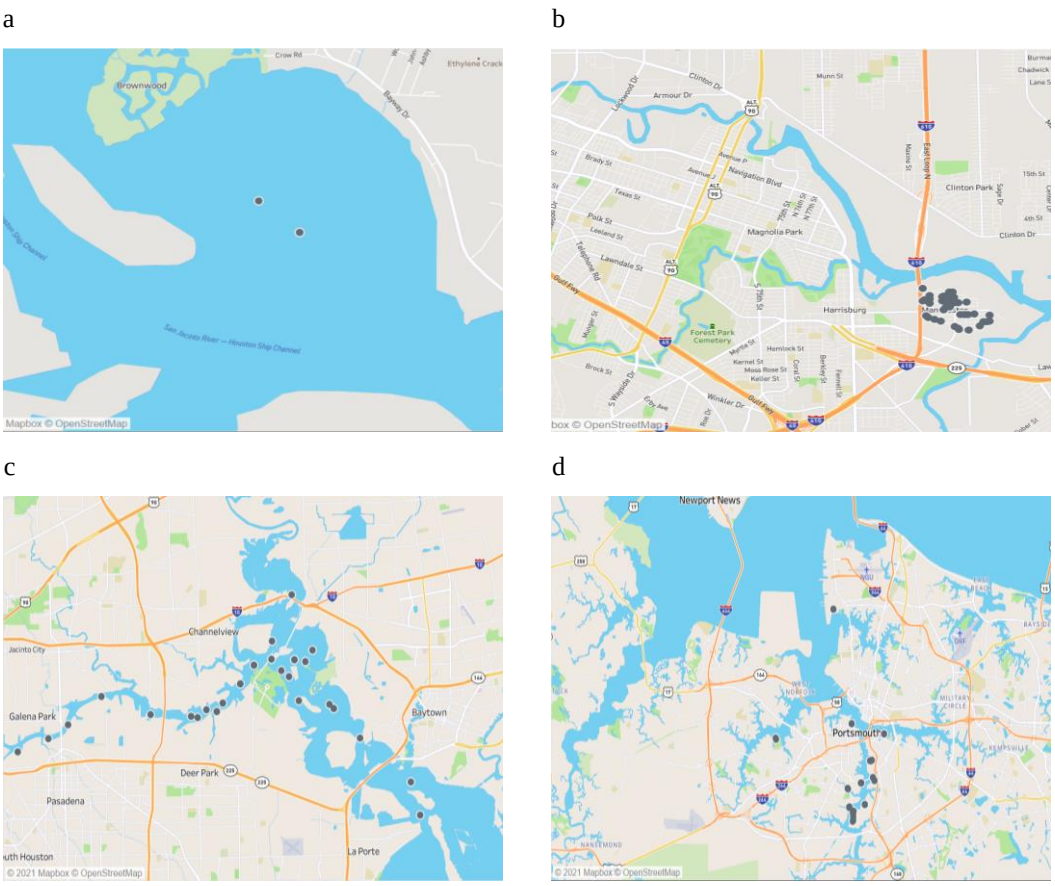

Figure 4-1 Study sites base map for all sediment and soil data collected in 2016 (pre-Harvey sediment cores), 2017 (post-Harvey soils), 2019 (post-Harvey surface sediments), and 2018 (Elizabeth River surface sediments). The 2016 data comprised of 2 sediment cores (a), while the 2017 data comprised of 44 soil samples taken within the Manchester Neighborhood (b). In 2019 43 surface sediment samples were collected from both Galveston Bay/Houston Ship Channel and Clear Lake (c), while 43 surface sediments were collected from the Elizabeth River (d). Each map demonstrates the four unique sites assessed in this project.

4.3.1.2. Elizabeth River, VA

Surface sediments from the Elizabeth River (ER) were collected in 2018 as a part of a killifish study seeking to understand tumor prevalence in local fish populations (Elizabeth River Project & Virginia Institute of Marine Science, 2020). These sediments were collected as previously described (insert collection methods citation here) (n=30) (Figure 4-1d). All sample geocoordinates are reported in Supplementary Table 3.

4.3.2. Soil Collection and Study Sites

The soil sample collection methodology has been previously described (Sansom et al., 2020 *In Press)* and their geocoordinates were also recorded (n=42) (Figure 4-1b).

4.3.3. Sediment and Soil Chemical Analyses for PAHs

All Galveston Bay/Houston Ship Channel sediment and Manchester soil PAH extraction and analysis methods have been previously described (Camargo et al., 2020; Garret T. Sansom et al., 2021). Elizabeth River sediment samples were analyzed for PAH concentrations with gas chromatography-mass spectrometry-selective ion monitoring (GC-MS-SIM) methods used previously (Spier et al., 2011; Unger et al., 2008). Briefly, the samples were lyophilized, spiked with deuterated surrogate standards, and extracted with dichloromethane in a Dionex accelerated solvent extractor. The extracts were reduced under dry nitrogen and separated by size exclusion chromatography and open column chromatography to isolate the compounds of interest. The internal standard p-terphenyl was added before analysis on a Varian Saturn GC/MS/MS ion trap mass spectrometer operated in electron ionization mode (EI). Six-

point calibration curves were generated for PAH analytes and identifications were based on retention time and matches to library spectra.

4.3.4. **Total Organic Carbon (TOC) Analyses**

The soil and sediment TOC analysis for the GB/HSC sediments and Manchester soils were analyzed by TDI-Brooks International, Inc. using the Lloyd Kahn procedure and the LECO corporation model 632 carbon analyzer with direct combustion/infrared detection (TDI-Brooks, 2019). The Elizabeth River sediment TOC analysis was completed using the Exeter CHN Nodel 440 CE analyzer. The samples (between 8-25 mg), were packed in a silver cup or nickel sleeve, were dropped into the combustion chamber (at 975 °C), which was purged with helium to removed atmospheric nitrogen. In the mixing volume, the sample gas was thoroughly homogenized at a precise volume, pressure, and temperature. The sample gas was passed between three thermal conductivity cells measuring, first the differential between the gas before and after the first trap measures (H), then the second trap removing CO_2 measures (C), and the third trap, which removed helium measures (N). The role of TOC data in this project is to quantify the presence of organic content per sampling site. As each site will be unique, the TOC data also serve as a marker for potential material PAHs can sorb to that can then be detected by GC/MS in the whole sediment/soil analyses.

4.3.5. **Porewater PAH Analysis**

Porewater was extracted through centrifugation (3500g X 15 min), where the porewater extracts were then filtered using 0.45 µm Teflon Millipore filters to exclude particulate matter in the extracts. To quantify the total 3-5 ring PAHs in the extracts, the

2G8 antibody with a fluorescent tag was used to analyze each sample (Li et al., 2016b). The biosensor's automated sample handling procedure allows mixing of the fluorescent antibody with each sample as previously described (Spier et al., 2011). A standard curve for final porewater concentrations was determined using Phenanthrene standards from 0.5 to 2.5 µg/L. Each Phenanthrene standard was made daily before sample analysis through a serial dilution of a stock solution. If a sample exceeded the calibration curve, it was diluted with deionized water to make the detection response linearly proportional to the calibrated concentration range. The minimum detection limit (MDL) for all porewater samples was <0.5µ/L, where this value was halved to standardized the <MDL detection values.

4.3.6. **Regional Screening Level (RSL) Calculations**

To aid in risk characterization, the USEPA RSL Calculator was used to estimate potential oral, dermal, and inhalation risk of the Manchester soils. Each parent PAH value detected by GC-MS was inputted to the RSL Calculator using the following settings: Screening Level Type: Regional Screening Levels (RSLs); Hazard Quotient: 0.1; Target Risk: 10^{-6}; Scenario: Resident; Media selected: 'Soil'; Screening Level Choice: Site-Specific/User-Provided; Risk Output: Yes; RfD/RfC Choice: both Chronic and Subchronic were analyzed for each soil site; all of the USEPA 16 PAH (parent compounds) were selected and retrieved. All RSL Calculator outputs were downloaded as Excel files that were then compiled into a singular excel sheet for further data analysis.

4.3.7. **Statistical Analyses**

All statistical analyses were carried out in GraphPad Prism 9.0.0. and the raw data were processed using Microsoft 365 Excel. Tableau 2020.2.9 was used to construct the sampling maps.

	SAMP	mg C	% TOC	foc	Cfree	Total EPA 16	Totals w/ alkylated	Pyrogenic Index	Perylene Index (%)
Min	2016 Cores	0.96	0.38	0.00	0.00	115	176	0.21	15.80
	2017 Soils	0.54	0.21	0.00	0.25	87	121	0.06	4.89
	2019 GB/HSC Sed	0.28	0.11	0.00	0.00	41	51	0.15	5.19
	2018 ER Sediments	0.00	0.19	0.00	0.25	714	1029	0.00	4.68
Median	2016 Cores	2.33	0.93	0.01	0.42	414	607	0.56	63.75
	2017 Soils	4.86	1.94	0.02	0.60	1481	1883	2.28	8.28
	2019 GB/HSC Sed	2.40	0.97	0.01	0.87	763	1019	1.48	26.98
	2018 ER Sediments	-	0.97	0.01	0.69	11498	15636	-	8.22
Max	2016 Cores	3.56	1.41	0.01	1.94	794	1270	1.29	92.02
	2017 Soils	64.14	25.82	0.26	27.37	14953	17809	3.72	25.89
	2019 GB/HSC Sed	5.81	2.37	0.02	5.65	18086	21320	5.38	98.34
	2018 ER Sediments	-	11.38	0.11	129.06	6792632	7019023	-	19.19
IQR	2016 Cores	1.58, 2.69	0.63, 1.06	0.01, 0.01	0.00, 0.69	297, 499	386, 845	0.38, 0.68	34.93, 78.12
	2017 Soils	3.59, 7.00	1.49, 2.77	0.01, 0.03	0.25, 1.25	759, 2684	1013, 3565	1.69, 2.68	7.25, 12.11
	2019 GB/HSC Sed	1.14, 3.44	0.44, 1.36	0.00, 0.01	0.50, 1.46	307, 1709	475, 2053	1.13, 2.00	19.80, 38.36
	2018 ER Sediments	-	0.43, 2.03	0.00, 0.03	0.25, 1.31	4048, 38583	9292, 46628	-, -	6.92, 9.18

Table 4-1 Summarized are detected soil and sediment Total Organic Carbon (TOC) measurements, total PAH concentrations in porewater (C_{free}), PAH totals (Total EPA 16; Totals w/alkylated), a pyrogenic index, and a perylene index. TOC measurements are reported in milligrams per gram Carbon (mg C), percentage TOC (%TOC) , or as the fractional organic carbon (f_{OC}). The C_{free} values are reported in µg/L, while both the Total Priority 16 EPA PAHs (Total EPA 16) and Total PAHs with alkylated PAHs (Totals w/alkylated) sums are reported in µg/kg. A detailed list of the PAHs included for the two PAH totals listed is in Supplementary Table 1. The pyrogenic index is unitless while the perylene index is reported as a percentage.

Original GC-MS data are reported in µg/kg Table 4-1, while these concentrations are log-transformed comparative analysis in consequent figures. Double-plot ratios for BaA/(BaA+CHR) vs Fl/(Fl+PY) and An/(An+PHE) vs. Fl/(Fl+PY) were used to determine PAH sourcing. The log-10 of the RSL Calculator hazard quotient (HQ) results for both children and adults were taken for a comparative analysis of the soil samples.

4.4. Results

4.4.1. Soil and Sediment Chemistry

4.4.1.1. Total Organic Carbon (TOC)

In the 2016 sediment cores, the %TOC ranged from 0.38-1.41%, with differing depth profiles for SB1 compared to SB2. For instance, SB1 has a similar %TOC at the surface as at 40-45cm depth, while the %TOC was higher at depths of 25-30cm and 30-35cm (Figure C 1). The 2019 surface sediments TOC range was 0.11-2.37%, with the HSC having higher %TOC values compared to the Clear Lake samples. In contrast to the GB/HSC/CL sediments, the soils contain the highest %TOC, with the range of 0.21-25.82%. The highest %TOC within the soil samples was at site 98 (25.82%), which is in a recreational park with several other sites in this area also having elevated %TOC (sites: 85, 97, 99) that may be attributed to leafy substances and/or added peat moss.

Compared to the GB/HSC sediments, the soils in most sites exceed both the highest 2016 and 2019 %TOC values while the ER sites are comparable with the GB/HSC sites (%TOC range: 0.19-11.38%). The highest Elizabeth River %TOC was at site CS-A, which is an industrialized site adjacent to an active shipyard and is the location of a historical wood treatment facility

4.4.1.2. PAH Distributions

Four distinct sample groups were analyzed by GC-MS in this study: sediment cores (2016 Cores), soils (2017 soils), GB/HSC surface sediments (2019 GB/HSC Sed), and ER surface sediments (2018 ER Sediments). To verify the variability between each group's PAH distribution, a one-way ANOVA analysis was run between all four sample groups' EPA Priority PAHs (Figure 4-2a) and Total PAHs with alkylated PAHs (Figure 4-2b). The Total PAHs with alkylated PAHs included a short list of alkylated PAHs, which are summarized in Table C 1. Both the EPA Priority PAHs and the Total PAHs with alkylated PAHs groups were found to be statistically distinct (EPA PAHs: $p<0.0001$; $R^2= 0.4543$ and Total PAHs with alkylated PAHs: ($p<0.0001$; $R^2=0.4816$).

The Total 16 EPA Priority PAHs (Total EPA 16) for Galveston Bay sediments ranged between 115-794 µg/kg (2016 Cores) and 41-18,086 µg/kg (2019 GB/HSC surface sediments), while the Elizabeth River sediments ranged from of 714-6,792,632 µg/kg. These range differences indicate both regions have unique PAH sediment source loading with distinct PAH concentrations. In contrast to these sediment samples, the Manchester soils have relatively low Total EPA 16 concentrations (range of 87-14,953 µg/kg) compared to the Elizabeth River sediments, but a comparable range to the Galveston Bay sediments. Similar ranges are observed for the Total PAHs with alkylated PAHs (Figure 4-2a & 4-2b; Table 4-1) as this sum included several alkylated PAHs also determined in the soils by GC-MS.

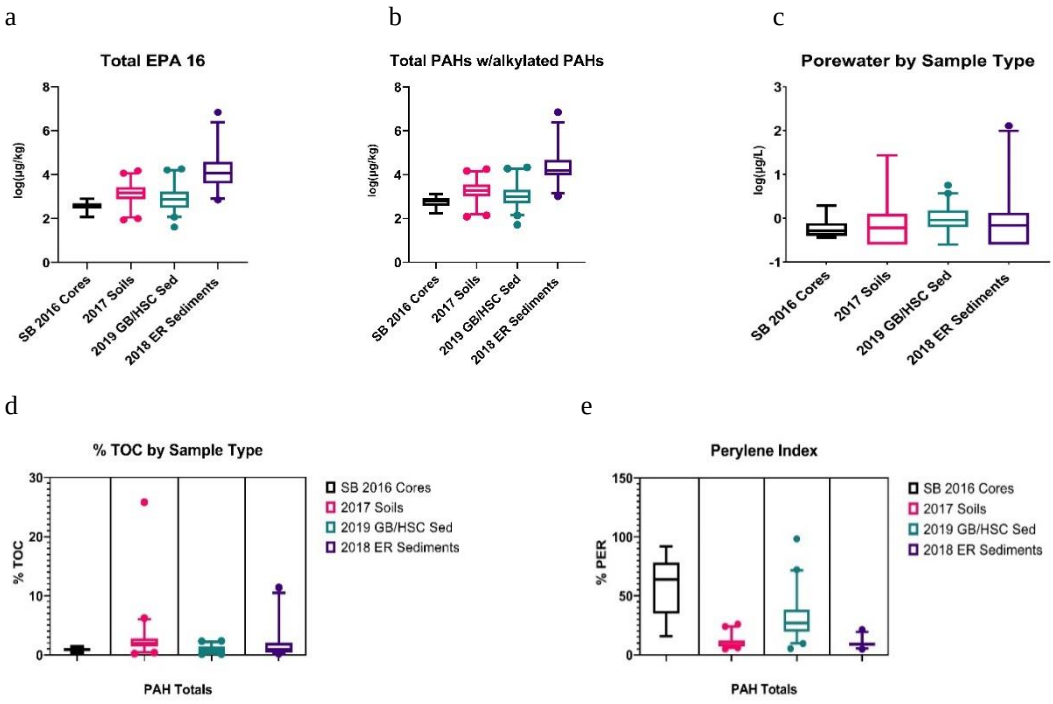

Figure 4-2 Comparative PAH distributions between the EPA 16 PAHs (a) and Total PAHs with VIMS alkylated PAHs (b) in log(µg/kg). Both (a) and (b) boxplots illustrate sample type differences: the 2016 sediment cores (black), GB/HSC surface sediments (pink), Manchester soils (green), and Elizabeth River surface sediments (purple) with a one-way ANOVA confirming each sample type is unique and different from the others (EPA 16 PAHs: $p<0.0001$; $R^2=0.4543$ and VIMS alkyl PAHs: $p<0.0001$; 0.4861). Panel (c) demonstrates the ranges of each sample type porewater values in log-normalized µg/L, while panel (d) compares the percent perylene (% PER) ranges between sample types.

Given the biosensor's sensitivity for 3-5 ring PAHs (Li et al., 2016b; Spier et al., 2009), these ring structures along with a portion of 2-Ring PAHS were observed in all four sample types (Figure C 2). A one-way ANOVA confirmed each variability between each ring structure group (Figure C 2: (a): $p<0.0001$, $R^2=0.8065$; (b): $p<0.0001$, $R^2=0.5688$; (c): $p<0.0001$, $R^2=0.4137$; (d): $p<0.0001$, $R^2=0.1880$). In each of the sample types, the median values for 4 and 5-Ring PAHs were 210 and 203 µg/kg for the 2016 sediment cores, 836 and 448 µg/kg for the 2017 soils, 365 and 340 µg/kg for the 2019 GB/HSC sediments, and 6,483 and 3230 µg/kg for the Elizabeth River sediments suggesting when combined, there are detectable PAHs in these sediment porewaters. Figure 4-3 illustrates the predictivity of the biosensor with a goodness of fit being 0.766, which further supports its utility as a rapid tool for PAH characterization in both sediments and soils.

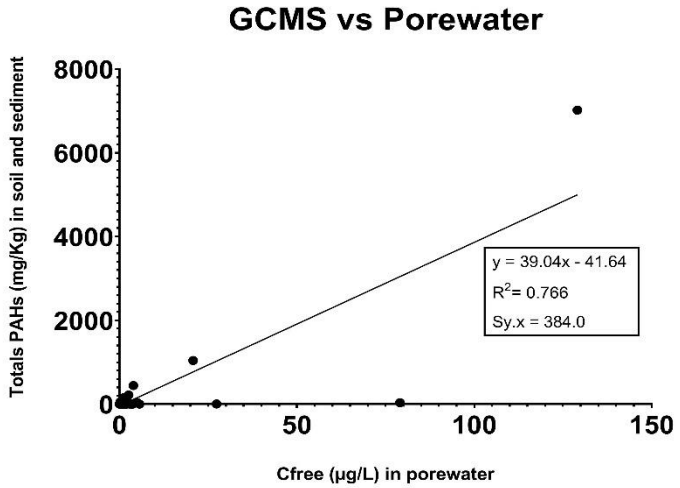

Figure 4-3 A correlation analysis between the GC-MS total PAH concentrations (mg/kg) versus porewater C_{free} (µg/L) for the predictivity of PAH detection by the KinExA Inline Biosensor where y = 39.04x - 41.6 (Goodness of Fit: R^2 = 0.766 and the standard deviation of the residuals (Sy.x) = 384.0).

4.4.2. **PAH Sourcing**

To understand potential PAH inputs, double-plot ratios were analyzed for all four sample groups using BaA/(BaA + CHR) vs Fl/(Fl + PY) (Figure 4-4). Both pyrogenic indices and perylene indices were calculated for the GB/HSC sediments and soils; however, only the perylene index was calculated for the Elizabeth River sediments as the alkylated PAHs detected by VIMS were not the same as GERG (Table C 1). The pyrogenic index suggests the predominance of petrogenic or pyrogenic origins in a sample where a range of 0-0.05 indicates petroleum sources and an excess of this range indicates pyrogenic sources (Wang et al., 2014). In contrast, the perylene index is the percentage of perylene detected within the total of the parent 5-ring PAH isomers (Wang

et al., 2014). This latter index is useful for indicating whether detected PAHs occurred due to anoxic conditions transforming organic matter, which is also known as biogenic or diagenetic origins (Boehm, 2005; Stogiannidis & Laane, 2015; Wang et al., 2014).

a

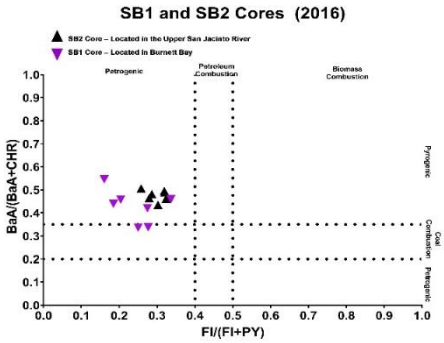

b

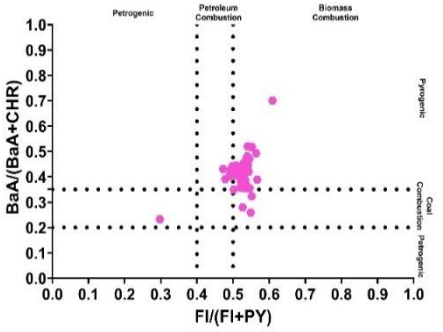

c

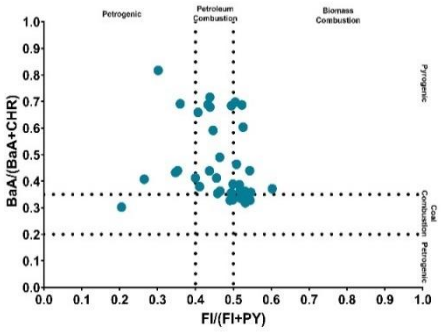

d

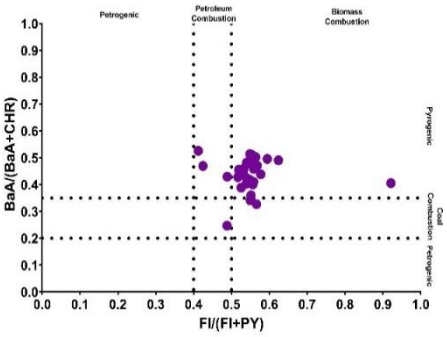

Figure 4-4 The double-ratio plot of BaA/(BaA+CHR) vs Fl/(Fl+PY) are illustrated for the 2016 sediment cores (a), the 2017 soils (b - pink), the 2019 sediments from GB/HSC (c – green), and the 2020 sediments from the Elizabeth River (d - purple). Both cores indicate petrogenic/pyrogenic sourcing (a) while both the 2017 soils (b) and 2019 GB/HSC sediments have mixed sourcing.

However, a unique pyrogenic PAH source is creosote, a distillate of coal tar, both of which are predominated by 5-6 ring PAHs and there is a distinct prevalence of these PAHs parent compounds compared to their alkylated homologs (Boehm, 2005; Merrill & Wade, 1985). Due in part to the historical wood treatment facilities along the Elizabeth River, such as Atlantic Wood, the Elizabeth River sediments are known for predominantly creosote contamination (Brown et al., 2017; Di Giulio & Clark, 2015; Merrill & Wade, 1985). Consequently, the sediments collected within this tidal estuary served as a known creosote contaminated area to compare with the GB/HSC sediments and soils.

In Figure 4-4a, the two 2016 sediment cores predominantly originate from a mixture of petrogenic (0.15-0.35 Fl/(Fl+PY)) and pyrogenic (0.3-0.6 BaA/(BaA+PY)) sources. The pyrogenic index solidifies the pyrogenic inputs as all values exceed crude oil/heavy oil and fuel pyrogenic index range (Wang et al., 2014). The perylene index, on the other hand, indicates all core samples have a biogenic origin, which is sensible due to the sediments being under anoxic conditions at depth. The soils in comparison, consist of both petroleum and biomass combustion (0.45-0.60 Fl/(Fl+PY)) as well as coal combustion (0.25-0.35 BaA/(BaA+PY)) (Figure 4-4b). Two unique sites from this general trend are sites 59 and 61 both of which are comprised of more alkylated PAHs than the parent PAHs. However, like the sediment cores, all samples except site 61 have pyrogenic inputs. At site 61, the pyrogenic index of 0.06 indicates this site may have a heavy fuel or oil input. Unlike the sediment cores, the soil perylene index varied with a

few sites exceeding 10%, which indicated the biogenic origins may be associated with the organic matter in the floodwaters.

The 2019 GB/HSC sediments follow a similar trend as the soils for relative PAH sources, except for several sites with a petrogenic/pyrogenic source (HSC 7; HSC 13; HSC 15; HSC 17, HSC 18) and one with a petrogenic/coal combustion source (HSC 2) (Figure 4-4c). The five sites with petrogenic/pyrogenic sourcing are located within the upper HSC and near the more industrialized portions of the channel. Site HSC 2 is located near Morgan's Point and Atkins Island; both of which are secondary entry points to the Upper HSC from the Bolivar Roads/Gulf of Mexico HSC entry. Of the sites with petroleum combustion or biomass combustion and pyrogenic origins, there is a near split between these groupings from 0.4-0.46 Fl/(Fl+PY) and 0.49-0.54 (Fl/(Fl+PY) (Figure 4-4c). The former Fl/(Fl+PY) range could be attributed to roadway dust (Yunker et al., 2002), while the latter is bordering the transition range of petroleum sources to combustion sources (Yunker et al., 2002). The pyrogenic index for all the GB/HSC samples indicated pyrogenic origins, while the perylene index indicated biogenic origins influenced several sites. Compared to the 2016 sediment cores, most of the GB/HSC sediments did not have biogenic inputs as a key PAH source, except for site HSC 12, which is located across from the San Jacinto Park in Buffalo Bayou.

The Elizabeth River sediments are uniquely clustered within the range of 0.51-0.62 Fl/(Fl+PY) with five sites separate from this range (PC-A; SC1-A; SP-A; SP-B; RF-A) (Figure 4-4d). The clustered sites create a boundary within the range of coal tar's Fl/(Fl+PY) ratio value (0.58) (Yunker et al., 2002) implicating creosote, a distillate of

this PAH. The perylene index for the Elizabeth River is mostly below 10% indicating few sites have biogenic inputs; however, a few sites such as LF-A, MP2-B, SC1-A, and WB-A exceed 10% indicating these sites have some biogenic inputs.

4.4.3. **PAH Risk in Soils and Sediment**

The GC-MS PAH results for the soils were inputted into the RSL Calculator using the settings discussed in the methods section. Of the outputs, risks to both human children (Figure 4-5a) and adults (Figure 4-5b) were considered for three routes of exposure: ingestion, dermal, and inhalation. Both the ingestion and dermal exposure routes are of concern, because of documented sediment deposits being reported near residences after Hurricane Harvey (Karaye et al., 2019). However, each route of exposure for PAHs had a hazard quotient (HQ) value less than 1. Should these HQs exceed 1, additional soil studies for exposure assessment and soil management would have been required to determine specific site characteristics and potential health impacts from these soils.

a b

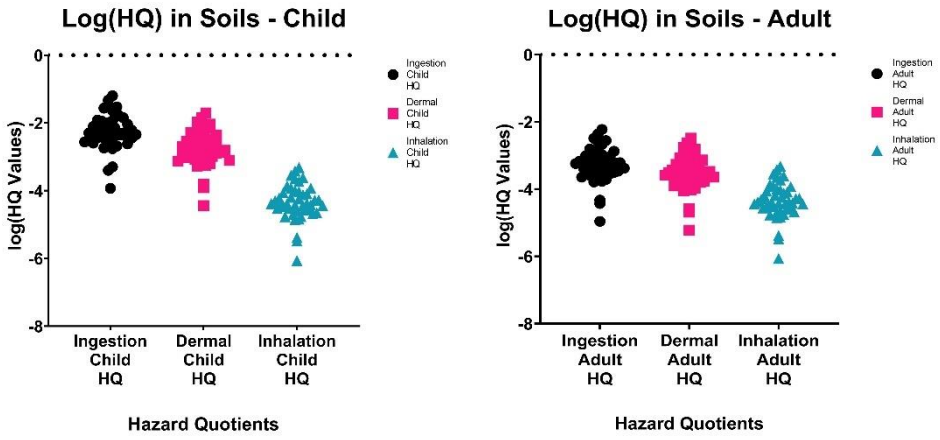

Figure 4-5 Given the GC/MS whole-soil analysis collected for PAHs, these values were inputted to the USEPA Regional Screening Level (RSL) Calculator (United States Environmental Protection Agency, 2017) to calculate the ingestion risk (black circles), dermal risk (pink squares), and inhalation risk (turquoise triangles) for both children (a) and adults (b). Should values exceed 1.00 (dotted line at y = 0) further investigation is required to determine the extent of the exposure risk. For all the soils analyzed in the Manchester Neighborhood, their risk values all fell well below 1.00 indicating low exposure risk in this particular media.

To understand the risk to benthic organisms in the sediments of both GB/HSC and the Elizabeth River, the USEPA's Region 4 Ecological Screening Value (R4-ESV) and the Refinement Screening Value (R4- RSV) are used to compare individual PAH parent compound concentrations to values of potential remedial concern. All PAH concentrations were normalized to organic carbon and are reported in μg/kg OC. Of the sediments analyzed, the 2016 sediment cores were above the R4-ESV values, but below the R4-RSV, thus indicating these sediments were within bounds and did not require additional lines of evidence for ecological risk assessment (Table C 3). However, of the 2019 GB/HSC sediments and the Elizabeth River (ER) sediments, all maximum values of the individual PAHs listed exceeded the R4-RSV values (Table 4-2). Since our sediment values for both ER and GB/HSC sediments exceed the R4-RSV, our results support a need for future investigations that consider mixture effects of these PAHs and the related toxicity mechanisms for ecological risk assessment (United States Environmental Protection Agency, 2018). These additional investigations are outside of the scope of this current study; however, our results will serve as a baseline for future research within these two regions.

	GB/HSC Min	ER Min	GB/HSC Median	ER Median	GB/HSC Max	ER Max	GB/HSC IQR	ER IQR	R4-ESV	Region 4 Refinement Screening Value (RSV)
LMW PAHs										
Acenaphthene	891	0	2178	20376	7176	1119096	1552; 4357	0; 130371	6.7	4910
Acenaphthylene	2889	0	7061	1656	23268	64538	5031; 14126	0; 19034	5.9	4520
Anthracene	4255	159	10401	18959	34274	13086420	7411; 20808	159; 141003	57	5940
Fluorene	1495	0	3655	22355	12044	4245043	2604; 7312	0; 171292	77	5380
Naphthalene	1773	0	4333	13327	14277	1809650	3087; 8668	0; 55693	176	3850
Phenanthrene	11219	477	27421	108269	90356	16126081	19537; 54855	477; 310825	204	5960
HMW PAHs										
Benzo(a)anthracene	15357	761	37535	108059	123683	1623022	26744; 75088	761; 337120	108	8410
Benzo(b)fluoranthene	51482	1118	125834	107456	414642	1059391	89657; 251728	1118; 418483	190	9790
Benzo(k)fluoranthene	11591	704	28330	114130	93351	993259	20185; 56673	704; 356973	240	9810
Benzo(g,h,i)perylene	18322	0	44783	66866	147568	723984	31908; 89588	0; 182012	170	10900
Benzo(a)pyrene	23288	925	56921	93767	187564	1262362	40557; 113870	925; 333496	150	9650
Chrysene	30368	991	74227	108236	244589	2079610	52887; 148489	991; 379116	166	8440
Dibenzo(a,h)anthracene	4591	0	11223	16739	36980	138340	7996; 22451	0; 73240	33	11200
Fluoranthene	40217	1322	98301	237071	323915	8812940	70039; 196648	1322; 1039797	423	7070
Indeno(1,2,3-c,d)pyrene	17889	314	43724	71648	144078	933460	31154; 87470	314; 198423	200	11200
Perylene	10337	724	25267	28826	83258	263957	18003; 50546	724; 107376	-	9680
Pyrene	37164	1162	90838	223798	299326	6443210	64723; 181720	1162; 964517	195	6970

Table 4-2 The summary statistics for individual PAHs in the 2018 Elizabeth River (ER) surface sediments and GB/HSC surface sediments are reported in µg/kg OC and compared to the USEPA Region 4's Ecological Screening Value (R4-ESV) and Refinement Screening Value (R4 – RSV) for freshwater sediments. These value comparisons contextualize how the individual PAHs may contribute to sediment toxicity.

4.5. Discussion

4.5.1. PAH Predictivity Using KinExA Biosensor

Environmental sampling is often extensive and the use of traditional analytical methods of HPLC or GC to characterize chemical compounds requires both time and money. When a natural disaster occurs, comparisons to pre-disaster baseline are sought to improve understanding of where contaminated environmental media may have traveled and the impact these shifted contaminants may pose for the environment and the public's health (Bera et al., 2019; Birch & Lee, 2018; Camargo et al., 2020; Dellapenna et al., 2020; Horney et al., 2018; Kiaghadi & Rifai, 2019). The biosensor technology applied and analyzed in this project demonstrates a rapid, flexible, and cost-effective method to assess for PAHs within both soils and sediments, two matrices often implicated with natural disasters, such as floods and hurricanes. Additionally, the freely dissolved PAH value (C_{free}) determined using the biosensor is representative of a general PAH total. With this C_{free} value, follow-up sediment or soil kinetic and toxicity studies can be prioritized for site characterization and potential exposures.

Since traditional guidance related to sediment toxicity utilize dry-weight concentrations or mass-based concentrations, a knowledge gap remains between how freely dissolved concentration (C_{free}) impacts sediment toxicity (United States Environmental Protection Agency, 2018). Therefore, efforts continue to improve understanding of the relationship between bulk-sediment and sediment porewater partitioning and sediment toxicity, since organic carbon and other organic matter present in sediments and soils can impact PAH partitioning (Arp et al., 2009; Ruby et al., 2016;

United States Environmental Protection Agency, 2018). In this study, despite variable %TOC, the porewater C_{free} detected provided initial predictions expected of the whole-soil/sediment GC-MS analysis. By characterizing dissolved PAH concentrations first through the biosensor, sample analysis by traditional GC-MS is streamlined for further PAH characterization.

4.5.2. **Implications for Disaster Research and Exposure Assessment**

The value of the biosensor in disaster research and exposure assessment is to serve as an adaptable tool both in the lab and in the field. The resulting PAH concentrations can serve as a guide to prioritizing environmental matrices for environmental health exposures after a disaster as well as provide preliminary data to share while in the field for risk communications. Due to the ubiquitous nature of PAHs found throughout the world, and especially within urban and industrialized environments, the biosensor offers the opportunity to determine follow-up experimental needs within a wide range of environments. The biosensor's comparable results to passive samplers also support its implementation for future fieldwork (Conder et al., 2021).

4.5.3. **Limitations**

This project has several important limitations. The quantities of porewater samples were low, despite centrifugation. This was in part due to there not being enough samples as well as the lack of porewater in the samples. For future experiments involving soil analysis, in particular, we recommend testing a wide range of soil types to understand how the porewater and soil chemistry impact porewater yield as well as the

PAH portioning properties. Regarding the sediment analysis, pre-disaster pollution sources are important to document, as many of the GB/HSC sediments were well below any of the Elizabeth River sediment PAH concentrations. Comparisons with known polluted samples can help gauge levels of potential contamination of sites with unknown PAH inputs.

4.6. Conclusions

This project demonstrates the screening ability of the KinExA Inline Biosensor within two tidal estuarine environments and for the first time in soils. The biosensor is an asset for DR2, especially when vulnerable human and ecological populations are located near a potential site of concern. The biosensor is capable of supplementing GC/MS analysis as well as passive sampler analysis (Conder et al., 2021). Data are provided in real-time and the biosensor is compatible with field-work analysis. Despite a lack of guidelines for freely dissolved PAHs, the biosensor offers insights into which fraction of PAHs are bioavailable or bioaccessible in the freely dissolved phase compared to the bulk sediment on which many sediment quality guidelines are based (McGrath et al., 2019; United States Environmental Protection Agency, 2018). These results offer preliminary PAH exposure risk considerations and ultimately will help streamline additional analytical analyses and lines of evidence required for environmental health.

5. SUMMARY & CONCLUSIONS

5.1. Summary

In summary, we show the applicability of three tools for chemical distribution characterization. Aim 1 applies a SEM to determine whether a baseline dataset existed for this region. This first tool helped us document multiple chemicals detected in GB/HSC, but recorded data varied between agency-based and peer-reviewed articles. We also found a need to improve environmental reporting methods through this unique approach.

As PAHs are common urban contaminants (Birch & Lee, 2018; Hartzell et al., 2017; Hussar et al., 2012; Kanzari et al., 2014; Rocha & Palma, 2019), Aim 2 focuses on their distribution under pre- and post-Hurricane Harvey conditions. In this study, we found a small, but detectable, increase in surface sediment PAH concentrations after Hurricane Harvey. The kriging results estimate that the regions of Morgan's Point and the Upper HSC as future areas to sample. Therefore, these results illustrated an approach that could be applied to other contaminated environments impacted by natural disasters.

The final tool in Aim 3 applies a technology called a KinExA Inline Biosensor (biosensor). This approach is rapid and cost-effective for PAH detection in environmental media. With the biosensor freely dissolved PAH concentrations in soils and sediments can be calculated; both of which play a role in DR2 and sediment management research. The real-time analysis and sensitivity of the biosensor also offer insights into the potential bioavailability or bioaccessibilty of PAHs in porewater. This

approach is a contrast to the traditional GC-MS analysis of bulk soils and sediments, which may over or underestimate the bioavailable or bioaccessible PAH fraction (Arp et al., 2009; Ruby et al., 2016).

Collectively, this dissertation offers several approaches to aid in DR2, while also considering relevant chemical exposures within an urban environment. These tools are not region specific and can therefore be applied to other urban environments. Our approaches also offer the opportunity to identify and characterize relevant environmental complex mixtures for future exposure assessments and toxicity testing.

5.2. Study Significance

With the possibility of natural disasters redistributing chemicals, there is a need for rapid exposure characterization. Therefore, this dissertation seeks to develop rapid sampling methods that help characterize contaminant exposure in Houston communities. GB/HSC serves as an excellent case-study region due to its historical and current contamination (Al Mukaimi, 2018b; Bera et al., 2019; Howell et al., 2011b; Lakshmanan et al., 2010; Louchouarn et al., 2018; Oziolor et al., 2014a; Qian et al., 2001; Yeager et al., 2007). With chemical exposures occurring as complex mixtures (Tsatsakis et al., 2016), a knowledge gap remains for protective mixture exposure measures. This dissertation research is therefore significant as it applies several tools for the synthesis and characterization of mixtures under normal and DR2 conditions. Collectively, the findings presented here help fill the following data gaps: 1) available chemical data in GB/HSC, 2) post-Hurricane Harvey PAH distributions, and 3) real-time detection of

PAHs in GB/HSC. Together these tools can improve sampling strategies under normal and DR2 contexts.

5.3. Limitations

Each study in this dissertation has limitations; however, this dissertation as a whole sheds light upon chemical distributions in GB/HSC and how these chemicals may be of concern for DR2. In Aim 1, a SEM is used to determine if a baseline chemical dataset existed in GB/HSC. This aim also sought to identify any potential chemical spatial or temporal patterns. During scoping development, specific terms such as "Houston Ship Channel" yielded too few studies, while "Gulf of Mexico" was too broad. Thus, a mixture of general key location terms, such as "Houston," "Galveston," and "Gulf Coast" were used to hone the study scope. However, even with our search strategy, our search may have missed articles, and with regular website development, any recent publications will not have been included in Aim 1.

Another limitation in Aim 1 were limited geolocation data. Both the federal and state monitoring programs provided specific geocoordinates, but many of the academic articles were inconsistent. This reporting discrepancy made it difficult to discern whether there were spatial or temporal trends.

Due to limited pre-Harvey sediment samples, the pre- and post-Hurricane Harvey PAH comparisons were not robust for quantitative analysis. Therefore, we used 1996 NOAA data to provide initial background PAH distributions. If additional data points were available for 2015 or 2016, PAH comparisons may have improved. This research aim therefore provides a reference baseline for future PAH characterization in GB/HSC.

Environmental analysis often possesses limited sample sizes, which can be exacerbated by natural disaster conditions. For example, there was limited porewater in several of the post-Hurricane Harvey soil samples analyzed in Aim 3. However, as long as samples were at least 2mL, the biosensor was able to analyze the sample for PAHs. The GB/HSC results in Aim 3 show low PAH concentrations in the porewater; therefore, we used contaminated Elizabeth River sediments to compare highly contaminated creosote sites to the low values seen in GB/HSC.

The limitations in each aim offer the opportunity for future monitoring studies to focus sample collections in the Upper HSC, while also targeting ecotoxicology studies for complex environmental mixtures. Overall, this dissertation provides additional data for the fields of public health, DR2, environmental toxicology, exposure science, environmental risk assessment, and human health risk assessment.

5.4. Future Directions

Given the tools outlined in this research, there is room to expand and further refine their utility in DR2 and other urban environments. If Aim 1 is reconducted, a specific online search for grey literature can be developed to identify relevant reports and white papers. However, a challenge to consider is the reproducibility of search engines used as websites and web-based platforms are regularly updated. A comparative analysis between GB/HSC and other urban estuaries' chemical data may yield additional insights regarding chemical contamination reporting. This comparison may also identify areas for future research.

Due to limited pre-Harvey data in Aim 2, our results provide a new reference PAH baseline for future spatial and temporal studies to expand upon. The pre- and post-sediment conditions and kriging results suggest general areas to sample in the future for both DR2 and normal conditions. By considering new kriging approaches for contaminant or human activity estimation (Kim et al., 2017; McLeod et al., 2017; Ver Hoef, 2018), additional environmental variables can be identified for future studies to model.

Aim 3 results suggest the biosensor is applicable for both rapid PAH detection in soils and sediments. The real-time data collected also indicates the biosensor is a useful technology for future DR2 projects conducted with GB/HSC as well as the City of Houston. The biosensor's relevance and applicability will continue, since PAHs are a common exposure within Houston and GB/HSC (Bera et al., 2019; Camargo et al., 2020; Horney et al., 2018; Karaye et al., 2019; Oziolor et al., 2014a; Sansom et al., 2018; Sansom et al., 2021). If the biosensor is incorporated into DR2 and regular monitoring programs, future studies could be developed to identify relevant PAH point sources, prioritize sediment or soil toxicity studies, and quantify preliminary PAH exposures in GB/HSC.

The key findings from this dissertation therefore include several applicable tools that can further our understanding of relevant chemical contaminant exposures within an estuarine urban environment.

6. REFERENCES

Agency for Toxic Substances and Disease Registry. (1995). *Toxicological Profile for Polycyclic Aromatic Hydrocarbons, U.S. Department of Health & Human Services, Public Health Service, Agency for Toxic Substances and Disease Registry, Washington, D.C., August, 1985*. 1–487. https://doi.org/10.3109/15569529909037564

Aguilar, L., Williams, E. S., Brooks, B. W., & Usenko, S. (2014). Development and application of a novel method for high-throughput determination of PCDD/Fs and PCBs in sediments. *Environmental Toxicology and Chemistry*, *33*(7), 1529–1536. https://doi.org/10.1002/etc.2579

Aiassa, E., Higgins, J. P. T., Frampton, G. K., Greiner, M., Afonso, A., Amzal, B., Deeks, J., Dorne, J. L., Glanville, J., Lövei, G. L., Nienstedt, K., O'connor, A. M., Pullin, A. S., Rajić, A., & Verloo, D. (2015). Applicability and Feasibility of Systematic Review for Performing Evidence-Based Risk Assessment in Food and Feed Safety. *Critical Reviews in Food Science and Nutrition*, *55*(7), 1026–1034. https://doi.org/10.1080/10408398.2013.769933

Al Mukaimi, M. E., Dellapenna, T. M., & Williams, J. R. (2018). Enhanced land subsidence in Galveston Bay, Texas: Interaction between sediment accumulation rates and relative sea level rise. *Estuarine, Coastal and Shelf Science*, *207*(February), 183–193. https://doi.org/10.1016/j.ecss.2018.03.023

Al Mukaimi, M. E., Kaiser, K., Williams, J. R., Dellapenna, T. M., Louchouarn, P., & Santschi, P. H. (2018). Centennial record of anthropogenic impacts in Galveston Bay: Evidence from trace metals (Hg, Pb, Ni, Zn) and lignin oxidation products. *Environmental Pollution*, *237*, 887–899. https://doi.org/10.1016/j.envpol.2018.01.027

Almukaimi, M. E. A. Y. S. (2016). *Geochemical and sedimentary record of urbanization and industrialization of the Galveston Bay watershed* [Texas A&M University]. http://proxy.library.tamu.edu/login?url=https://www.proquest.com/dissertations-theses/geochemical-sedimentary-record-urbanization/docview/1825269927/se-2?accountid=7082

Aly, N. A., Luo, Y. S., Liu, Y., Casillas, G., McDonald, T. J., Kaihatu, J. M., Jun, M., Ellis, N., Gossett,

S., Dodds, J. N., Baker, E. S., Bhandari, S., Chiu, W. A., & Rusyn, I. (2020). Temporal and spatial analysis of per and polyfluoroalkyl substances in surface waters of Houston ship channel following a large-scale industrial fire incident. *Environmental Pollution*, *265*, 115009. https://doi.org/10.1016/j.envpol.2020.115009

Apeti, D. A., Lauenstein, G. G., & Evans, D. W. (2012). Recent status of total mercury and methyl mercury in the coastal waters of the northern Gulf of Mexico using oysters and sediments from NOAA's mussel watch program. *Marine Pollution Bulletin*, *64*(11), 2399–2408. https://doi.org/10.1016/j.marpolbul.2012.08.006

Arp, H. P. H., Breedveld, G. D., & Cornelissen, G. (2009). Estimating the in situ sediment-porewater distribution of PAHs and chlorinated aromatic hydrocarbons in anthropogenic impacted sediments. *Environmental Science and Technology*, *43*(15), 5576–5585. https://doi.org/10.1021/es9012905

Bacosa, H. P., Steichen, J., Kamalanathan, M., Windham, R., Lubguban, A., Labonté, J. M., Kaiser, K., Hala, D., Santschi, P. H., & Quigg, A. (2020). Polycyclic aromatic hydrocarbons (PAHs) and putative PAH-degrading bacteria in Galveston Bay , TX (USA), following Hurricane Harvey (2017). *Environmental Science and Pollution Research*, *27*, 34987–34999. https://doi.org/10.1007/s11356-020-09754-5

Baird, S. J. S., Bailey, E. A., & Vorhees, D. J. (2007). Evaluating human risk from exposure to alkylated PAHs in an aquatic system. *Human and Ecological Risk Assessment*, *13*(2), 322–338. https://doi.org/10.1080/10807030701226277

Barron, M. G., & Wharton, S. R. (2005). Survey of methodologies for developing media screening values for ecological risk assessment. *Integrated Environmental Assessment and Management*, *1*(4), 320–332. https://doi.org/10.1897/1551-3793(2005)1[320:SOMFDM]2.0.CO;2

Behera, B. K., Das, A., Sarkar, D. J., Weerathunge, P., Parida, P. K., Das, B. K., Thavamani, P., Ramanathan, R., & Bansal, V. (2018). Polycyclic Aromatic Hydrocarbons (PAHs) in inland aquatic ecosystems: Perils and remedies through biosensors and bioremediation. *Environmental Pollution*, *241*, 212–233. https://doi.org/10.1016/j.envpol.2018.05.016

Behnke, N. L., Cronk, R., Shackelford, B. B., Cooper, B., Tu, R., Heller, L., & Bartram, J. (2020).

Environmental health conditions in protracted displacement: A systematic scoping review. *Science of the Total Environment*, *726*, 138234. https://doi.org/10.1016/j.scitotenv.2020.138234

Bera, G., Camargo, K., Sericano, J. L., Liu, Y., Sweet, S. T., Horney, J., Jun, M., Chiu, W., Rusyn, I., Wade, T. L., & Knap, A. H. (2019). Baseline data for distribution of contaminants by natural disasters : results from a residential Houston neighborhood during Hurricane Harvey flooding. *Heliyon*, *5*(August), e02860. https://doi.org/10.1016/j.heliyon.2019.e02860

Bernes, C., Bullock, J. M., Jakobsson, S., Rundlöf, M., Verheyen, K., & Lindborg, R. (2017). How are biodiversity and dispersal of species affected by the management of roadsides? A systematic map. *Environmental Evidence*, *6*(1), 1–16. https://doi.org/10.1186/s13750-017-0103-1

Betts, K. (2014). A Survey of Environmental Chemistry Around the World : Studies , Processes , Techniques , and Employment. *American Chemical Society*, 54.

Bilotta, G. S., Milner, A. M., & Boyd, I. (2014). On the use of systematic reviews to inform environmental policies. *Environmental Science and Policy*, *42*, 67–77. https://doi.org/10.1016/j.envsci.2014.05.010

Birch, G. F. (2018). A review of chemical-based sediment quality assessment methodologies for the marine environment. *Marine Pollution Bulletin*, *133*(November 2017), 218–232. https://doi.org/10.1016/j.marpolbul.2018.05.039

Birch, G. F., & Lee, S. B. (2018). Baseline physio-chemical characteristics of Sydney estuary water under quiescent conditions. *Marine Pollution Bulletin*, *137*(June), 370–381. https://doi.org/10.1016/j.marpolbul.2018.10.041

Blake, E. S., & Zelinsky, D. A. (2018). *NATIONAL HURRICANE CENTER TROPICAL CYCLONE REPORT HURRICANE HARVEY (AL092017)*. https://doi.org/https://www.nhc.noaa.gov/data/tcr/AL092017_Harvey.pdf

Boehm, P. D. (2005). Ch. 15 Polycyclic Aromatic Hydrocarbons (PAHs). In R. D. Morrison & B. L. Murphy (Eds.), *Environmental Forensics: Contaminant Specific Guide*. Pergamon Press Ltd. https://doi.org/10.1016/B978-0-12-507751-4.50037-9

Brown, D. R., Thompson, J., Chernick, M., Hinton, D. E., & Di Giulio, R. T. (2017). Later life swimming performance and persistent heart damage following subteratogenic PAH mixture exposure in the

Atlantic killifish (Fundulus heteroclitus). *Environmental Toxicology and Chemistry*, *36*(12), 3246–3253. https://doi.org/10.1002/etc.3877

Camargo, K., Sericano, J. L., Bhandari, S., Hoelscher, C., Mcdonald, T. J., Chiu, W. A., Wade, T. L., Dellapenna, T. M., Liu, Y., & Knap, A. H. (2020). Polycyclic aromatic hydrocarbon status in post-hurricane Harvey sediments : Considerations for environmental sampling in the Galveston Bay / Houston Ship Channel region. *Marine Pollution Bulletin*, *June*, 111872. https://doi.org/10.1016/j.marpolbul.2020.111872

Campo, R. (2020). *Trade Infrastructure for Global Competitiveness February 6, 2020 - Testimony of Ric Campo*. Port of Houston. https://waysandmeans.house.gov/sites/democrats.waysandmeans.house.gov/files/documents/Campo Testimony.pdf

Carr, R. S., Chapman, D. C., Howard, C. L., & Biedenbach, J. M. (1996). Sediment quality triad assessment survey of the Galveston Bay, Texas system. *Ecotoxicology*, *5*(6), 341–364. https://doi.org/10.1007/BF00351951

Chapman, P. M. (2002). Integrating toxicology and ecology: Putting the “eco” into ecotoxicology. *Marine Pollution Bulletin*, *44*(1), 7–15. https://doi.org/10.1016/S0025-326X(01)00253-3

Chapman, P. M. (2018). Environmental quality benchmarks—the good, the bad, and the ugly. *Environmental Science and Pollution Research*, *25*(4), 3043–3046. https://doi.org/10.1007/s11356-016-7924-2

Chiles, J.-P., & Delfiner, P. (2012). *Geostatistics: Modeling Spatial Uncertainty* (D. J. Balding, N. A. Cressie, G. M. Fitzmaurice, H. Goldstein, I. M. Johnstone, G. Molenberghs, D. W. Scott, A. F. Smith, R. S. Tsay, & S. Weisberg (eds.); 2nd ed.). John Wiley & Sons, Inc.

Chiou, C. T., Mcgroddy, S. E., & Kile, D. E. (1998). Partition characteristics of polycyclic aromatic hydrocarbons on soils and sediments. *Environmental Science and Technology*, *32*(2), 264–269. https://doi.org/10.1021/es970614c

Cochrane Library. (2020). *About Cochrane Reviews*. https://www.cochranelibrary.com/about/about-cochrane-reviews

Cohen Hubal, E. A., Frank, J. J., Nachman, R., Angrish, M., Deziel, N. C., Fry, M., Tornero-Velez, R., Kraft, A., & Lavoie, E. (2020). Advancing systematic-review methodology in exposure science for environmental health decision making. *Journal of Exposure Science and Environmental Epidemiology*. https://doi.org/10.1038/s41370-020-0236-0

Conder, J., Jalalizadeh, M., Luo, H., Bess, A., Sande, S., Healey, M., & Unger, M. A. (2021). Evaluation of a rapid biosensor tool for measuring PAH availability in petroleum-impacted sediment. *Environmental Advances*, *3*(January), 100032. https://doi.org/10.1016/j.envadv.2021.100032

Cuevas, N., Martins, M., & Costa, P. M. (2018). Risk assessment of pesticides in estuaries: a review addressing the persistence of an old problem in complex environments. *Ecotoxicology*, *27*(7), 1008–1018. https://doi.org/10.1007/s10646-018-1910-z

Cui, X., Mayer, P., & Gan, J. (2013). Methods to assess bioavailability of hydrophobic organic contaminants: Principles, operations, and limitations. *Environmental Pollution*, *172*, 223–234. https://doi.org/10.1016/j.envpol.2012.09.013

Davis, E., Walker, T. R., Adams, M., Willis, R., Norris, G. A., & Henry, R. C. (2019). Source apportionment of polycyclic aromatic hydrocarbons (PAHs) in small craft harbor (SCH) surficial sediments in Nova Scotia, Canada. *Science of the Total Environment*, *691*, 528–537. https://doi.org/10.1016/j.scitotenv.2019.07.114

Davis, F. R. (2018). *Spatiotemporal Patterns of Polycyclic Aromatic Hydrocarbons Contamination in the Houston Ship Channel's Sediment* [Texas Southern University]. https://doi.org/2054006125

de Zwart, D., Adams, W., Galay Burgos, M., Hollender, J., Junghans, M., Merrington, G., Muir, D., Parkerton, T., De Schamphelaere, K. A. C., Whale, G., & Williams, R. (2018). Aquatic exposures of chemical mixtures in urban environments: Approaches to impact assessment. *Environmental Toxicology and Chemistry*, *37*(3), 703–714. https://doi.org/10.1002/etc.3975

Dean, K. E., Suarez, M. P., Rifai, H. S., Palachek, R. M., & Larry, K. (2009). Bioaccumulation of polychlorinated dibenzodioxins and dibenzofurans in catfish and crabs along an estuarine salinity and contamination gradient. *Environmental Toxicology and Chemistry*, *28*(11), 2307–2317. https://doi.org/10.1897/08-646.1

Dellapenna, T. M., Hoelscher, C., Hill, L., Al Mukaimi, M. E., & Knap, A. (2020). How tropical cyclone flooding caused erosion and dispersal of mercury-contaminated sediment in an urban estuary : The impact of Hurricane Harvey on Buffalo Bayou and the San Jacinto Estuary, Galveston Bay, USA. *Science of the Total Environment*, *748*, 141226. https://doi.org/10.1016/j.scitotenv.2020.141226

Di Giulio, R. T., & Clark, B. W. (2015). The Elizabeth River Story: A Case Study in Evolutionary Toxicology. *Journal of Toxicology and Environmental Health - Part B: Critical Reviews*, *18*(6), 259–298. https://doi.org/10.1080/15320383.2015.1074841

Dobberstine, J. A. (2007). *Sediment triad approach to finding a suitable reference bayou for Patrick Bayou and similar sites located on the Houston Ship Channel* [Universtiy of Houston - Clear Lake]. http://proxy.library.tamu.edu/login?url=https://www.proquest.com/dissertations-theses/sediment-triad-approach-finding-suitable/docview/304718079/se-2?accountid=7082

Du, J., Park, K., Dellapenna, T. M., & Clay, J. M. (2019a). Corrigendum to "Dramatic hydrodynamic and sedimentary responses in Galveston Bay and adjacent inner shelf to Hurricane Harvey." *Science of the Total Environment*, *697*, 134219. https://doi.org/10.1016/j.scitotenv.2019.134219

Du, J., Park, K., Dellapenna, T. M., & Clay, J. M. (2019b). Dramatic hydrodynamic and sedimentary responses in Galveston Bay and adjacent inner shelf to Hurricane Harvey. *Science of the Total Environment*, *653*, 554–564. https://doi.org/10.1016/j.scitotenv.2018.10.403

Du, J., Park, K., Yu, X., Zhang, Y. J., & Ye, F. (2020). Massive pollutants released to Galveston Bay during Hurricane Harvey: Understanding their retention and pathway using Lagrangian numerical simulations. *Science of the Total Environment*, *704*, 135364. https://doi.org/10.1016/j.scitotenv.2019.135364

Elizabeth River Project, & Virginia Institute of Marine Science. (2020). *State of the Elizabeth River Scorecard*. http://elizabethriver.org/sites/default/files/ERP-State-of-the-River-2020.pdf

Evidence, C. for E. (2018). *Section 3. Planning a CEE Evidence Synthesis*. http://www.environmentalevidence.org/guidelines/section-3

Evidence, C. for E. (2019). *Section 5: Conducting a Search*. http://www.environmentalevidence.org/guidelines/section-5

Farrington, J. W., Tripp, B. W., Tanabe, S., Subramanian, A., Sericano, J. L., Wade, T. L., & Knap, A. H. (2016). Edward D. Goldberg's proposal of "the Mussel Watch": Reflections after 40 years. *Marine Pollution Bulletin*, *110*(1), 501–510. https://doi.org/10.1016/j.marpolbul.2016.05.074

Galveston Bay Estuary Program; TCEQ, USEPA, H. (2019). *Metals in Galveston Bay Sediments*. https://www.galvbaydata.org/www.galvbaydata.org/WaterSediment/WaterandSedimentQuality/Indicators/Metals/tabid/2210/Default.html

Gao, P., da Silva, E. B., Townsend, T., Liu, X., & Ma, L. Q. (2019). Emerging PAHs in urban soils: Concentrations, bioaccessibility, and spatial distribution. *Science of the Total Environment*, *670*, 800–805. https://doi.org/10.1016/j.scitotenv.2019.03.247

Gardinali, P. R. (1996). *Assessment of halogenated aromatic compounds contamination in the Galveston Bay ecosystem* [Texas A&M University]. http://proxy.library.tamu.edu/login?url=https://www.proquest.com/dissertations-theses/assessment-halogenated-aromatic-compounds/docview/304360226/se-2?accountid=7082

Ghosh, U., Luthy, R. G., Cornelissen, G., Werner, D., & Menzie, C. A. (2011). In-situ sorbent amendments: A new direction in contaminated sediment management. *Environmental Science and Technology*, *45*(4), 1163–1168. https://doi.org/10.1021/es102694h

Ghosh, U., Talley, J. W., & Luthy, R. G. (2001). Particle-scale investigation of PAH desorption kinetics and thermodynamics from sediment. *Environmental Science and Technology*, *35*(17), 3468–3475. https://doi.org/10.1021/es0105820

Golash-Boza, T. (2015). *No TitleWriting a Literature Review: Six Steps to Get You from Start to Finish*. The Wiley Network. https://www.wiley.com/network/researchers/preparing-your-article/writing-a-literature-review-six-steps-to-get-you-from-start-to-finish

Haddaway, Neal R. (2018). Open Synthesis: On the need for evidence synthesis to embrace Open Science. *Environmental Evidence*, *7*(1), 4–8. https://doi.org/10.1186/s13750-018-0140-4

Haddaway, Neal R., & Crowe, S. (2018). Experiences and lessons in stakeholder engagement in environmental evidence synthesis: A truly special series Neal Haddaway, Sally Crowe. *Environmental Evidence*, *7*(1), 10–11. https://doi.org/10.1186/s13750-018-0123-5

Haddaway, Neal R., Macura, B., Whaley, P., & Pullin, A. S. (2018). ROSES Reporting standards for Systematic Evidence Syntheses: Pro forma, flow-diagram and descriptive summary of the plan and conduct of environmental systematic reviews and systematic maps. *Environmental Evidence*, *7*(1), 4–11. https://doi.org/10.1186/s13750-018-0121-7

Haddaway, Neal Robert, & Macura, B. (2018). The role of reporting standards in producing robust literature reviews. *Nature Climate Change*, *8*(6), 444–447. https://doi.org/10.1038/s41558-018-0180-3

Hanrahan, G. (2012). Environmental Toxicology and Hazardous Waste Characterization. *Key Concepts in Environmental Chemistry*, 265–293. https://doi.org/10.1016/b978-0-12-374993-2.10009-3

Hanrahan, G., & Hanrahan, G. (2012). Chapter 8 – Soil Chemistry. *Key Concepts in Environmental Chemistry*, 245–262. https://doi.org/10.1016/B978-0-12-374993-2.10008-1

HARC and Galveston Bay Foundation. (2017a). *Galveston Bay*. https://www.galvbaygrade.org/wp-content/uploads/2017/08/2017_Galveston_Bay_Full_Report.pdf

HARC and Galveston Bay Foundation. (2017b). *Galveston Bay Report Card 2017*.

HARC and Galveston Bay Foundation. (2018). *Galveston Bay Report Card 2018*. WWW.GALVBAYGRADE.ORG

HARC, & Foundation, G. B. (2019). *Galveston Bay Report Card 2019*. HARC and Galveston Bay Foundation. https://www.galvbaygrade.org/wp-content/uploads/2019/08/2019_Galveston_Bay_Full_Report.pdf

HARC, & Galveston Bay Foundation. (2020). *Galveston Bay Report Card 2020*. https://www.galvbaygrade.org/wp-content/uploads/2020/09/2020_Galveston_Bay_Full_Report.pdf

Harris County Flood Control District. (2018). *Hurricane Harvey: Impact and Response in Harris County*. https://www.hcfcd.org/Portals/62/Harvey/harvey-impact-and-response-book-final-re.pdf

Hartzell, S. E., Unger, M. A., McGee, B. L., & Yonkos, L. T. (2017). Effects-based spatial assessment of contaminated estuarine sediments from Bear Creek, Baltimore Harbor, MD, USA. *Environmental Science and Pollution Research*, *24*(28), 22158–22172. https://doi.org/10.1007/s11356-017-9667-0

Hartzell, S. E., Unger, M. A., Vadas, G. G., & Yonkos, L. T. (2018). Evaluating porewater polycyclic

aromatic hydrocarbon–related toxicity at a contaminated sediment site using a spiked field-sediment approach. *Environmental Toxicology and Chemistry*, *37*(3), 893–902. https://doi.org/10.1002/etc.4023

Hieke, A. S. C., Brinkmeyer, R., Yeager, K. M., Schindler, K., Zhang, S., Xu, C., Louchouarn, P., & Santschi, P. H. (2016). Widespread Distribution of Dehalococcoides mccartyi in the Houston Ship Channel and Galveston Bay, Texas, Sediments and the Potential for Reductive Dechlorination of PCDD/F in an Estuarine Environment. *Marine Biotechnology*, *18*(6), 630–644. https://doi.org/10.1007/s10126-016-9723-7

Horney, J.A., Casillas, G. A., Baker, E., Stone, K. W., Kirsch, K. R., Camargo, K., Wade, T. L., & McDonald, T. J. (2018). Comparing residential contamination in a Houston environmental justice neighborhood before and after Hurricane Harvey. *PLoS ONE*, *13*(2). https://doi.org/10.1371/journal.pone.0192660

Horney, Jennifer A., Rios, J., Cantu, A., Ramsey, S., Montemayor, L., Raun, L., & Miller, A. (2019). Improving hurricane Harvey disaster research response through academic–practice partnerships. *American Journal of Public Health*, *109*(9), 1198–1201. https://doi.org/10.2105/AJPH.2019.305166

Hou Aixin, DeLaune Ronald D, Tan MeiHuey, Reams Margaret, and L. E. (2009). Toxic Elements in Aquatic Sediments: Distinguishing Natural Variability from Anthropogenic Effects. *Water Air Soil Pollution*, *203*(1), 179–191. https://doi.org/10.1007/s11270-009-0002-3

Houston, C. of. (2021). *Planning and Development: Demographics*. https://www.houstontx.gov/planning/Demographics/

Howell, N. L., Rifai, H. S., & Koenig, L. (2011a). Chemosphere Comparative distribution , sourcing , and chemical behavior of PCDD/Fs and PCBs in an estuary environment. *Chemosphere*, *83*, 873–881. https://doi.org/10.1016/j.chemosphere.2011.02.082

Howell, N. L., Rifai, H. S., & Koenig, L. (2011b). Comparative distribution, sourcing, and chemical behavior of PCDD/Fs and PCBs in an estuary environment. *Chemosphere*, *83*(6), 873–881. https://doi.org/10.1016/j.chemosphere.2011.02.082

Howell, N. L., Rifai, H. S., & Koenig, L. (2011c). Comparative distribution, sourcing, and chemical

behavior of PCDD/Fs and PCBs in an estuary environment. *Chemosphere*, *83*(6), 873–881. https://doi.org/10.1016/j.chemosphere.2011.02.082

Huang, L., Chernyak, S. M., & Batterman, S. A. (2014). PAHs (polycyclic aromatic hydrocarbons), nitro-PAHs, and hopane and sterane biomarkers in sediments of southern Lake Michigan, USA. *Science of the Total Environment*, *487*(1), 173–186. https://doi.org/10.1016/j.scitotenv.2014.03.131

Hussar, E., Richards, S., Lin, Z.-Q., Dixon, R. P., & Johnson, K. A. (2012). Human Health Risk Assessment of 16 Priority Polycyclic Aromatic Hydrocarbons in Soils of Chattanooga, Tennessee, USA. *Water Air Soil Pollution*, *223*(9), 5535–5548. https://doi.org/10.1007/s11270-012-1265-7.

Hwang, H. M., & Foster, G. D. (2006). Characterization of polycyclic aromatic hydrocarbons in urban stormwater runoff flowing into the tidal Anacostia River, Washington, DC, USA. *Environmental Pollution*, *140*(3), 416–426. https://doi.org/10.1016/j.envpol.2005.08.003

Jackson, T. J., Wade, T. L., Sericano, J. L., Brooks, J. M., Wong, J. M., Garcia-Romero, B., & McDonald, T. J. (1998). Galveston Bay: Temporal changes in the concentrations of trace organic contaminants in national status and trends oysters (1986-1994). *Estuaries*, *21*(4 B), 718–730. https://doi.org/10.2307/1353276

James, K. L., Randall, N. P., & Haddaway, N. R. (2016). A methodology for systematic mapping in environmental sciences. *Environmental Evidence*, *5*(1), 1–14. https://doi.org/10.1186/s13750-016-0059-6

Jun, M., & Park, E. S. (2013). Multivariate receptor models for spatially correlated multipollutant data. *Technometrics*, *55*(3), 309–320. https://doi.org/10.1080/00401706.2013.765321

Kanzari, F., Syakti, A. D., Asia, L., Malleret, L., Piram, A., Mille, G., & Doumenq, P. (2014). Distributions and sources of persistent organic pollutants (aliphatic hydrocarbons, PAHs, PCBs and pesticides) in surface sediments of an industrialized urban river (Huveaune), France. *Science of the Total Environment*, *478*, 141–151. https://doi.org/10.1016/j.scitotenv.2014.01.065

Karaye, I., Stone, K. W., Casillas, G. A., Newman, G., & Horney, J. A. (2019). A Spatial Analysis of Possible Environmental Exposures in Recreational Areas Impacted by Hurricane Harvey Flooding, Harris County, Texas. *Environmental Management*, *64*(4), 381–390. https://doi.org/10.1007/s00267-

019-01204-4

Karlsson, M., & Gilek, M. (2020). Mind the gap: Coping with delay in environmental governance. *Ambio*, *49*(5), 1067–1075. https://doi.org/10.1007/s13280-019-01265-z

Kennicutt II, M. C. (2017a). Chapter 4: Sediment Contaminants of the Gulf of Mexico. In *Habitats and Biota of the Gulf of Mexico: Before the Deepwater Horizon Oil Spill* (Vol. 1). https://doi.org/10.1007/978-1-4939-3447-8

Kennicutt II, M. C. (2017b). Chapter 4 - SEDIMENT CONTAMINANTS OF THE GULF OF MEXICO. In *Habitats and Biota of the Gulf of Mexico: Before the Deepwater Horizon Oil Spill*. https://doi.org/10.1007/978-1-4939-3447-8

Kiaghadi, A., & Rifai, H. S. (2019). Physical, Chemical, and Microbial Quality of Floodwaters in Houston Following Hurricane Harvey. *Environmental Science and Technology*, *53*(9), 4832–4840. https://doi.org/10.1021/acs.est.9b00792

Kim, A. W., Vane, C. H., Moss-Hayes, V. L., Beriro, D. J., Nathanail, C. P., Fordyce, F. M., & Everett, P. A. (2019). Polycyclic aromatic hydrocarbons (PAHs) and polychlorinated biphenyls (PCBs) in urban soils of Glasgow, UK. *Earth and Environmental Science Transactions of the Royal Society of Edinburgh*, *108*(2–3), 231–247. https://doi.org/10.1017/S1755691018000324

Kim, S. M., Choi, Y., Yi, H., & Park, H. D. (2017). Geostatistical prediction of heavy metal concentrations in stream sediments considering the stream networks. *Environmental Earth Sciences*, *76*(2). https://doi.org/10.1007/s12665-017-6394-2

Knap, A. H., & Rusyn, I. (2016). Environmental exposures due to natural disasters. *Reviews on Environmental Health*, *31*(1), 89–92. https://doi.org/10.1515/reveh-2016-0010

Kohl, C., McIntosh, E. J., Unger, S., Haddaway, N. R., Kecke, S., Schiemann, J., & Wilhelm, R. (2018). Online tools supporting the conduct and reporting of systematic reviews and systematic maps: A case study on CADIMA and review of existing tools. *Environmental Evidence*, *7*(1), 1–18. https://doi.org/10.1186/s13750-018-0115-5

Kwok, K. W. H., Batley, G. E., Wenning, R. J., Zhu, L., Vangheluwe, M., & Lee, S. (2014). Sediment quality guidelines: Challenges and opportunities for improving sediment management.

Environmental Science and Pollution Research, *21*(1), 17–27. https://doi.org/10.1007/s11356-013-1778-7

Lakshmanan, D., Howell, N. L., Rifai, H. S., & Koenig, L. (2010). Spatial and temporal variation of polychlorinated biphenyls in the Houston Ship Channel. *Chemosphere*, *80*(2), 100–112. https://doi.org/10.1016/j.chemosphere.2010.04.014

Leonard, L. E. (2018). *Pollutant Loads and Distributions Following a Major Flooding Event in Galveston Bay, Texas* [Texas A&M University]. http://hdl.handle.net/1969.1/166541

Li, X., Kaattari, S. L., Vogelbein, M. A., Vadas, G. G., & Unger, M. A. (2016a). A highly sensitive monoclonal antibody based biosensor for quantifying 3-5 ring polycyclic aromatic hydrocarbons (PAHs) in aqueous environmental samples. *Sens Biosensing Res, March 7*(7), 115–120. https://doi.org/doi:10.1016/j.sbsr.2016.02.003

Li, X., Kaattari, S. L., Vogelbein, M. A., Vadas, G. G., & Unger, M. A. (2016b). A highly sensitive monoclonal antibody based biosensor for quantifying 3-ring polycyclic aromatic hydrocarbons (PAHs) in aqueous environmental samples. *Sensing and Bio-Sensing Research*, *7*, 115–120. https://doi.org/10.1016/j.sbsr.2016.02.003

Louchouarn, P., Seward, S. M., Cornelissen, G., Arp, H. P. H., Yeager, K. M., Brinkmeyer, R., & Santschi, P. H. (2018). Limited mobility of dioxins near San Jacinto super fund site (waste pit) in the Houston Ship Channel, Texas due to strong sediment sorption. *Environmental Pollution*, *238*, 988–998. https://doi.org/10.1016/j.envpol.2018.02.003

M. Oziolor, E., De Schamphelaere, K., & Matson, C. W. (2016). Evolutionary toxicology: Meta-analysis of evolutionary events in response to chemical stressors. *Ecotoxicology*, *25*(10), 1858–1866. https://doi.org/10.1007/s10646-016-1735-6

Macura, B., Suškevičs, M., Garside, R., Hannes, K., Rees, R., & Rodela, R. (2019). Systematic reviews of qualitative evidence for environmental policy and management: An overview of different methodological options. *Environmental Evidence*, *8*(1), 1–12. https://doi.org/10.1186/s13750-019-0168-0

Mangano, M. C., Sarà, G., & Corsolini, S. (2017). Monitoring of persistent organic pollutants in the polar

regions: knowledge gaps & gluts through evidence mapping. *Chemosphere*, *172*, 37–45. https://doi.org/10.1016/j.chemosphere.2016.12.124

Mark Vincent, P., Glahan, L. F., & Raphaelson, R. D. (2015). Proceedings of the Western Dredging Association and Texas A&M Univestiy Center for Dreding Studies' "Dredging Summit and Expo 2015." *The History of Dredging at the Port of Houston: Ditching High and Low To Build A Port*, 469–486. https://www.westerndredging.org/phocadownload/Proceedings/2015/7a-1 Vincent-Glahn-Raphaelson Dredge Houston 2015 rer (2).pdf

McGrath, J. A., Joshua, N., Bess, A. S., & Parkerton, T. F. (2019). *Review of Polycyclic Aromatic Hydrocarbons (PAHs) Sediment Quality Guidelines for the Protection of Benthic Life*. *15*(4), 505–518. https://doi.org/10.1002/ieam.4142

McLeod, L., Bharadwaj, L., Epp, T., & Waldner, C. L. (2017). Use of principal components analysis and kriging to predict groundwater-sourced rural drinkingwater quality in saskatchewan. *International Journal of Environmental Research and Public Health*, *14*(9). https://doi.org/10.3390/ijerph14091065

Merrill, E. G., & Wade, T. L. (1985). Carbonized coal products as a source of aromatic hydrocarbons to sediments from a highly industrialized estuary. *Environmental Science & Technology*, *19*(7), 597–603. https://doi.org/10.1021/es00137a003

Miake-Lye, I. M., Hempel, S., Shanman, R., & Shekelle, P. G. (2016). What is an evidence map? A systematic review of published evidence maps and their definitions, methods, and products. *Systematic Reviews*, *5*(28), 1–21. https://doi.org/10.1186/s13643-016-0204-x

Moffatt & Nichol. (2010). *Galveston Bay Regional Sediment Management Galveston , Texas Programmatic Sediment*. *M&N Projec*(Document No. 6731-02RP002 Rev: 1). https://www.epa.gov/sites/production/files/2017-04/documents/galveston_odmds_smmp_2016_0.pdf

Munn, Z., MClinSc, S. M., Lisy, K., Riitano, D., & Tufanaru, C. (2015). Methodological guidance for systematic reviews of observational epidemiological studies reporting prevalence and cumulative incidence data. *International Journal of Evidence-Based Healthcare*, *13*(3), 147–153.

https://doi.org/10.1097/XEB.0000000000000054

Munn, Z., Peters, M. D. J., Stern, C., Tufanaru, C., McArthur, A., & Aromataris, E. (2018). Systematic review or scoping review? Guidance for authors when choosing between a systematic or scoping review approach. *BMC Medical Research Methodology*, *18*(1), 1–7. https://doi.org/10.1186/s12874-018-0611-x

Munn, Z., Stern, C., Aromataris, E., Lockwood, C., & Jordan, Z. (2018a). What kind of systematic review should i conduct? A proposed typology and guidance for systematic reviewers in the medical and health sciences. *BMC Medical Research Methodology*, *18*(1), 1–9. https://doi.org/10.1186/s12874-017-0468-4

Munn, Z., Stern, C., Aromataris, E., Lockwood, C., & Jordan, Z. (2018b). What kind of systematic review should I conduct? A proposed typology and guidance for systematic reviewers in the medical and health sciences. *BMC Medical Research Methodology*, *18*(1), 1–9. https://doi.org/10.1186/s12874-017-0468-4

Muz, M., Escher, B. I., & Jahnke, A. (2020). Bioavailable environmental pollutant patterns in sediments from passive equilibrium sampling. *Environmental Science and Technology*. https://doi.org/10.1021/acs.est.0c05537

National Centers for Environmental Information. (2021). *State of the Climate: National Climate Report for Annual 2020*. https://www.ncdc.noaa.gov/sotc/national/202013

National Oceanic & Atmospheric Administration. (2008). *NOAA Screening Quick Reference*. https://response.restoration.noaa.gov/environmental-restoration/environmental-assessment-tools/squirt-cards.html

National Oceanic & Atmospheric Administration. (2017). *NOAA's National Status and Trends More Data: Gulf of Mexico - Galvestion Bay Organics - Sediment*. National Centers for Coastal Ocean Science. https://products.coastalscience.noaa.gov/collections/ltmonitoring/nsandt/data2.aspx

National Oceanic & Atmospheric Administration. (2020a). *DIVER Explorer - Data Integration Visualization Exploration and Reporting*. Natural Resource Damage Assessment & Restoration. https://www.diver.orr.noaa.gov/web/guest/diver-explorer?siteid=4&subtitle=Southeast

National Oceanic & Atmospheric Administration. (2020b). *Record-breaking Atlantic hurricane season draws to an end*. https://www.noaa.gov/media-release/record-breaking-atlantic-hurricane-season-draws-to-end

National Oceanic & Atmospheric Administration Estuarine Programs Office. (1988). *Galveston Bay: issues, resources, status, and management* (Issue 13).

National Toxicology Program. (2011). *Polycyclic Aromatic Hydrocarbons : 15 Listings*. *205*. https://ntp.niehs.nih.gov/ntp/roc/content/profiles/polycyclicaromatichydrocarbons.pdf

Nevalainen, L., Tuomisto, J., Haapasaari, P., & Lehikoinen, A. (2021). Spatial aspects of the dioxin risk formation in the Baltic Sea: A systematic review. *Science of the Total Environment*, *753*, 142185. https://doi.org/10.1016/j.scitotenv.2020.142185

O'Brien, A. L., Dafforn, K. A., Chariton, A. A., Johnston, E. L., & Mayer-Pinto, M. (2019). After decades of stressor research in urban estuarine ecosystems the focus is still on single stressors: A systematic literature review and meta-analysis. *Science of the Total Environment*, *684*, 753–764. https://doi.org/10.1016/j.scitotenv.2019.02.131

Oswer, U. S. E. P. A. (2002). *MEMO REGARDING THE PRINCIPLES FOR MANAGING CONTAMINATED SEDIMENT RISKS AT HAZARDOUS WASTE SITES OSWER 9285.6-08*.

Oziolor, E. (2017). *Evolution to Pollution in Gulf Killifish (Fundulus grandis) from Galveston Bay, TX, USA* [Baylor University]. http://proxy.library.tamu.edu/login?url=https://www.proquest.com/dissertations-theses/evolution-pollution-gulf-killifish-i-fundulus/docview/1952999029/se-2?accountid=7082

Oziolor, E. M., Apell, J. N., Winfield, Z. C., Back, J. A., Usenko, S., & Matson, C. W. (2018a). Polychlorinated biphenyl (PCB) contamination in Galveston Bay, Texas: Comparing concentrations and profiles in sediments, passive samplers, and fish. *Environmental Pollution*, *236*, 609–618. https://doi.org/10.1016/j.envpol.2018.01.086

Oziolor, E. M., Apell, J. N., Winfield, Z. C., Back, J. A., Usenko, S., & Matson, C. W. (2018b). Polychlorinated biphenyl (PCB) contamination in Galveston Bay, Texas: Comparing concentrations and profiles in sediments, passive samplers, and fish. *Environmental Pollution*, *236*, 609–618.

https://doi.org/10.1016/j.envpol.2018.01.086

Oziolor, E. M., Bigorgne, E., Aguilar, L., Usenko, S., & Matson, C. W. (2014a). Evolved resistance to PCB- and PAH-induced cardiac teratogenesis, and reduced CYP1A activity in Gulf killifish (Fundulus grandis) populations from the Houston Ship Channel, Texas. *Aquatic Toxicology*, *150*, 210–219. https://doi.org/10.1016/j.aquatox.2014.03.012

Oziolor, E. M., Bigorgne, E., Aguilar, L., Usenko, S., & Matson, C. W. (2014b). Evolved resistance to PCB- and PAH-induced cardiac teratogenesis , and reduced CYP1A activity in Gulf killifish (Fundulus grandis) populations from the Houston Ship Channel, Texas. *Aquatic Toxicology*, *150*, 210–219. https://doi.org/10.1016/j.aquatox.2014.03.012

Pardue, J. H., Moe, W. M., McInnis, D., Thibodeaux, L. J., Valsaraj, K. T., Maciasz, E., Van Heerden, I., Korevec, N., & Yuan, Q. Z. (2005). Chemical and microbiological parameters in New Orleans floodwater following hurricane Katrina. *Environmental Science and Technology*, *39*(22), 8591–8599. https://doi.org/10.1021/es0518631

Park, J. S., Wade, T. L., & Sweet, S. (2001a). Atmospheric deposition of organochlorine contaminants to Galveston Bay, Texas. *Atmospheric Environment*, *35*(19), 3315–3324. https://doi.org/10.1016/S1352-2310(00)00503-3

Park, J. S., Wade, T. L., & Sweet, S. (2001b). Atmospheric distribution of polycyclic aromatic hydrocarbons and deposition to Galveston Bay, Texas, USA. *Atmospheric Environment*, *35*(19), 3241–3249. https://doi.org/10.1016/S1352-2310(01)00080-2

PRISMA. (2015). *PRISMA - Transparent Reporting of Systematic Reviews and Meta-analyses*. http://www.prisma-statement.org/

Qian, Y., Wade, T. L., & Sericano, J. L. (2001). Sources and bioavailability of polynuclear aromatic hydrocarbons in Galveston Bay, Texas. *Estuaries*, *24*(6 A), 817–827. https://doi.org/10.2307/1353173

Rabodonirina, S., Net, S., Ouddane, B., Merhaby, D., Dumoulin, D., Popescu, T., & Ravelonandro, P. (2015). Distribution of persistent organic pollutants (PAHs, Me-PAHs, PCBs) in dissolved, particulate and sedimentary phases in freshwater systems. *Environmental Pollution*, *206*, 38–48.

https://doi.org/10.1016/j.envpol.2015.06.023

Randall, N. P., Donnison, L. M., Lewis, P. J., & James, K. L. (2015). How effective are on-farm mitigation measures for delivering an improved water environment? A systematic map. *Environmental Evidence*, *4*(1), 1–16. https://doi.org/10.1186/s13750-015-0044-5

Rhitu, C. (2007). Environmental News. *Environmental Science and Technology*, *41*(15), 5172.

Riding, M. J., Doick, K. J., Martin, F. L., Jones, K. C., & Semple, K. T. (2013). Chemical measures of bioavailability/bioaccessibility of PAHs in soil: Fundamentals to application. *Journal of Hazardous Materials*, *261*, 687–700. https://doi.org/10.1016/j.jhazmat.2013.03.033

Rocha, A. C., & Palma, C. (2019). Source identification of polycyclic aromatic hydrocarbons in soil sediments: Application of different methods. *Science of the Total Environment*, *652*, 1077–1089. https://doi.org/10.1016/j.scitotenv.2018.10.014

Romanok, K. M., Szabo, Z., Reilly, T. J., Defne, Z., & Ganju, N. K. (2016). Sediment chemistry and toxicity in Barnegat Bay, New Jersey: Pre- and post-Hurricane Sandy, 2012-13. *Marine Pollution Bulletin*, *107*(2), 472–488. https://doi.org/10.1016/j.marpolbul.2016.04.018

Rooney, A. A., Boyles, A. L., Wolfe, M. S., Bucher, J. R., & Thayer, K. A. (2014). Systematic Review and Evidence Integration for Literature-Based Environmental Health Science Assessments. *Environmental Health Perspectives*, *122*(7), 711–718. https://doi.org/10.4135/9781412950602.n267

Roth, D. (n.d.). *Texas Hurricane History*. 80. https://www.weather.gov/media/lch/events/txhurricanehistory.pdf

Ruby, M. V., Lowney, Y. W., Bunge, A. L., Roberts, S. M., Gomez-Eyles, J. L., Ghosh, U., Kissel, J. C., Tomlinson, P., & Menzie, C. (2016). Oral Bioavailability, Bioaccessibility, and Dermal Absorption of PAHs from Soil - State of the Science. *Environmental Science and Technology*, *50*(5), 2151–2164. https://doi.org/10.1021/acs.est.5b04110

Sansom, Garett T., Kirsch, K. R., Stone, K. W., McDonald, T. J., & Horney, J. A. (2018). Domestic exposure to polycyclic aromatic hydrocarbons in a Houston, Texas, environmental justice neighborhood. *Environmental Justice*, *11*(5), 183–191. https://doi.org/10.1089/env.2018.0004

Sansom, Garret T., Kirsch, K. R., Casillas, G. A., Camargo, K., Wade, T. L., Knap, A. H., Baker, E. S., &

Horney, J. A. (2021). Spatial Distribution of Polycyclic Aromatic Hydrocarbon Contaminants after Hurricane Harvey in a Houston Neighborhood. *Journal of Health and Pollution*, *11*(29), 210308. https://doi.org/10.5696/2156-9614-11.29.210308

Santschi, P. H., Presley, B. J., Wade, T. L., Garcia-Romero, B., & Baskaran, M. (2001). Historical contamination of PAHs, PCBs, DDTs, and heavy metals in Mississippi River Delta, Galveston Bay and Tampa Bay sediment cores. *Marine Environmental Research*, *52*(1), 51–79. https://doi.org/10.1016/S0141-1136(00)00260-9

Sappington, E. N., Balasubramani, A., & Rifai, H. S. (2015). Polychlorinated dibenzo-p-dioxins and polychlorinated dibenzofurans (PCDD/Fs) in municipal and industrial effluents. *Chemosphere*, *133*, 82–89. https://doi.org/10.1016/j.chemosphere.2015.04.019

Saran, A., & White, H. (2018). Evidence and gap maps: a comparison of different approaches. *Campbell Systematic Reviews*, *14*(1), 1–38. https://doi.org/10.4073/cmdp.2018.2

Schabenberger, O., & Gotway, C. A. (2005). *Statistical Methods for Spatial Data Analysis* (B. P. Carlin, C. Chatfield, M. Tanner, & J. Zidek (eds.)). Chapman & Hall/CRC.

Seward, S. M. (2010). *Using Sediment Records to Determine Sources, Distribution, Bioavailabiltiy, and Potential Toxicity of Dioxins in the Houston Ship Channel: A Multi-Proxy Approach* [Texas A&M University]. http://hdl.handle.net/1969.1/ETD-TAMU-2010-05-7903

Sheehan, M. C., & Lam, J. (2015). Use of Systematic Review and Meta-Analysis in Environmental Health Epidemiology: a Systematic Review and Comparison with Guidelines. *Current Environmental Health Reports*, *2*(3), 272–283. https://doi.org/10.1007/s40572-015-0062-z

Simons, J. D., & Smith, C. R. (2009). Texas National Coastal Assessment (2000-2004): Challenges, solutions, lessons learned and future directions. *Environmental Monitoring and Assessment*, *150*(1–4), 167–179. https://doi.org/10.1007/s10661-008-0684-9

Soliman, Y. S., Alansari, E. M. A., Sericano, J. L., & Wade, T. L. (2019). Science of the Total Environment Spatio-temporal distribution and sources identifications of polycyclic aromatic hydrocarbons and their alkyl homolog in surface sediments in the central Arabian Gulf. *Science of the Total Environment*, *658*, 787–797. https://doi.org/10.1016/j.scitotenv.2018.12.093

Spier, C. R., Bromage, E. S., Harris, T. M., Unger, M. A., & Kaattari, S. L. (2009). The development and evaluation of monoclonal antibodies for the detection of polycyclic aromatic hydrocarbons. *Analytical Biochemistry*, *387*(2), 287–293. https://doi.org/10.1016/j.ab.2009.01.020

Spier, C. R., Vadas, G. G., Kaattari, S. L., & Unger, M. A. (2011). Near real-time, on-site, quantitative analysis of PAHs in the aqueous environment using an antibody-based biosensor. *Environmental Toxicology and Chemistry*, *30*(7), 1557–1563. https://doi.org/10.1002/etc.546

Stogiannidis, E., & Laane, R. (2015). Source Characterization of Polycyclic Aromatic Hydrocarbson by Using Their Molecular Indices: An Overview of Possibilities. In D. Witacre (Ed.), *Reviews of Environmental Contamination and Toxicology* (Volume 234, pp. 49–133). https://doi.org/10.1007/978-3-319-10638-0_2

Suarez, M. P., Rifai, H. S., Palachek, R., Dean, K., & Koenig, L. (2006). Distribution of polychlorinated dibenzo-p-dioxins and dibenzofurans in suspended sediments, dissolved phase and bottom sediment in the Houston Ship Channel. *Chemosphere*, *62*(3), 417–429. https://doi.org/10.1016/j.chemosphere.2005.04.088

Suarez, M. P., Rifai, H. S., Palachek, R. M., Dean, K. E., & Koenig, L. (2005). Polychlorinated Dibenzo-. *Environmental Engineering Science*, *22*(6), 891–906.

Suarez, M. P., Rifai, H. S., Schimek, J., Bloom, M., Jensen, P., & Koenig, L. (2006). Dioxin in storm-water runoff in Houston, Texas. *Journal of Environmental Engineering*, *132*(12), 1633–1643. https://doi.org/10.1061/(ASCE)0733-9372(2006)132:12(1633)

TDI-Brooks. (2019). *Analytical Services*. https://www.tdi-bi.com/analytical-services/#geotechnical

Texas Commission on Environmental Quality. (1994). *Chapter Six: Water and Sediment Quality: Status and Trends*. https://www.tceq.texas.gov/assets/public/comm_exec/pubs/gbnep/gbnep-44/gbnep_44_95-137.pdf

Texas Commission on Environmental Quality. (2018). *Hurricane Harvey Response 2017 After-Action Review Report*. https://www.tceq.texas.gov/assets/public/response/hurricanes/hurricane-harvey-after-action-review-report.pdf

Texas Commission on Environmental Quality. (2020a). *Surface Water Quality Viewer*.

https://tceq.maps.arcgis.com/apps/webappviewer/index.html?id=b0ab6bac411a49189106064b70bbe778

Texas Commission on Environmental Quality. (2020b). *Surface Water Quality Web Reporting Tool*. https://www80.tceq.texas.gov/SwqmisPublic/index.htm

Texas Commission on Environmental Quality. (2020c). *The Texas Clean Rivers Program*. https://www.tceq.texas.gov/waterquality/clean-rivers/index.html

The Texas Clean Rivers Program. (2020). *CRP Data Tool*. https://www80.tceq.texas.gov/SwqmisWeb/public/crpweb.faces#

Thyng, K. M. (2019). Deepwater Horizon Oil could have naturally reached Texas beaches. *Marine Pollution Bulletin*, *149*(March), 110527. https://doi.org/10.1016/j.marpolbul.2019.110527

Tobiszewski, M., & Namieśnik, J. (2012). PAH diagnostic ratios for the identification of pollution emission sources. *Environmental Pollution*, *162*, 110–119. https://doi.org/10.1016/j.envpol.2011.10.025

Tsatsakis, A. M., Docea, A. O., & Tsitsimpikou, C. (2016). New challenges in risk assessment of chemicals when simulating real exposure scenarios; simultaneous multi-chemicals' low dose exposure. *Food and Chemical Toxicology*, *96*, 174–176. https://doi.org/10.1016/j.fct.2016.08.011

Unger, M., Harvey, E., Vadas, G., & Veccione, M. (2008). Persistent Pollutants in nine species of deep-sea cephalopods. *Marine Pollution Bulletin*, *56*(8), 1498–1500. https://doi.org/10.1016/j.marpolbul.2008.04.018

United States Environmental Protection Agency. (1996a). *SW-846 Test Method 4000: Immunoassay*. https://www.epa.gov/hw-sw846/sw-846-test-method-4000-immunoassay

United States Environmental Protection Agency. (1996b). *SW-846 Test Method 4030: Soil Screening for Petroleum Hydrocarbons by Immunoassay*. https://www.epa.gov/hw-sw846/sw-846-test-method-4030-soil-screening-petroleum-hydrocarbons-immunoassay

Appendix A to 40 CFR, Part 423–126 Priority Pollutants, (2014). https://www.epa.gov/eg/toxic-and-priority-pollutants-under-clean-water-act

United States Environmental Protection Agency. (2017). *RSL Calculator*. Regional Screening Levels.

https://epa-prgs.ornl.gov/cgi-bin/chemicals/csl_search

United States Environmental Protection Agency. (2018). Region 4 Ecological Risk Assessment Supplemental Guidance. In *Scientific Support Section - Superfund Division*. https://www.epa.gov/sites/production/files/2018-03/documents/era_regional_supplemental_guidance_report-march-2018_update.pdf

United States Environmental Protection Agency. (2020). *Search for Superfund Sites Where You Live: National Priorities List and Superfund Alternative Approach Sites*. https://www.epa.gov/superfund/search-superfund-sites-where-you-live

University of Houston-Clear Lake and the University of Houston Houston, T. (2003). *Environmental Institute of Houston 2003 Annual Report*. 1–46. https://www.uhcl.edu/environmental-institute/outreach/publications/files/ar2003.pdf

US Army Corps of Engineers. (2017). *Houston Ship Channel - Expansion Channel Improvement Project*. 1–8. http://www.swg.usace.army.mil/Missions/Projects/Houston-Ship-Channel-Expansion

Valentyne, A., Crawford, K., Cook, T., & Mathewson, P. D. (2018). Polycyclic aromatic hydrocarbon contamination and source profiling in watersheds serving three small Wisconsin, USA cities. *Science of the Total Environment*, *627*, 1453–1463. https://doi.org/10.1016/j.scitotenv.2018.01.200

Valle-Levinson, A., Olabarrieta, M., & Heilman, L. (2020). Compound flooding in Houston-Galveston Bay during Hurricane Harvey. *Science of the Total Environment*, *747*, 141272. https://doi.org/10.1016/j.scitotenv.2020.141272

Vane, C. H., Kim, A. W., Beriro, D. J., Cave, M. R., Knights, K., Moss-Hayes, V., & Nathanail, P. C. (2014). Polycyclic aromatic hydrocarbons (PAH) and polychlorinated biphenyls (PCB) in urban soils of Greater London, UK. *Applied Geochemistry*, *51*, 303–314. https://doi.org/10.1016/j.apgeochem.2014.09.013

Ver Hoef, J. M. (2018). Kriging models for linear networks and non-Euclidean distances: Cautions and solutions. *Methods in Ecology and Evolution*, *9*(6), 1600–1613. https://doi.org/10.1111/2041-210X.12979

Wang, Z., Yang, C., Parrott, J. L., Frank, R. A., Yang, Z., Brown, C. E., Hollebone, B. P., Landriault, M.,

Fieldhouse, B., Liu, Y., Zhang, G., & Hewitt, L. M. (2014). Forensic source differentiation of petrogenic, pyrogenic, and biogenic hydrocarbons in Canadian oil sands environmental samples. *Journal of Hazardous Materials*, *271*, 166–177. https://doi.org/10.1016/j.jhazmat.2014.02.021

Wei, B. (2016). Geospatial Characterization of Environmental Pollution and its Impact on Human Health in the Houston Ship Channel Region [Texas Southern University]. In *ProQuest Dissertations and Theses*. http://proxy.library.tamu.edu/login?url=https://www.proquest.com/docview/1909353497?accountid=7082

Wikoff, D. S., & Miller, G. W. (2018). Systematic reviews in toxicology. *Toxicological Sciences*, *163*(2), 335–337. https://doi.org/10.1093/toxsci/kfy109

Wolffe, T. A. M., Vidler, J., Halsall, C., Hunt, N., & Whaley, P. (2020). A Survey of Systematic Evidence Mapping Practice and the Case for Knowledge Graphs in Environmental Health and Toxicology. *Toxicological Sciences*, *175*(1), 35–49. https://doi.org/10.1093/toxsci/kfaa025

Wuebbles, D. J., Fahey, D. W., Hibbard, K. A., DeAngelo, B., Doherty, S., Hayhoe, K., Horton, R., Kossin, J. P., Taylor, P. C., Waple, A. M., & Weaver, C. P. (2017). *2017: Executive summary. In: Climate Science Special Report: Fourth National Climate Assessment.* https://doi.org/10.7930/J0DJ5CTG

Xia, H., Gomez-Eyles, J. L., & Ghosh, U. (2016). Effect of Polycyclic Aromatic Hydrocarbon Source Materials and Soil Components on Partitioning and Dermal Uptake. *Environmental Science and Technology*, *50*(7), 3444–3452. https://doi.org/10.1021/acs.est.5b06164

Yao, L., Hui, L., Yang, Z., Chen, X., & Xiao, A. (2020). Freshwater microplastics pollution: Detecting and visualizing emerging trends based on Citespace II. *Chemosphere*, *245*, 125627. https://doi.org/10.1016/j.chemosphere.2019.125627

Yeager, K. M., Brinkmeyer, R., Rakocinski, C. F., Schindler, K. J., & Santschi, P. H. (2010). Impacts of Dredging Activities on the Accumulation of Dioxins in Surface Sediments of the Houston Ship Channel, Texas. *Journal of Coastal Research*, *264*, 743–752. https://doi.org/10.2112/jcoastres-d-09-00009.1

Yeager, K. M., Santschi, P. H., Rifai, H. S., Suarez, M. P., Brinkmeyer, R., Hung, C. C., Schindler, K. J., Andres, M. J., & Weaver, E. A. (2007). Dioxin chronology and fluxes in sediments of the Houston ship channel, Texas: Influences of non-steady-state sediment transport and total organic carbon. *Environmental Science and Technology*, *41*(15), 5291–5298. https://doi.org/10.1021/es062917p

Yuill, R. M. (1991). *A paleoecological study of a one-hundred year sedimentary record of Galveston Bay, Texas* [Rice University]. http://proxy.library.tamu.edu/login?url=https://www.proquest.com/dissertations-theses/paleoecological-study-one-hundred-year/docview/303944040/se-2?accountid=7082

Yunker, M. B., Macdonald, R. W., Vingarzan, R., Mitchell, H., Goyette, D., & Sylvestre, S. (2002). *PAHs in the Fraser River basin: a critical appraisal of PAH ratios as indicators of PAH source and composition*. *33*, 489–515.

Zhang, C., Gabriel, Z., Gregory, H., & George, L. (2003). *Potential PAH Release from Contaminated Sediment in Galveston Bay-Houston Ship Channel*. https://tamug-ir.tdl.org/handle/1969.3/26336

APPENDIX A

SUPPLEMENTARY MATEIRALS FOR: CHARACTERIZING BASELINE LEGACY CHEMICAL CONTAMINATION IN URBAN ESTUARIES FOR DISASTER-RESEARCH THROUGH SYSTEMATIC EVIDENCE MAPPING: GALVESTON BAY CASE STUDY.

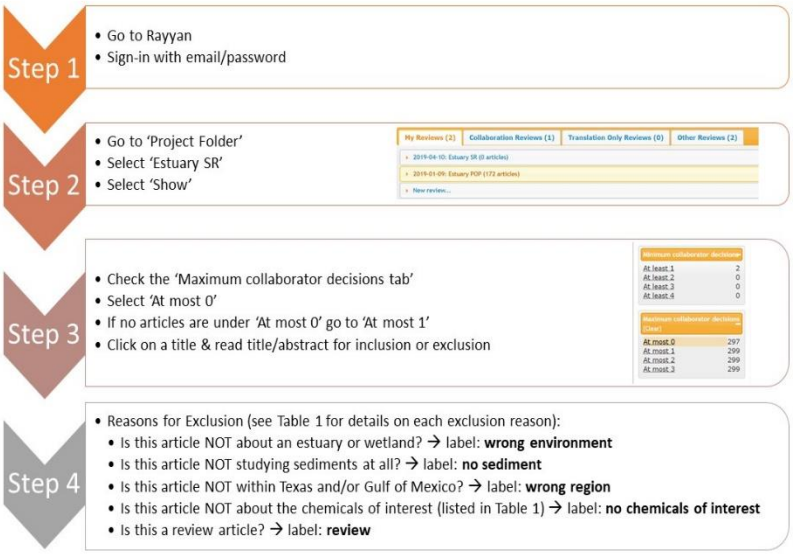

Figure A 1 Rayyan Screening process for all articles collected from scientific database search.

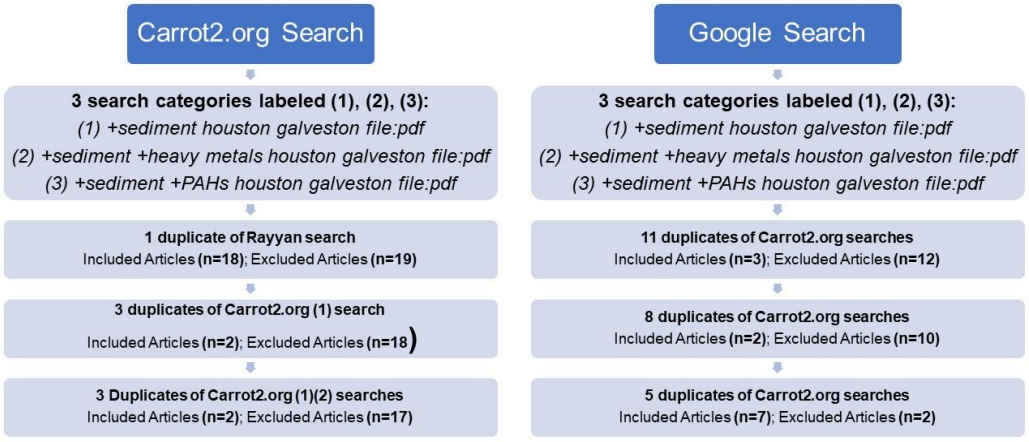

Figure A 2 Internet Screening Process for all Articles Searched on Carrot2.org and Google – Appendix and under search section discussion. Each row provides the number of articles screened for inclusion or exclusion as well as the number of duplicates observed.

NOAA DIVER					NOAA NCOOS					TCEQ Surface Water Quality Web Reporting Tool				
1	2	3	4	5	1	2	3	4	5	1	2	3	4	5
PCB_SUM	Nap	Chlor-dane alpha	Dibenzo-furan	Al	PCB 5/8	Nap	2,4'-DDD	Dibenzo-furan	Al	PCB 1254	AY	Alachlor	1,2378-PECDF	Al
PCB 5/8	AY	DDD_SUM		Sb	PCB 18	AY	2,4'-DDE		Sb	PCB 1	AE	Aldrin	1234678-HPCDD	As
PCB 18	AE	DDE_SUM		As	PCB 28	AE	2,4'-DDT		As	PCB 10	A	Atrazine	1234678-HPCDD	Ba
PCB 28	F	DDT_SUM		Ba	PCB 44	F	4,4'-DDD		Cd	PCB 103	BaA	B-BHC Beta	1234678-HPCDF	Cd
PCB 44	A	DDT_TOTAL		Be	PCB 52	A	4,4'-DDE		Cr	PCB 104	BbF	BHC Alpha	1234678-HPCDF	Cr
PCB 52	P	OP_DDE		Cd	PCB 66	P	Aldrin		Cu	PCB 105	ghi	Chlordane cis	1234789-HPCDF	Cu
PCB 66	FL	OP_DDT		Cr	PCB 90/101	FL	Alpha-Chlordane		Fe	PCB 106	BkF	Chlordane gamma	123478-HXCDD	Fe
PCB 101	PY	Aldrin		Co	PCB 105	PY	Alpha-Hexachlorocyclohexane		Pb	PCB 107		Chlordane (Tech Mix&Metabs)	123478-HXCDF	Pb
PCB 105	BaA	Dieldrin		Cu	PCB 118	BaA	Cis-Nonachlor		Mg	PCB 109	C	DDD	123678-HXCDD	Mg
PCB 118	C	Heptachlor epoxide		Fe	PCB 128	C	Delta-Hexachlorocyclohexane		Hg	PCB 11	FL	DDE	123678-HXCDF	Hg
PCB 128	BbF	Heptachlor		Pb	PCB 138/160	BbF	Dieldrin		Ni	PCB 111	F	DDT	123789-HXCDD	Ni
PCB 132/153	BkF	OP_DDD		Mn	PCB 53/132/168	BkF	Endosulfan II		Se	PCB 112	IP	Dieldrin	123789-HXCDF	Se
PCB 138	BaP	PP_DDD		Hg	PCB 170/190	BaP	Endrin		Ag	PCB 114	Nap	Endosulfan sulfate	2,378-TCDD	Ag
PCB 170/190	PER	PP_DDE		Mo	PCB 180	PER	Gamma-Chlordane		Sn	PCB 118	P	Endosulfan alpha	234678-HXCDF	Zn
PCB 180	IP	Endrin		Ni	PCB 187	IP	Gamma-Hexachlorocyclohexane		Zn	PCB 120	PY	Endosulfan beta	23478-PECDF	
PCB 187	DA	Chlordane gamma		Se	PCB 195/208	DA	Heptachlor			PCB 121		Endrin	2378-TCDF	
PCB 195/208	ghi	Chlorpyrifos		Ag	PCB 206	ghi	Heptachlor-Epoxide			PCB 122		Gama BHC (Lindane)	2378-TCDF	
PCB 206	C1Nap	Endosulfan alpha		Sr	PCB 209	C1Nap	Hexachlorobenzene			PCB 123		Guthion	OCDD	

PCB 209	C2Nap	Endosulfan beta		Tl		C2Nap	Mirex			PCB 126		Heptachlor epoxide	OCDF	
PCB 8	C3Nap	Endosulfan sulfate		Sn		C3Nap	Oxychlordane			PCB 127		Heptachlor	TOTALHXCDD	
PCB 29	C4Nap	Chlordane		Ti		C4Nap				PCB 130		Hexachlorophene	TOTALHXCDD	
PCB 31	C1F			Zn		C1F				PCB 131		Malathion	TOTALPECDD	
PCB 45	C2F			V		C2F				PCB 132		Methoxychlor	TOTALPECDF	
PCB 49	C3F					C3F				PCB 133		Mirex	TOTALPECDF	
PCB 56	C1PA					C1PA				PCB 137		Parathion	TOTALTCDD	
PCB 70	C2PA					C2PA				PCB 14			TOTALTCDF	
PCB 74	C3PA					C3PA				PCB 141			TOTALTCDF	
PCB 87	C4PA					C4PA				PCB 142			TOTAL-HPCDD	
PCB 95	C1C					C1C				PCB 144			TOTAL-HPCDD	
PCB 99	C2C					C2C				PCB 145			TOTAL-HPCDF	
PCB 101	C3C					C3C				PCB 146			TOTAL-HPCDF	
PCB 110	C4C					C4C				PCB 147			TOTAL-HXCDF	
PCB 146	C1FP					C1FP				PCB 148			TOTAL-HXCDF	
PCB 149	C2FP					C2FP				PCB 15				
PCB 151	C3FP					C3FP				PCB 150				
PCB 153	Total PAH					C4FP				PCB 152				
PCB 156										PCB 154				
PCB 158										PCB 155				
PCB 170										PCB 158				
PCB 174										PCB 159				

PCB 183										PCB 16				
PCB 194										PCB 160				
PCB 195										PCB 161				
PCB 201										PCB 162				
PCB126										PCB 164				
PCB 137										PCB 165				
										PCB 167				
										PCB 169				
										PCB 17				
										PCB 170				
										PCB 172				
										PCB 174				
										PCB 175				
										PCB 176				
										PCB 177				
										PCB 178				
										PCB 179				
										PCB 181				
										PCB 182				
										PCB 183				
										PCB 184				
										PCB 185				
										PCB 186				
										PCB 187				
										PCB 188				
										PCB 189				
										PCB 19				
										PCB 190				
										PCB 191				
										PCB 192				
										PCB 194				
										PCB 195				
										PCB 196				
										PCB 197				
										PCB 200				
										PCB 201				
										PCB 202				

										PCB 203				
										PCB 204				
										PCB 205				
										PCB 206				
										PCB 208				
										PCB 209				
										PCB 22				
										PCB 23				
										PCB 24				
										PCB 25				
										PCB 26				
										PCB 27				
										PCB 2				
										PCB 3				
										PCB 31				
										PCB 32				
										PCB 34				
										PCB 35				
										PCB 36				
										PCB 37				
										PCB 38				
										PCB 39				
										PCB 4				
										PCB 42				
										PCB 43				
										PCB 46				
										PCB 48				
										PCB 5				
										PCB 52				
										PCB 54				
										PCB 55				
										PCB 56				
										PCB 57				
										PCB 58				
										PCB 6				
										PCB 60				
										PCB 63				
										PCB 64				
										PCB 65				
										PCB 66				
										PCB 67				
										PCB 68				
										PCB 7				
										PCB 72				
										PCB 73				
										PCB 77				
										PCB 78				
										PCB 79				
										PCB 8				
										PCB 80				
										PCB 81				
										PCB 82				
										PCB 83				
										PCB 84				
										PCB 89				
										PCB 9				
										PCB 92				
										PCB 94				
										PCB 95				
										PCB 96				
										PCB 99				
										PCB Congeners Grp IUPAC 109+119+86+97+125				
										PCB 1016				

										PCB 1221				
										PCB 1232				
										PCB 1242				
										PCB 1248				
										PCB 1260				
										PCB GRP#1 13/12				
										PCB GRP#10 59/62/75				
										PCB GRP#11 61/70/74/76				
										PCB GRP#12 69/49				
										PCB GRP#13 88/91				
										PCB GRP#14 100/93/102/98				
										PCB GRP#15 110/115				
										PCB GRP#16 113/90/101				
										PCB GRP#17 117/116/85				
										PCB GRP#18 128/166				
										PCB GRP#19 134/143				
										PCB GRP#2 21/33				
										PCB GRP#20 138/163/129				
										PCB GRP#21 139/140				
										PCB GRP#22 147/149				
										PCB GRP#23 151/135				
										PCB GRP#24 153/168				
										PCB GRP#25 171/173				
										PCB GRP#26 193/180				
										PCB GRP#27 198/199				
										PCB GRP#3 26/29				
										PCB GRP#31 108/119/86/97/125/87				
										PCB GRP#32 107/124				
										PCB GRP#33 183/185				
										PCB GRP#34 197/200				
										PCB GRP#35 156/157				
										PCB GRP#4 28/20				
										PCB GRP#5 30/18				
										PCB GRP#6 40/41/71				
										PCB GRP#7 44/47/65				
										PCB GRP#8 45/51				

										PCB GRP#9 53/50			
										PCBs Bottom Deposits			

Table A 1 Chemicals Searched for in NOAA DIVER, NOAA NCCOS, and TCEQ Surface Water Quality Web Reporting Tool. PCBs are listed under columns with 1, PAHs are listed under columns with 2, Pesticides are listed under columns with 3, Dx/F are listed under columns with 4, and Metals are listed under columns with 5.

PAHs	
Naphthalene	Nap
Acenaphthylene	AY
Acenaphthene	AE
Fluorene	F
Anthracene	A
Phenanthrene	P
Fluoranthene	FL
Pyrene	PY
Benz[a]anthracene	BaA
Chrysene	C
Benzo[b]fluoranthene	BbF
Benzo[k]fluoranthene	BkF
Benzo[a]pyrene	BaP
Perylene	PER
Indeno[1,2,3-c,d]pyrene	IP
Dibenzo[a,h]anthracene	DA
Benzo[g,h,i]perylene	ghi
C1-Naphthalenes	C1Nap
C2-Naphthalenes	C2Nap
C3-Naphthalenes	C3Nap
C4-Naphthalenes	C4Nap
C1-Fluorenes	C1F
C2-Fluorenes	C2F
C3-Fluorenes	C3F
C1-Phenanthrenes_Anthracenes	C1PA
C2-Phenanthrenes_Anthracenes	C2PA
C4-Phenanthrenes_Anthracenes	C3PA
C4-Phenanthrenes_Anthracenes	C4PA
C1-Chrysenes	C1C
C2-Chrysenes	C2C
C3-Chrysenes	C3C
C4-Chrysenes	C4C
C1-Fluoranthenes_Pyrenes	C1FP

C2-Fluoranthenes_Pyrenes	C2FP
C3-Fluoranthenes_Pyrenes	C3FP
C4-Fluoranthenes_Pyrenes	C4FP

Table A 2 Polycyclic Aromatic Hydrocarbon shorthand abbreviations for reference in all manuscript tables.

Article Descriptors	Authors(s), Article title, Publication Year
Geographical Descriptors	Latitude, Longitude, General Location
Sample Descriptors	Estuary, Bay, Sub-Bay, Number of Samples, Sampling Year, Sampling Season, Sample Depth
Chemical Descriptors	Chemical Name, Reported Concentration(s)
Analytical Methods	
Additional Descriptors	Grain Size, Total Organic Carbon
Reported Outcomes	Sediment Quality, Sediment Management, Remedial Action, Environmental Policy, Dredging, etc.

Table A 3 Data coding descriptors used in the Google form.

	Median	Range	IQR	Sampling Timeframe	Reference(s)
HSC	ng/g	ng/g	ng/g		
Ship Channel	9	0.0000840; 162	8, 19.5	2005-2010; 2010-2012	Apeti et al. 2012; Al Mukaimia et al. 2018
Upper GB					
Yacht Club	0.00003	-	-	2005-2010	Apeti et al. 2012
Clear Lake	27.5	6; 47	7; 46.5	2010-2015	Al Mukaimia et al. 2018
Taylor Lake	41	25; 49	27; 49	2010-2015	Al Mukaimia et al. 2018
Lower GB					
Trinity Bay	0.047465	0.00008; 50.500	0.00094; 13.6995	1995-2000; 2010-2015	Santschi et al. 2001; Al Mukaimia et al. 2018
Galveston Bay	0.04088	0.0000472; 45	0.0045868; 26.250	2000-2005	Simmons and Smith 2009
Confederate Reef	0.000031	-	-	2005-2010	Apeti et al. 2012
Hannah Reef	0.000049	-	-	2005-2010	Apeti et al. 2012
Offatts Bayou	0.000109	-	-	2005-2010	Apeti et al. 2012
Todd's Dump	0.000018	-	-	2005-2010	Apeti et al. 2012
West Bay	11	8; 20	8; 16.625	2010-2015	Al Mukaimia et al. 2018
East Bay	13.5	6; 18	7.5; 17.250	2010-2015	Al Mukaimia et al. 2018
Texas City	17	15; 19	15; 19	2010-2015	Al Mukaimia et al. 2018

Table A 4 Trends by general location for metals reported in peer-reviewed articles.

	Median	Range	IQR	Sampling Timeframe	Reference(s)
HSC	ng/g	ng/g	ng/g		
General HSC averages	14.10	9.6; 26	9.6, 26	2000-2005	Lakshmanan et al. 2010
Upper Galveston Bay/HSC	13.80	0.6; 5840	2.625, 65.25	2000-2005	Suarez et al 2006
inlet off Burnett Bay	2.10	0.000210; 7312	0.00121; 0.0117	2005-2010	Louchourarn et al 2018; Hieke et al. 2016
Lower San Jacinto Bay	2.86	0.000200; 6.321	0.00103; 0.0194	2005-2010	Louchourarn et al 2018; Hieke et al. 2016
Negrohead Lake	2.80	0.000390; 4.646	0.000895; 0.0188	2005-2010	Louchourarn et al 2018; Hieke et al. 2016
San Jacinto Waste Pits	80.01	0.000582; 15.510	0.0155; 0.467	2005-2010	Aguilar et al. 2014; Hieke et al. 2016; Louchourarn et al 2018
Bear Lake	0.37	0.000045; 4.606	0.000108; 0.00218	2005-2010	Louchourarn et al 2018; Hieke et al. 2016
inlet by Kirby Inland Marine Oper Center	0.34	0.000108; 3.411	0.0000885; 0.00149	2005-2010	Yeager et al. 2007; Hieke et al. 2016
inlet south of Greens/Baffalo Bayou split	0.00	0; 3.204	0; 0.0163	2005-2010	Yeager et al. 2007; Hieke et al. 2016
inlet off entry to Buffalo Bayou	0.00	0; 3.239	0; 0.0548	2005-2010	Yeager et al. 2007; Hieke et al. 2016
near Bay Shore Park	0.00	0; 9.358	0; 0.00405	2005-2010	Yeager et al. 2007; Hieke et al. 2016
inlet off Tabbs Bay	0.00	0; 4.0115	0; 0.00383	2005-2010	Yeager et al. 2007; Hieke et al. 2016
Atkinson Island	0.00	0; 5.00270	0; 0.00958	2005-2010	Hieke et al. 2016
S. of I10 Bridge	5858.60	0.227; 6.092	1.609; 5.859	2005-2010	Louchourarn et al 2018
Hog Island	1821.70	0.227; 3.527	0.648; 2.677	2005-2010	Yeager et al 2010
Alexander Island	1.84	0.000032 0; 4.332	0.000667; 0.0112	2005-2010	Yeager et al 2010
inlet off Upper San Jacinto Bay	3.64	0.000628; 0.0322	0.00196; 0.00825	2005-2010	Yeager et al. 2007
inlet off Buffalo Bayou near BB Toll Bridge	9.80	0.00260; 0.0690	0.00460; 0.0136	2005-2010	Yeager et al. 2007
Upper GB					
Anahuac Channel	0.00	0; 0.00120	0; 0.000168	2005-2010	Louchourarn et al 2018; Hieke et al. 2016
transcect in GB	0.00	0; 0.0300	0;0	2005-2010	Hieke et al. 2016
terrestrial control off of Trinity River	0.00	0; 0.0430	0; 0.00128	2005-2010	Yeager et al. 2007
Lower GB					
Offatts Bayou	1242.0	124; 9997	461; 1747.250	1995-2000	Qian et al. 2001

Table A 5 Trends by general location for organics reported in peer-reviewed articles.

	Min	Median	Max	IQR	ERL	ERM
Units	mg/kg or ug/g	mg/kg or ug/g	mg/kg or ug/g	mg/kg or ug/g	mg/kg	mg/kg
Aluminum	4,800	49,514	93,100	33,650; 66,584	-	-
Antimony	0	0.52	1.97	0.32; 0.80	-	-
Arsenic	0	5.91	13.85	3.80; 8.03	8,200	70,000
Barium	0	0	553	0.00; 0.00	-	-
Beryllium	0	0	0.80	0.00; 0.00	-	-
Cadmium	0	0.1	0.84	0.05; 0.16	1,400	9,600
Chromium	0	45	91	29.50; 59.44	141,000	370,00
Cobalt	0	0	8.5	0.00; 59.44	-	-
Copper	0	11.7	57.8	6.90; 15.86	108,000	270,000
Iron	0	20,600	44,000	12,428; 31,180	-	-
Lead	2.51	17.5	64.95	11.81; 23.10	112,000	218,000
Manganese	0	324	2,483	222.50; 481.80	-	-
Mercury	0	0.042	0.194	0.03; 0.06	150	710
Molybdenum	0	0	0.60	0.00; 0.06	-	-
Nickel	0	15.9	36.4	10.82; 23.90	20,900	51,600
Selenium	0	0.25	1.86	0.10; 0.42	-	-
Silver	0	0.11	0.52	0.08; 0.15	1,000	3,700
Strontium	0	0	377.80	0.00; 0.15	-	-
Thallium	0	0	0.51	0.00; 0.00	-	-
Tin	0	1.2	6.9	0.75; 1.89	-	-
Titanium	0	0	2,581	0.00; 0.00	-	-
Vanadium	0	0	73.30	0.00; 0.00	-	-
Zinc	5.60	65.55	313.5	44.00; 94.34	150,000	410,000

Table A 6 Trends for metals reported by NOAA across all sampling years.

	Min	Median	Max	IQR	ERL	ERM
Units	mg/kg	mg/kg	mg/kg	mg/kg	mg/kg	mg/kg
Aluminum	2	21,000	72,200	10,250; 72,200	-	-
Arsenic	0.127	4.5325	75,800	2.97; 75,800	8,200	70,000
Barium	5	193	1,770	122; 1,770	1,400	9,600
Cadmium	0	0.397	3	0.171; 3	141,000	370,00
Chromium	0.5	26	359	15; 359	108,000	270,000
Copper	0.175	14	345	7; 345	-	-
Iron	600	15,900	39,800	9,755; 39,800	112,000	218,000
Lead	0.004	0.075	5,000	0.025; 5,000	-	-
Magnesium	2,710	2,910	3,110	-; 3,110	150	710
Mercury	0.004	0.0826	92	0.0316; 92	-	-
Nickel	0.605	16	80	10; 80	20,900	51,600
Selenium	0.008	0.404	6	0.237; 6	-	-
Silver	0.095	0.387	4	0.245; 4	1,000	3,700
Zinc	2	79	710	42; 710	150,000	410,000

Table A 7 Trends for metals reported by TCEQ across all sampling years.

	Min	Median	Max	IQR	ERL	ERM
Units	ug/kg	ug/kg	ug/kg	ug/kg	ug/kg	ug/kg
2,4'-DDD	0	0.09	2.66	0; 0.2	-	-
2,4'-DDE	0	0	0.25	0; 0.2	-	-
2,4'-DDT	0	0	3.03	0; 0	-	-
4,4'-DDD	0	0.05	5.4	0; 255	2	20
4,4'-DDE	0	0.045	2.16	0; 0.2	2.2	27
4,4'-DDT	0	0	6.68	0; 0.55	1	7
Acenaphthene	0.3	0.95	34.9	0.6; 1.7	16	500
Acenaphthylene	0.2	2.2	26.6	0.925; 4.525	44	640
Aldrin	0	0	0.35	0; 0.55	-	-
Alpha-Chlordane	0	0.03	0.45	0; 875	-	-
Alpha-Hexachlorocyclohexane	0	0.03	0.34	0; .07	-	-
Anthracene	0.2	3	228.3	0.2; 0.2.55	85.3	1100
Benz[a]anthracene	0.2	5.45	676.4	2.425; 575	261	1600
Benzo[a]pyrene	0.2	9.25	684.4	3.75; 025	430	1600
Benzo[b]fluoranthene	0.2	11.25	800.4	4.45; 325	-	-
Benzo[g,h,i]perylene	0.3	8.6	289.5	3.575; 625	-	-
Benzo[k]fluoranthene	0.1	3.6	178.7	1.25; 025	-	-
C1-Chrysenes	0	6.85	254.9	2.95; 225	-	-
C1-Fluoranthenes_Pyrenes	0	0.35	22.6	0; 875	-	-
C1-Fluorenes	0	9.65	669.9	4.725; .05	-	-
C1-Naphthalenes	0.5	3.5	18.8	1.925; 5.8	-	-
C1-Phenanthrenes_Anthracenes	0	5.45	228.5	2.8; 475	-	-
C2-Chrysenes	0	8.5	194.7	2.75; 875	-	-
C2-Fluorenes	0	0	47.2	0; 0.55	-	-
C2-Naphthalenes	0	4.8	27.3	0; 7.4	-	-
C2-Phenanthrenes_Anthracenes	0	7.1	235.1	3.225; 6.5	-	-
C3-Chrysenes	0	0.35	12.3	0; 075	-	-
C3-Fluorenes	0	0	111.4	0; 0.55	-	-
C3-Naphthalenes	0	6.8	67	0; 775	-	-
C3-Phenanthrenes_Anthracenes	0	9.6	240.3	4.125; 1.5	-	-
C4-Chrysenes	0	1.7	68.8	0; 875	-	-
C4-Naphthalenes	0	0	52.3	0; 0.55	-	-
C4-Phenanthrenes_Anthracenes	0	6.65	156.2	2.625; 225	-	-
Chrysene	0.2	7.15	711.6	2.775; 775	384	2800
Cis-Nonachlor	0	0.02	0.41	0; 575	-	-
Delta-Hexachlorocyclohexane	0	0.01	0.17	0; .04	-	-
Dibenzo[a,h]anthracene	0.1	0.04	0.04	0.04; .04	63.4	260
Dieldrin	0	0	0.63	0; 0.55	0.02	4.3
Endosulfan II	0	0.01	0.16	0; .05	-	-
Endrin	0	0	0.2	0; 0.55	-	-
Fluoranthene	0.6	9.75	1473	4.6; 975	600	5100
Fluorene	0.2	1.3	34.5	0.7; 275	19	540
Gamma-Chlordane	0	0.06	0.97	0; .12	-	-
Gamma-Hexachlorocyclohexane	0	0.015	0.18	0; .04	-	-
Heptachlor	0	0	0	0; 0.55	-	-
Heptachlor-Epoxide	0	0	10.4	0; 0.55	-	-
Hexachlorobenzene	0	0.185	15.22	0.04; 675	-	-
Indeno[1,2,3-c,d]pyrene	0.1	5	291.5	0.1; 0.1.55	-	-
Mirex	0	0.005	0.12	0; .02	-	-
Naphthalene	0.5	3.8	18.4	2.7; .75	160	2100
Oxychlordane	0	0	0.44	0; 0.55	-	-
PCB101_90	0	0.09	1.51	0.04; 205	-	-
PCB105	0	0.015	0.55	0; .04	-	-
PCB118	0	0.06	1.51	0; 0.2	-	-
PCB128	0	0	0.23	0; 0.55	-	-
PCB138_160	0	0.115	1.69	0.0525; 825	-	-
PCB153_132_168	0	0.08	2.03	0.04; 375	-	-
PCB170_190	0	0.125	3	0; 275	-	-
PCB18	0	0	0.8	0; 0.55	-	-
PCB180	0	0.09	1.01	0.03; .16	-	-
PCB187	0	0.03	0.9	0; 775	-	-
PCB195_208	0	0.01	0.23	0; 575	-	-
PCB206	0	0.04	0.35	0; .09	-	-
PCB209	0	0.205	10.92	0.0225; 075	-	-
PCB28	0	0.05	0.62	0; 175	-	-
PCB44	0	0.075	1.14	0.0325; .13	-	-
PCB52	0	0.16	2.78	0.06; 305	-	-
PCB66	0	0.02	1.02	0; 475	-	-
PCB8_5	0	0	0.84	0; 0.55	-	-

Perylene	0.4	8	187.2	0.4; 0.4.55	-	-
Phenanthrene	0.2	4.1	501.5	2.025; .05	240	1500
Pyrene	0.6	15.15	1502.7	6.025; .45	665	2600

Table A 8 Trends for organics reported by NOAA NCOOS across all sampling years.

	Min	Median	Max	IQR	ERL	ERM
Units	ug/kg	ug/kg	ug/kg	ug/kg	ug/kg	ug/kg
Nap	0	0	21.398	0; 1.9	160	2100
AY	0	0	69	0; 0.725	16	500
AE	0	0	66.45	0; 0.325	44	640
F	0	0	7600	0; 0.425	19	540
A	0	0	9000	0; 1.15	85.3	1100
P	0	0	12600	0; 4.45	240	1500
FL	0	2.25	18300	0; 14.575	600	5100
PY	0	3.1	15200	0; 17.4845	665	2600
BaA	0	0	12700	0; 4.3475	261	1600
C	0	0	22800	0; 6.075	384	2800
BbF	0	0.7	25800	0; 9.2	-	-
BkF	0	0	11900	0; 6.2	-	-
BaP	0	0	22300	0; 5.775	430	1600
PER	0	0	314.5	0; 6.2	-	-
IP	0	0	16900	0; 4.825	-	-
DA	0	0	10800	0; 1.225	63.4	260
ghi	0	0	14400	0; 7.4	-	-
C1Nap	0	0	30.08	0; 1.225	-	-
C2Nap	0	0	38.92	0; 0	-	-
C3Nap	0	0	40.44	0; 0	-	-
C4Nap	0	0	21.85	0; 0	-	-
C1F	0	0	36.17	0; 0	-	-
C2F	0	0	82.91	0; 0	-	-
C3F	0	0	144.27	0; 0	-	-
C1PA	0	0	309.91	0; 0	-	-
C2PA	0	0	203.23	0; 0	-	-
C3PA	0	0	90.55	0; 0	-	-
C4PA	0	0	40.24	0; 0	-	-
C1FP	0	0	555.91	0; 2.425	-	-
C2FP	0	0	324.14	0; 0	-	-
C3FP	0	0	169.68	0; 0	-	-
C1C	0	0	482.73	0; 1.85	-	-
C2C	0	0	203.23	0; 1.85	-	-
C3C	0	0	56.5	0; 0	-	-
C4C	0	0	73.36	0; 0	-	-
TOTAL_PAH	0	23.73521	107100	0; 83.25	4022	44792
PCB_SUM	0	0	62.2	0; 3.555	22.7	180
PCB 5/8	0	0	0.35	0; 0	-	-
PCB 18	0	0	6.2	0; 0	-	-
PCB 28	0	0	5.5	0; 0	-	-
PCB 44	0	0	4.8	0; 0	-	-
PCB 52	0	0	5	0; 0	-	-
PCB 66	0	0	4	0; 0	-	-
PCB 101	0	0	0.43	0; 0	-	-
PCB 105	0	0	3.626	0; 0	-	-
PCB 118	0	0	15.657	0; 0	-	-
PCB 128	0	0	7.7	0; 0	-	-
PCB 132/153	0	0	0.88	0; 0	-	-
PCB 138	0	0	4.4	0; 0	-	-
PCB 170/190	0	0	1.12	0; 0	-	-
PCB 180	0	0	3.499	0; 0.03	-	-
PCB 187	0	0	1.5	0; 0	-	-
PCB 195/208	0	0	0.06	0; 0	-	-
PCB 206	0	0	0.68	0; 0	-	-
PCB 209	0	0	3.05	0; 0	-	-
PCB 8	0	0	1	0; 0	-	-
PCB 29	0	0	0.23999	0; 0	-	-
PCB 31	0	0	0.4	0; 0	-	-
PCB 45	0	0	0.11999	0; 0	-	-
PCB 49	0	0	2.57	0; 0	-	-
PCB 56	0	0	0.51999	0; 0	-	-
PCB 70	0	0	1.31	0; 0	-	-
PCB 74	0	0	0.33	0; 0	-	-
PCB 87	0	0	0.91	0; 0	-	-
PCB 95	0	0	2.38	0; 0	-	-
PCB 99	0	0	2.86	0; 0	-	-
PCB 101	0	0	4.74	0; 0	-	-
PCB 110	0	0	3.61	0; 0	-	-
PCB 146	0	0	0.55	0; 0	-	-

PCB 149	0	0	2.13	0; 0	-	-
PCB 151	0	0	0.57999	0; 0	-	-
PCB 153	0	0	16.569	0; 0.1	-	-
PCB 156	0	0	2.08	0; 0	-	-
PCB 158	0	0	0.27	0; 0	-	-
PCB 170	0	0	4.518	0; 0	-	-
PCB 174	0	0	0.68	0; 0	-	-
PCB 183	0	0	0.38999	0; 0	-	-
PCB 194	0	0	0.23	0; 0	-	-
PCB 195	0	0	0.73	0; 0	-	-
PCB 201	0	0	0.03999	0; 0	-	-
PCB126_-_PPB_-_Result_(0_DL)	0	0	0.7	0; 0	-	-
PCB 137	0	0	16.839	0; 0	-	-
Chlordane alpha	0	0	7.13	0; 0	-	-
DDD_SUM	0	0	3.02	0; 0	-	-
DDE_SUM	0	0	22.588	0; 0	-	-
DDT_SUM	0	0	0.4	0; 0	-	-
DDT_TOTAL	0	0	22.588	0; 0	1.58	46.1
OP_DDE	0	0	0.34	0; 0	-	-
OP_DDT	0	0	3.4	0; 0	-	-
ALDRIN	0	0	0.36	0; 0	-	-
DIELDRIN	0	0	0.8	0; 0	0.02	4.3
Heptachlor expoxide	0	0	0.91	0; 0	-	-
Heptachlor	0	0	0.20999	0; 0	-	-
OP_DDD	0	0	3.8	0; 0	-	-
PP_DDD	0	0	0.7	0; 0	2	20
PP_DDE	0	0	22.588	0; 0.1	2.2	27
Endrin	0	0	0.23999	0; 0	-	-
Chlordane gamma	0	0	1.36	0; 0	-	-
Chlorpyrifos	0	0	0.54	0; 0	-	-
Endosulfan alpha	0	0	0.01	0; 0	-	-
Endosulfan beta	0	0	0.73	0; 0	-	-
Endosulfan sulfate	0	0	1.2	0; 0	-	-
Chlordane	0	0	1.93	0; 0	0.5	6
Dibenzofuran	0.6	2.375	36.28	0.6; 11.8	-	-

Table A 9 Trends for organics reported by NOAA DIVER across all sampling years.

	Min	Median	Max	IQR	ERL	ERM
Units	ug/kg	ug/kg	ug/kg	ug/kg	ug/kg	ug/kg
AE	0.5	189.5	3050	117.25; 284.75	16	500
AY	0.5	193	5450	118.125; 295.75	44	640
A	0.5	203	5450	120.5; 298	85.3	1100
BaA	0.5	193.5	5450	118.125; 284.625	261	1600
BbF	0.5	187.5	5450	112.25; 296.5	-	-
Bghi	0.5	190.5	5450	114.75; 304.75	-	-
BkF	0.5	190.5	5450	119.25; 284.75	-	-
BaP	0.5	189.5	5450	119; 285	430	1600
C	0.5	183.5	5450	114.75; 291.5	384	2800
FL	0.5	183.5	5450	110; 302	600	5100
F	0.5	199.75	5450	119.125; 298.375	19	540
IP	0.5	185.5	5450	116.375; 284.875	-	-
Nap	0.5	196.5	5450	119; 285	160	2100
P	0.5	187	5450	115.125; 297.25	240	544
PY	0.5	183.5	3050	110; 320.75	665	2,600
Arachlor	2.15	-	3.3	-; -	-	-
Aldrin	0.00125	6.3	160	1.5; 16	-	-
Atrazine	7	182.25	5450	85.25; 2267.5	-	-
B-BHC Beta	0.0005	8.1	160	2.1; 16.5	-	-
B-BHC alpha	0.0005	5.275	160	2; 14.2625	-	-
Chlordane gamma	0.415	19.5	82	17.5; 20	-	-
DDD	0.0075	7.125	320	3; 23.25	2	20
DDE	0.00375	4.975	320	1.75; 10	2.2	27
DDT	0.0075	10	320	2.675; 25	1	7
Dieldrin	0.0025	5.6	320	2.3; 17.4375	0.02	4.3
Endosulfan alpha	0.0015	7.95	320	3; 25.625	-	-
Endosulfan Beta	0.415	12.85	82	4.39375; 33.4875	-	-
Endosulfan	0.00125	4.525	125	1.25; 12.5	-	-
Endrin	0.00375	10	43	2.3125; 24.25	-	-
Gamma BHC	0.0005	5.025	160	1.5125; 17.2125	-	-
Heptachlor epoxide	0.00125	8.1625	350	1.75; 20	-	-
Heptachlor	0.00065	10	160	1.5; 27.375	-	-
Heptachlorophene	0.175	10	7750	3.5; 20.8	-	-
Malathion	0.0025	25	376	7.35; 51	-	-
Methoxychlor	0.0125	20	305	5; 64.625	-	-
Mirex	0.002	3	95	1.5; 9	-	-
Parathion	0.00375	35.5	376	25; 68.5	-	-

Table A 10 Trends for organics (PAHs & Pesticides) reported by TECQ across all sampling years.

	Min	Median	Max	IQR	ERL	ERM
Units	ug/kg	ug/kg	ug/kg	ug/kg	ug/kg	ug/kg
1,2378-PECDF	0.00006	0.0008	0.21	0.000265; 0.0025	-	-
1234678-HPCDD	0.000315	0.15	2.4	0.0608; 0.24	-	-
1234678-HPCDF	0.0001	0.017	2.41	0.0049; 0.042	-	-
1234789-HPCDF	0.00012	0.00145	0.651	0.0025; 0.0025	-	-
123478-HXCDD	0.00006	0.0011	0.0498	0.00032; 0.0025	-	-
123478-HXCDD	0.000095	0.00245	0.363	0.00034; 0.007	-	-
123478-HXCDF	0.00013	0.0025	2.1	0.0006; 0.0074	-	-
123678-HXCDF	0.000095	0.00115	0.39	0.000245; 0.0025	-	-
123789-HXCDD	0.00018	0.00245	0.25	0.0004925; 0.0063	-	-
123789-HXCDF	0.000055	0.00055	0.088	0.000265; 0.0025	-	-
12378-PECDD	4.65E-05	0.000438	0.0421	0.000325; 0.0024375	-	-
2,378-TCDD	0.000115	0.006495	0.65	0.00047875; 0.015	-	-
234678-HXCDF	0.00007	0.00055	0.042	0.00023; 0.00245	-	-
23478-PECDF	0.000065	0.0021	0.18	0.000315; 0.0025	-	-
2378-TCDF	0.000085	0.023	1.9	0.00355; 0.0485	-	-
DIBENZOFURAN	0.11	0.316	5.45	0.15425; 2.2675	-	-
OCDD	0.0016	2.7	41	0.83725; 4.6	-	-
OCDF	0.000415	0.11	357.37	0.0265; 0.315	-	-
TOTAL HXCDD	0.0002	0.074	2.8	0.022; 0.14	-	-
TOTAL PECDD	0.00011	0.013	2	0.0017; 0.0235	-	-
TOTAL PECDF	0.000055	0.013	1.3	0.0016; 0.031	-	-
TOTAL TCDD	0.00012	0.022	5.8	0.006; 0.037	-	-
TOTAL TCDF	0.000085	0.051	3.1	0.0135; 0.1	-	-
TOTAL-HPCDD	0.000315	0.28	7.9	0.063; 0.62	-	-
TOTAL-HPCDF	0.000125	0.032	2.9	0.0084; 0.0785	-	-
TOTAL-HXCDF	0.00011	0.019	3.4	0.00245; 0.047	-	-

Table A 11 Trends for organics (Dx/F) reported by TECQ across all sampling years.

	Min	Median	Max	IQR	ERL	ERM
Units	ug/kg	ug/kg	ug/kg	ug/kg	ug/kg	ug/kg
PCB 1254	0	0.048275	1.6	0.0119; 0.15	-	-
PCB 1	0	0	0.124	0; 0.0223	-	-
PCB 10	0	0.02245	0.124	0.0009; 0.0144	-	-
PCB 103	0	0.01535	0.124	0; 0.0244	-	-
PCB 104	0	0.023725	0.124	0.0007; 0.0247	-	-
PCB 105	0	0	0.04985	0; 0	-	-
PCB 106	0	0.023775	0.124	0.0006; 0.0247	-	-
PCB 107	0	0	0.1495	0; 0.0468	-	-
PCB 109	0	0	0.124	0; 0.0235	-	-
PCB 11	0	0	0.1495	0; 0.0720	-	-
PCB 111	0	0.0238	0.124	0.0008; 0.0248	-	-
PCB 112	0	0.02385	0.124	0.0013; 0.0248	-	-
PCB 114	0	0.0228	0.124	0; 0.0245	-	-
PCB 118	0	0	0.049	0; 0.0000	-	-
PCB 120	0	0.02345	0.124	0; 0.0246	-	-
PCB 121	0	0.023825	0.124	0.0012; 0.0248	-	-
PCB 122	0	0.02325	0.124	0; 0.0245	-	-
PCB 123	0	0.023225	0.124	0; 0.0245	-	-
PCB 126	0	0.023525	0.124	0; 0.0246	-	-
PCB 127	0	0.023775	0.124	0.0005; 0.0248	-	-
PCB 130	0	0	0.124	0; 0.0240	-	-
PCB 131	0	0.022975	0.124	0; 0.0245	-	-
PCB 132	0	0	0.04985	0; 0.0000	-	-
PCB 133	0	0.022125	0.124	0; 0.0245	-	-
PCB 136	0	0	0.124	0; 0.0230	-	-
PCB 137	0	0	0.124	0; 0.0243	-	-
PCB 14	0	0.0227	0.124	0.0013; 0.0243	-	-
PCB 141	0	0	0.124	0; 0.0230	-	-
PCB 142	0	0.023775	0.124	0.0028; 0.0247	-	-
PCB 144	0	0.003248	0.124	0; 0.0245	-	-
PCB 145	0	0.0238	0.124	0.0010; 0.0248	-	-
PCB 146	0	0	0.124	0; 0.0232	-	-
PCB 147	0	0.0242	0.124	0.0233; 0.0247	-	-
PCB 148	0	0.0137	0.04985	0; 0.0247	-	-
PCB 15	0	0	0.025	0; 0.0000	-	-
PCB 150	0	0.02365	0.124	0.0006; 0.0246	-	-
PCB 152	0	0.0237	0.124	0.0009; 0.0247	-	-
PCB 154	0	0.0033	0.124	0; 0.0245	-	-
PCB 155	0	0.0238	0.124	0.0006; 0.0248	-	-
PCB 158	0	0	0.124	0; 0.0236	-	-
PCB 159	0	0.02345	0.124	0; 0.0246	-	-
PCB 16	0	0	0.124	0; 0.0122	-	-
PCB 160	0	0.0238	0.124	0.0022; 0.0247	-	-
PCB 161	0	0.02375	0.124	0.0007; 0.0247	-	-
PCB 162	0.075	24.3	124	23.1500; 24.9500	-	-
PCB 164	2.325	24.4	124	23.6500; 46.5500	-	-
PCB 165	0	0.023825	0.124	0.0023; 0.0248	-	-
PCB 167	0	0	0.124	0; 0.0243	-	-
PCB 169	0	0.0237	0.124	0.0050; 0.0247	-	-
PCB 17	0	0	0.124	0; 0.0117	-	-
PCB 170	0	0	0.04985	0; 0.0056	-	-
PCB 172	0	0	0.124	0; 0.0241	-	-
PCB 174	0	0	0.04985	0; 0.0000	-	-
PCB 175	0	0.0229	0.124	0; 0.0245	-	-
PCB 176	0	0	0.124	0; 0.0243	-	-
PCB 177	0	0	0.124	0; 0.0228	-	-
PCB 178	0	0	0.124	0; 0.0240	-	-
PCB 179	0	0	0.124	0; 0.0233	-	-
PCB 181	0	0.023625	0.124	0; 0.0246	-	-
PCB 182	0	0.023825	0.124	0.0019; 0.0248	-	-
PCB 183	0	0	0	0; 0	-	-
PCB 184	0	0.0238	0.124	0.0010; 0.0248	-	-
PCB 185	0.000085	0.0007	0.01	0.0002; 0.0019	-	-
PCB 186	0	0.023825	0.124	0.0017; 0.0248	-	-
PCB 187	0	0	0.049	0; 0	-	-
PCB 188	0	0.0238	0.124	0.0012; 0.0247	-	-
PCB 189	0	0.02325	0.124	0; 0.0245	-	-
PCB 19	0	0.000875	0.124	0; 0.0234	-	-
PCB 190	0	0	0.124	0; 0.0241	-	-

PCB 191	0	0.02325	0.124	0; 0.0245	-	-
PCB 192	0	0.023775	0.124	0.0013; 0.0247	-	-
PCB 194	0	0	0.124	0; 0.0244	-	-
PCB 195	0	0	0.124	0; 0.0248	-	-
PCB 196	0	0	0.1735	0; 0.0342	-	-
PCB 197	0	0.00065	0.017	0; 0.0032	-	-
PCB 200	0	0.00084	0.037	0; 0.0016	-	-
PCB 201	0	0.002425	0.124	0; 0.0350	-	-
PCB 202	0	0	0.124	0; 0.0343	-	-
PCB 203	0	0	0.124	0; 0.0245	-	-
PCB 204	0	24.35	173.5	23.2000; 28.4500	-	-
PCB 205	0	0.02365	0.124	0; 0.0358	-	-
PCB 206	0	0	0.124	0; 0.0241	-	-
PCB 207	0	0	0.124	0; 0.0346	-	-
PCB 208	0	0	0.124	0; 0.0351	-	-
PCB 209	0	0	0.0735	0; 0	-	-
PCB 22	0	0	0.124	0; 0	-	-
PCB 23	0	0.0227	0.124	0.0006; 0.0243	-	-
PCB 24	0	0.01265	0.124	0; 0.0242	-	-
PCB 25	0	0.007375	3.025	0; 0.0245	-	-
PCB 26	0	0	0	0; 0	-	-
PCB 27	0	0.00168	0.124	0; 0.0237	-	-
PCB 2	0	0.01145	0.124	0; 0.0240	-	-
PCB 3	0	0	0.124	0; 0.0229	-	-
PCB 31	0	0	0.0245	0; 0	-	-
PCB 32	0	0	0.124	0; 0.0119	-	-
PCB 34	0	0.012225	0.124	0; 0.0241	-	-
PCB 35	0	0.01205	0.124	0; 0.0240	-	-
PCB 36	0	0.0228	0.124	0; 0.0243	-	-
PCB 37	0	0	0.124	0; 0	-	-
PCB 38	0	0.0228	0.124	0.0006; 0.0243	-	-
PCB 39	0	0.01225	0.124	0; 0.0241	-	-
PCB 4	0	0	0.124	0; 0.0232	-	-
PCB 42	0	0	0.124	0; 0.0041	-	-
PCB 42	0	0	0.124	0; 0.0237	-	-
PCB 46	0	0	0.124	0; 0.0244	-	-
PCB 48	0	0	0.124	0; 0.0240	-	-
PCB 5	0	0.01875	0.124	0; 0.0243	-	-
PCB 52	0	0	0.049	0; 0.0000	-	-
PCB 54	0	0.0229	0.124	0; 0.0245	-	-
PCB 55	0	0.02405	0.124	0.0001; 0.0248	-	-
PCB 56	0	0	3.035	0; 0.0016	-	-
PCB 57	0	0.0233	0.124	0; 0.0246	-	-
PCB 57	0	0.023425	0.124	0; 0.0246	-	-
PCB 6	0	0	0.124	0; 0.0232	-	-
PCB 60	0	0	0.124	0; 0.0241	-	-
PCB 63	0	0.021975	0.124	0; 0.0244	-	-
PCB 64	0	0	0.04985	0; 0.0000	-	-
PCB 65	0	0	0	0; 0.0000	-	-
PCB 66	0	0	2.795	0; 0.0000	-	-
PCB 67	0	0.022825	0.124	0; 0.0245	-	-
PCB 68	0	0.023225	0.124	0; 0.0245	-	-
PCB 7	0	0.01225	0.124	0; 0.0240	-	-
PCB 72	0	0.02285	0.124	0; 0.0245	-	-
PCB 73	0	0.023225	0.124	0.0001; 0.0244	-	-
PCB 73	0	0	0.124	0; 0.0241	-	-
PCB 78	0	0.0238	0.124	0.0013; 0.0248	-	-
PCB 79	0	0.02325	0.124	0; 0.0246	-	-
PCB 8	0	0	0.745	0; 0	-	-
PCB 80	0	0.023675	0.124	0.0001; 0.0246	-	-
PCB 81	0	0.02365	0.124	0.0017; 0.0247	-	-
PCB 82	0	0	0.124	0; 0.0241	-	-
PCB 83	0	0	0.04985	0; 0.0240	-	-
PCB 84	0	0	0.124	0; 0.0020	-	-
PCB 89	0	0.023275	0.124	0; 0.0246	-	-
PCB 9	0	0.01225	0.124	0; 0.0241	-	-
PCB 92	0	0.00445	0.124	0; 0.0244	-	-
PCB 94	0	0.02315	0.124	0; 0.0246	-	-
PCB 95	0	0	0.049	0; 0	-	-
PCB 96	0	0	0.124	0; 0.0229	-	-
PCB 99	0	0.02335	0.124	0; 0.0245	-	-

PCB IUPAC 109+119+86+97+125+87	0	0	0.02825	0; 0.0001	-	-
PCB 1016	0.00001	0.0705	1.6	0.0209; 0.1713	-	-
PCB 1221	0.00001	0.07	1.6	0.0218; 0.1713	-	-
PCB 1232	0.00001	0.07125	1.6	0.0218; 0.1750	-	-
PCB 1242	0.00001	0.071	1.6	0.0218; 0.1750	-	-
PCB 1248	0	0.0354	1.6	0.0013; 0.1188	-	-
PCB 1260	0	0.0665	1.6	0.0160; 0.1600	-	-
PCB Grp 1 (13/12)	0	0.022125	0.124	0; 0.0245	-	-
PCB Grp 10 (59/62/75)	0	0	0.1495	0; 0.0680	-	-
PCB Grp 11 (61/70/74/76)	0	0	0.1995	0; 0	-	-
PCB Grp 12 (69/49)	0	0	0.0995	0; 0	-	-
PCB Grp 13 (88/91)	0	0	0.124	0; 0.0241	-	-
PCB Grp 14 (100/93/102/98)	0	0	0.1995	0; 0.0915	-	-
PCB Grp 15 (110/115)	0	0	0.0995	0; 0	-	-
PCB Grp 16 (113/90/101)	0	0	0.1495	0; 0	-	-
PCB Grp 17 (117/116/85)	0	0	0.1495	0; 0.0294	-	-
PCB Grp 18 (128/166)	0	0	0.248	0; 0.0461	-	-
PCB Grp 19 (134/143)	0	0	0.124	0; 0.0250	-	-
PCB Grp 2 (21/33)	0	0	0.124	0; 0	-	-
PCB Grp 20 (138/163/129)	0	0	0.1495	0; 0	-	-
PCB Grp 21 (139/140)	0	0.014	0.139	0; 0.0454	-	-
PCB Grp 22 (147/149)	0	0	0.098	0; 0	-	-
PCB Grp 23 (151/135)	0	0	0.0995	0; 0	-	-
PCB Grp 24 (153/168)	0	0	0.098	0; 0	-	-
PCB Grp 25 (171/173)	0	0	0.124	0; 0.0249	-	-
PCB Grp 26 (193/180)	0	0	0.0995	0; 0	-	-
PCB Grp 27 (198/199)	0	0	0.1495	0; 0.0246	-	-
PCB Grp 3 (26/29)	0	0	0.1195	0; 0.0245	-	-
PCB Grp 31 (108/119/86/97/125/87)	0	0	0.299	0; 0.1358	-	-
PCB Grp 32 (107/124)	0	0.024025	0.1195	0; 0.0488	-	-
PCB Grp 33 (183/185)	0	0	0.124	0; 0.0245	-	-
PCB Grp 34 (197/200)	0	0.0244	0.62	0; 0.1210	-	-
PCB Grp 35 (156/157)	0	0.02285	0.605	0; 0.0925	-	-
PCB Grp 4 (28/20)	0	0	0.049	0; 0	-	-
PCB Grp 5 (30/18)	0	0	0.124	0; 0.0045	-	-
PCB Grp 6 (40/41/71)	0	0	0.1495	0; 0.0017	-	-
PCB Grp 7 (44/47/65)	0	0	0.1495	0; 0	-	-
PCB Grp 8 (45/51)	0	0	0.124	0; 0.0244	-	-
PCB Grp 9 (53/50)	0	0	0.124	0; 0.0248	-	-
PCBs	0	0.0015	0.6	0; 0.0505	4,022	44,792

Table A 12 Trends for organics (PCBs) reported by TECQ across all sampling years.

	Min	25th	Median	75th	Max	ERL	ERM
Units	ug/kg	ug/kg	ug/kg	ug/kg	ug/kg	ug/kg	ug/kg
As	1540	1760	2240	2840	3270		
Cd	-	-	-	-	-		
Cr	898	4175	6890	8705	12900		
Cu	866	2855	9110	9720	16800		
Pb	1020	4735	10500	19250	34500		
Ni	776	3325	6660	8475	10200		
Sn	-	-	-	-	-		
Zn	4160	12700	33100	46250	88400		
Hg	7.5	8.4	17.5	36.4	51.6		

Table A 13 Trends for metals reported by Dobberstine 2007.

	Min	25th	Median	75th	Max	ERL	ERM
Units	ug/kg	ug/kg	ug/kg	ug/kg	ug/kg	ug/kg	ug/kg
DDT	-	-	11	-	-	1	7
Dieldren	-	-	4.3	-	-	0.02	4.3
A	12	12	14	20	20	85.3	1100
BaA	16	16	27	107.5	120	261	1600
BaP	17	20.5	33	124.5	160	430	1600
BbF & BkF	43	53	82	310.5	430	-	-
C	21	24.5	32	145.5	177	384	2800
DA	11	16	16.5	36.75	42	63.4	135
FL	29	39	99	213	258	600	5100
PY	25	35	66	182	221	665	2,600
P	16	23.75	54.5	63.5	64	240	544

Table A 14 Trends for organics reported by Dobberstine 2007.

	Min	25th	Median	75th	Max	ERL	ERM
Units	ug/kg	ug/kg	ug/kg	ug/kg	ug/kg	ug/kg	ug/kg
Sum PCDD/F	0.132	0.9275	2.093	4.09	16.806	-	-
Total PCBs	0.14	0.99	28.5	224.5	1407	4,022	44,792
77	0.88	6.62	10.5	45.8	1568	-	-
81	0.391	0.475	0.954	15.78	31.46	-	-
126	0.236	0.6965	1.93	36.8	95.2	-	-
169	0.094	0.18375	0.53	3.1	10	-	-
105	0.0185	0.0309	0.263	1.1	2.401	-	-
114	0.000941	0.0018	0.0119	0.0553	0.122	-	-
118	0.0544	0.0944	0.665	2.402	6.585	-	-
123	0.000841	0.00161	0.00927	0.04	0.134	-	-
156	0.00846	0.0147	0.109	0.46	1.598	-	-
157	0.00301	0.005628	0.0585	0.154	0.301	-	-
167	0.00185	0.00336	0.0446	0.184	0.623	-	-
189	0.00172	0.00182	0.00822	0.0431	0.191	-	-
128	0.0168	0.0194	0.172	0.801	2.178	-	-
138	0.0618	0.0844	0.726	3.326	11.917	-	-
158	0.00629	0.0125	0.071	0.419	1.249	-	-
166	0.000219	0.000465	0.00822	0.0214	0.0358	-	-
170	0.0385	0.0447	0.329	2.365	9.233	-	-

Table A 15 Trends for organics (Dx/F & PCBs) reported by Gardinali 1996.

APPENDIX B

SUPPLEMENTARY MATERIALS FOR: POLYCYCLIC AROMATIC HYDROCARBON STATUS IN POST-HURRICANE HARVEY SEDIMENTS: CONSIDERATIONS FOR ENVIRONMENTAL SAMPLING IN THE GALVESTON BAY/HOUSTON SHIP CHANNEL REGION

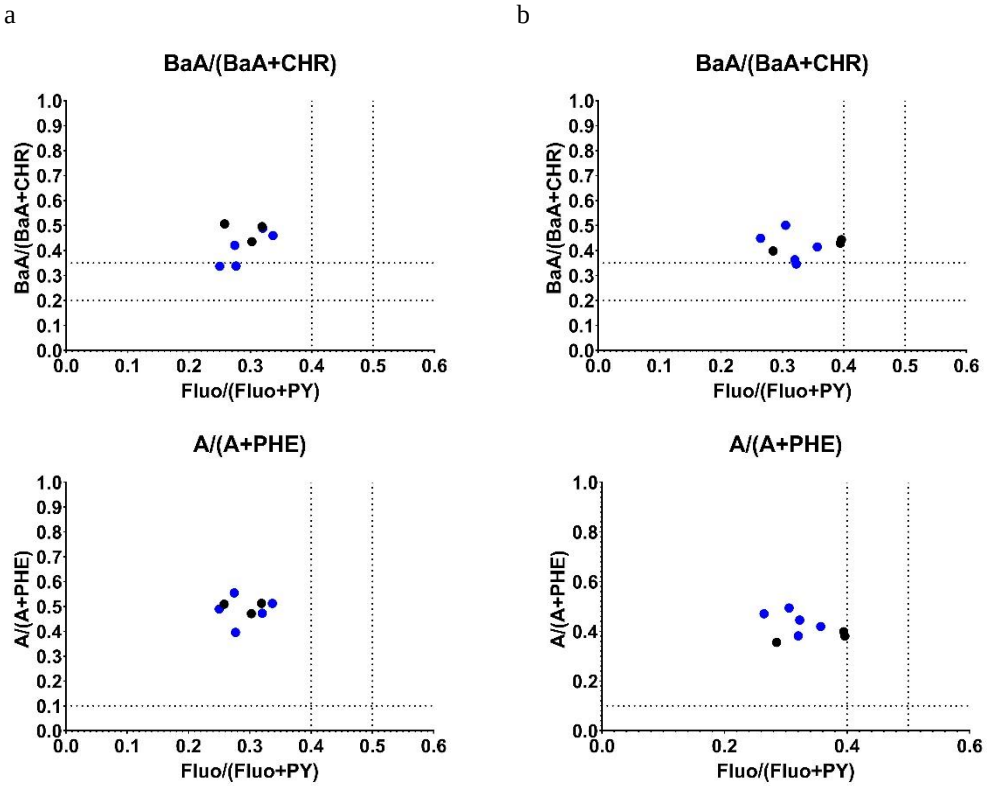

Figure B 1 Double Ratio sourcing plots comparing pre-Harvey data (a, c) and post-Harvey data (b, d). Panels a and b show BaA/(BaA+CHR) vs. Fluo/(Fluo+PY); panels c and d show A/A(PHE) vs. Fluo/(Fluo+PY). The black circles show cores collected south of Bear Lake in the San Jacinto River; the blue circles show cores collected in Burnett Bay.

Sample ID	General Descriptor	Latitude	Longitude	Date of Sample
GAL_001	Upper Houston Ship Channel	29.74	-95.0572	1996
GAL_002A1	Upper Houston Ship Channel	29.7617	-95.067	1996
GAL_003	Upper Houston Ship Channel	29.76	-95.0783	1996
GAL_004	Scott Bay	29.735	-95.0533	1996
GAL_005	Scott Bay	29.7217	-95.0227	1996
GAL_006	Scott Bay	29.745	-95.0353	1996
GAL_007	Upper San Jacinto Bay	29.7067	-95.0323	1996
GAL_008	Upper San Jacinto Bay	29.7033	-95.0318	1996
GAL_009A1	Upper San Jacinto Bay	29.7017	-95.0258	1996
GAL_010	Lower San Jacinto Bay	29.6867	-94.9883	1996
GAL_011	Lower San Jacinto Bay	29.6867	-94.985	1996
GAL_012	Lower San Jacinto Bay	29.695	-94.99	1996
GAL_013	Tabbs Bay	29.7033	-94.9783	1996
GAL_014	Tabbs Bay	29.7033	-94.9867	1996
GAL_015	Tabbs Bay	29.7083	-94.98	1996
GAL_016	Upper Galveston Bay - East	29.6317	-94.935	1996
GAL_017A1	Upper Galveston Bay - East	29.6233	-94.935	1996
GAL_018	Upper Galveston Bay - East	29.6567	-94.9483	1996
GAL_019	Upper Galveston Bay - West	29.64	-95.0032	1996
GAL_020	Upper Galveston Bay - West	29.6217	-94.9817	1996
GAL_021	Upper Galveston Bay - West	29.6383	-94.9967	1996
GAL_022	Clear Lake	29.5633	-95.0597	1996
GAL_023	Clear Lake	29.5533	-95.0605	1996
GAL_024	Clear Lake	29.5567	-95.0383	1996
GAL_025	Central Galveston Bay- West	29.56	-94.98	1996
GAL_026	Central Galveston Bay- West	29.535	-94.9533	1996
GAL_027	Central Galveston Bay- West	29.5983	-94.9567	1996
GAL_028	Central Galveston Bay- West	29.5683	-94.9717	1996
GAL_029	Central Galveston Bay- East	29.58	-94.9117	1996
GAL_030	Central Galveston Bay- East	29.62	-94.89	1996
GAL_031	Central Galveston Bay- East	29.6117	-94.9283	1996
GAL_032	Central Galveston Bay- East	29.5333	-94.8367	1996
GAL_033	Lower Galveston Bay	29.4217	-94.82	1996
GAL_034	Lower Galveston Bay	29.45	-94.7433	1996
GAL_035	Lower Galveston Bay	29.52	-94.77	1996
GAL_036	Lower Galveston Bay	29.4417	-94.8	1996
GAL_037	Lower Galveston Bay	29.4133	-94.865	1996
GAL_038	Trinity Bay - Offshore	29.695	-94.815	1996
GAL_039	Trinity Bay - Offshore	29.59	-94.7967	1996
GAL_040	Trinity Bay - Offshore	29.6667	-94.7517	1996
GAL_041	Trinity Bay - Offshore	29.6667	-94.73	1996
GAL_042	Trinity Bay - Nearshore	29.7233	-94.765	1996
GAL_043	Trinity Bay - Nearshore	29.7183	-94.8317	1996
GAL_044	Trinity Bay - Nearshore	29.7417	-94.8067	1996
GAL_045	East Bay	29.5033	-94.6117	1996
GAL_046	East Bay	29.4417	-94.7133	1996
GAL_047	East Bay	29.5317	-94.705	1996
GAL_048	East Bay	29.535	-94.505	1996
GAL_049	East Bay	29.5267	-94.6417	1996
GAL_050	Texas City	29.315	-94.8233	1996
GAL_051	Texas City	29.3467	-94.8433	1996
GAL_052	Texas City	29.3033	-94.8783	1996
GAL_053	West Bay	29.2183	-95.025	1996
GAL_054	West Bay	29.2617	-94.965	1996
GAL_055	West Bay	29.1317	-95.1307	1996
GAL_056	West Bay	29.1883	-95.0717	1996
GAL_057	West Bay	29.29	-94.945	1996
GAL_058	Bolivar Roads	29.3417	-94.765	1996
GAL_059	Bolivar Roads	29.355	-94.7717	1996
GAL_060	Bolivar Roads	29.3483	-94.5533	1996
GAL_061	Galveston Bay - Entrance	29.335	-94.6517	1996

GAL_062	Galveston Bay - Entrance	29.3333	-94.695	1996
GAL_063	Galveston Bay - Entrance	29.3533	-94.7133	1996
GAL_064	Galveston Island - Nearshore	29.315	-94.735	1996
GAL_065	Galveston Island - Nearshore	29.3133	-94.7217	1996
GAL_066	Galveston Island - Nearshore	29.3067	-94.7233	1996
GAL_067	Bolivar Peninsula - Nearshore	29.415	-94.685	1996
GAL_068	Bolivar Peninsula - Nearshore	29.3967	-94.7083	1996
GAL_069	Bolivar Peninsula - Nearshore	29.3867	-94.7083	1996
GAL_070	Galveston Island - Offshore	29.29	-94.715	1996
GAL_071	Galveston Island - Offshore	29.3033	-94.6933	1996
GAL_072	Galveston Island - Offshore	29.3	-94.71	1996
GAL_073	Bolivar Peninsula - Offshore	29.3483	-94.6767	1996
GAL_074	Bolivar Peninsula - Offshore	29.3567	-94.6467	1996
GAL_075	Bolivar Peninsula - Offshore	29.36	-94.6517	1996
Confederate Reef	MW1997GBCRSED	29.2633	-94.9163	1997
Hanna Reef	MW1997GBHRSED	29.4803	-94.7418	1997
Offatts Bayou	MW1997GBOBSED	29.284	-94.8363	1997
Todd's Dump	MW1997GBTDSED	29.503	-94.896	1997
Yacht Club	MW1997GBYCSED	29.622	-94.9958	1997
Confederate Reef	MW2007GBCRSED	29.2633	-94.9163	2007
Hanna Reef	MW2007GBHRSED	29.4803	-94.7418	2007
Offatts Bayou	MW2007GBOBSED	29.284	-94.8363	2007
Ship Channel	MW2007GBSCSED	29.7045	-94.993	2007
Todd's Dump	MW2007GBTDSED	29.503	-94.896	2007
Yacht Club	MW2007GBYCSED	29.622	-94.9958	2007
Confederate Reef	SS2010GBCR1SED	29.2633	-94.9163	2010
Hanna Reef	SS2010GBHR1SED	29.4803	-94.7418	2010
Offatts Bayou	SS2010GBOB1SED	29.284	-94.8363	2010
Ship Channel	SS2010GBSC1SED	29.7045	-94.993	2010
Todd's Dump	SS2010GBTD1SED	29.503	-94.896	2010
Yacht Club	SS2010GBYC1SED	29.622	-94.9958	2010
Confederate Reef	SS2011GBCR2SED	29.2633	-94.9163	2011
Hanna Reef	SS2011GBHR2SED	29.4803	-94.7418	2011
Offatts Bayou	SS2011GBOB2SED	29.284	-94.8363	2011
Ship Channel	SS2011GBSC2SED	29.7045	-94.993	2011
Todd's Dump	SS2011GBTD2SED	29.503	-94.896	2011
Yacht Club	SS2011GBYC2SED	29.622	-94.9958	2011
HARV 12	Upper	29.55273	-95.0452	October/December 2017
C20	Upper	29.70192	-94.989	October/December 2017
C22	Upper	29.739	-95.0381	October/December 2017
VCPROP 4	Upper	29.80582	-95.0714	October/December 2017
VCPROP 2	Upper	29.76833	-95.0517	October/December 2017
BC-6	Upper	29.67577	-94.9789	October/December 2017
BC-7	Upper	29.68537	-94.9833	October/December 2017
BC-8	Upper	29.69895	-94.999	October/December 2017
BC-9	Upper	29.72408	-95.0216	October/December 2017
BC-10	Upper	29.74302	-95.0606	October/December 2017
BC-11	Upper	29.76237	-95.077	October/December 2017
BC-12	Upper	29.75192	-95.0955	October/December 2017
BC-13	Upper	29.7344	-95.125	October/December 2017
HARV 1	Mid	29.55485	-94.9665	October/December 2017
HARV 17	Mid	29.62388	-94.9294	October/December 2017
Harv 14	Mid	29.54763	-95.0798	October/December 2017
C18	Mid	29.66038	-94.991	October/December 2017
C10	Mid	29.73602	-94.7696	October/December 2017
GB5	Mid	29.61011	-94.89	October/December 2017
HARV10	Mid	29.55308	-95.0059	October/December 2017
Harv15	Mid	29.53338	-95.0795	October/December 2017
ML1	Mid	29.56663	-95.0725	October/December 2017
ML-2	Mid	29.57133	-95.0722	October/December 2017
ML3	Mid	29.57407	-95.0701	October/December 2017

C09	Lower	29.63788	-94.8042	October/December 2017
GB1	Lower	29.3571	-94.7557	October/December 2017
HARV 7A	Lower	29.57782	-94.9026	October/December 2017
HARV11	Lower	29.55293	-95.0353	October/December 2017
GB2	Lower	29.43529	-94.8062	October/December 2017
GB3	Lower	29.51241	-94.8571	October/December 2017
GB4	Lower	29.56184	-94.893	October/December 2017
HARV05	Lower	29.60983	-94.8305	October/December 2017

Table B 1 Latitude & Longitude Location of Samples.

APPENDIX C

SUPPLEMENTARY MATERIALS FOR: BIOSENSOR APPLICATIONS IN GALVESTON BAY: IMPLICATIONS FOR DISASTER RESEARCH RESPONSE

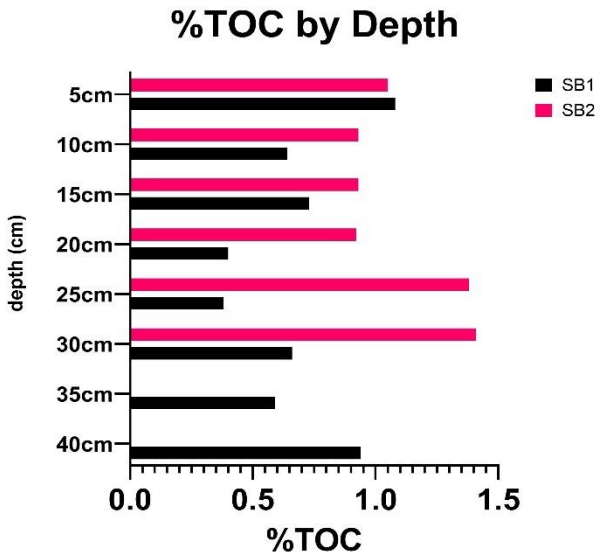

Figure C 1 Comparisons of %TOC at depth for the 2016 SB1 (black) and SB2 (pink) cores.

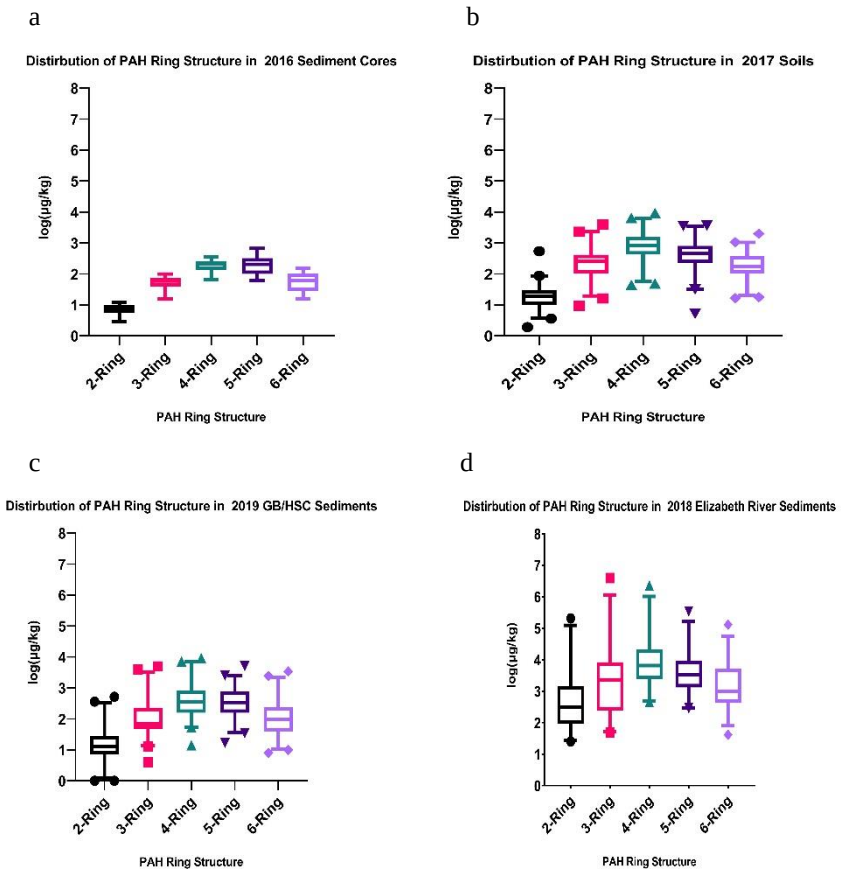

Figure C 2 Boxplots comparing each sampling type based on PAH ring structure with (a) 2016 Sediment Cores, (b) 2017 Soils, (c) 2019 GB/HSC Sediments, and (d) 2018 Elizabeth River Sediments.

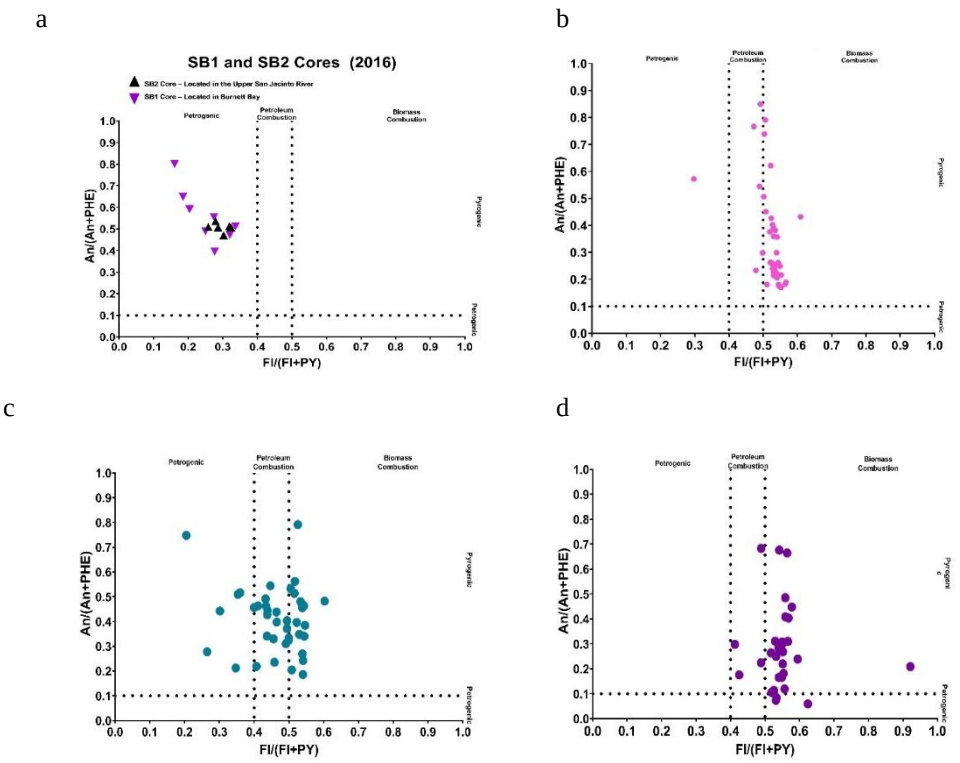

Figure C 3 The double-ratio plot of An/(An+PHE) vs Fl/(Fl+PY) are illustrated for the 2016 sediment cores (a), the 2017 soils (b - pink), the 2019 sediments from GB/HSC (c - green), and the 2020 sediments from the Elizabeth River (d - purple). Both cores indicate petrogenic/pyrogenic sourcing (a) while both the 2017 soils (b) and 2019 GB/HSC (c) sediments have mixed sourcing.

GERG Parent PAHs	GERG Alkylated PAHs	VIMS Parent PAHs	VIMS Alkyl
Nap	C1-Naphthalenes	Nap	2-Methyl Nap
Biphenyl	C2-Naphthalenes	Biphenyl	1-Methyl Nap
AY	C3-Naphthalenes	AY	2,6 & 2,7-Dimethyl Nap
AE	C4-Naphthalenes	AE	1-Methyl P
F	C1-Fluorenes	F	
A	C2-Fluorenes	A	
P	C3-Fluorenes	P	
Dibenzothiophene	C1-Phenanthrenes/Anthracenes	FL	
FL	C2-Phenanthrenes/Anthracenes	PY	
PY	C3-Phenanthrenes/Anthracenes	BaA	
BaA	C4-Phenanthrenes/Anthracenes	C	
C	C1-Dibenzothiophenes	BbF	
BbF	C2-Dibenzothiophenes	BjF & BkF	
BeP	C3-Dibenzothiophenes	BeP	
BaP	C1-Fluoranthenes/Pyrenes	BaP	
PER	C2-Fluoranthenes/Pyrenes	PER	
IP	C3-Fluoranthenes/Pyrenes	IP	
DA	C1-Chrysenes	DA	
ghi	C2-Chrysenes	ghi	
BeP	C3-Chrysenes		
	C4-Chrysenes		
	2-Methylnaphthalene		
	1-Methylnaphthalene		
	2,6-Dimethylnaphthalene		
	1,6,7-Trimethylnaphthalene		
	1-Methylphenanthrene		

Table C 1 Summary table of all parent PAH compounds and alkylated PAH compounds detected by the Geochemical Environmental Research Group (GERG) and the Virginia Institute of Marine Science (VIMS). Each of these PAHs were used in both the Total PAH calculations and Total Alkylated PAH calculations.

Client Sample ID	Latitude	Longitude
HSC 20	29.717100	-95.239390
HSC 19	29.723810	-95.220030
HSC 18	29.730640	-95.207440
HSC 17	29.745136	-95.186364
HSC 16	29.736050	-95.154920
HSC 15	29.734400	-95.124967
HSC 14	29.737444	-95.112750
HSC 13	29.741722	-95.108861
HSC 12	29.751333	-95.097639
HSC 11	29.760778	-95.089028
HSC 9	29.768333	-95.051667
HSC 8	29.763389	-95.063444
HSC 6	29.743017	-95.060617
HSC 5	29.739000	-95.038083
HSC 4	29.724083	-95.021633
HSC 3	29.701917	-94.989017
HSC 2	29.685367	-94.983333
HSC 1	29.623883	-94.929383
CL 3	29.552933	-95.035250
CL 4	29.552733	-95.045183
CL6	29.560750	-95.051383
CL 5	29.558792	-95.044042
CL 7	29.563061	-95.061103
CL 8	29.561131	-95.070975
CL 9	29.553789	-95.072292
CL 10	29.547633	-95.079833
CL 11	29.544875	-95.084633
CL 12	29.533383	-95.079450
CL 13	29.542847	-95.079447
CL 14	29.547269	-95.072350
HSC 2	29.796139	-95.065028
HSC 5	29.772694	-95.077611
HSC 5A	29.763667	-95.078028
HSC 6A	29.760778	-95.089028
HSC 7	29.751333	-95.097639
HSC 8	29.741722	-95.108861
HSC 9	29.738472	-95.119194
HSC 10	29.735056	-95.128944
HSC 12	29.763389	-95.063444
HSC 13	29.762417	-95.056361
HSC 14	29.758111	-95.071583
HSC 15	29.755083	-95.066861
PB 1	29.737444	-95.112750
SB1	29.768330	-95.051700
SB2	29.805820	-95.071400
BC-A	36.7915167	-76.3054333
BC-B	36.7915833	-76.3053333
BC-C	36.7918	-76.3049833
LF-A	36.9134833	-76.3196833
LF-B	36.9136	-76.3195333
LF-C	36.9133833	-76.31975
WB-A	36.8333	-76.3719333
WB-B	36.8334333	-76.3717167
WB-C	36.8342667	-76.3722167
MP1-A	36.7834667	-76.3015167
MP1-B	36.78325	-76.3017833
MP1-C	36.7829333	-76.3022667
PC-A	36.8033167	-76.3066667
PC-B	36.8033	-76.3065667
PC-C	36.80295	-76.3063
SP-A	36.8430167	-76.3030167

SP-B	36.8429667	-76.3029833
SP-C	36.8428833	-76.3029667
MP2-A	36.7853	-76.30155
MP2-B	36.78595	-76.3015333
MP2-C	36.7867	-76.3015333
MP3-A	36.7878667	-76.3016833
MP3-B	36.7883833	-76.3014833
MP3-C	36.7889833	-76.3013167
CF-A	36.8206	-76.2844833
CF-B	36.8203	-76.2856833
CF-C	36.8202	-76.2866667
CS-A	36.8365667	-76.2735333
CS-B	36.8366167	-76.2735667
CS-C	36.8367	-76.2734667
MP4- bucket	36.7880833	-76.3020167
RF-A	36.7931667	-76.2911833
RF-B	36.7931833	-76.2911833
RF-C	36.79325	-76.2909167
AW-A	36.8064833	-76.29445
AW-B	36.8065833	-76.2946833
AW-C	36.80655	-76.2942833
SC1-A	36.8079	-76.28225
SC1-B	36.80785	-76.28215
SC1-C	36.8080333	-76.2822167
SC2-A	36.8096333	-76.2836167
SC2-B	36.8096833	-76.2835833
SC2-C	36.8096833	-76.28385

Table C 2 Summary table of all sediment samples collected in 2016 (SB1 & SB2), Elizabeth River sediments in 2018, and 2019 (HSC and CL Samples).

	Min	Median	Max	IQR	R4-ESV	R4-RSV
LMW PAHs						
Acenaphthene	100	184	668	157; 295	6.7	4910
Acenaphthylene	834	1612	2422	1286; 1861	5.9	4520
Anthracene	1021	2162	5200	1862; 2455	57	5940
Fluorene	289	420	484	344; 458	77	5380
Naphthalene	764	1185	2782	905; 1390	176	3850
Phenanthrene	1261	1828	2362	1542; 2142	204	5960
HMW PAHs						
Benzo(a)anthracene	846	1872	6726	1601; 2372	108	8410
Benzo(b)fluoranthene	1512	4884	6995	2383; 6171	190	9790
Benzo(k)fluoranthene	415	1412	2342	552; 1604	240	9810
Benzo(g,h,i)perylene	1322	4841	7282	3385; 6563	170	10900
Benzo(a)pyrene	1503	2329	4422	1656; 2995	150	9650
Chrysene	1658	2249	5598	2003; 2593	166	8440
Dibenzo(a,h)anthracene	115	550	814	290; 706	33	11200
Fluoranthene	3274	4787	5917	4077; 5373	423	7070
Indeno(1,2,3-c,d)pyrene	690	2927	4346	1169; 3713	200	11200
Perylene	1739	13695	56107	5007; 31774	-	9680
Pyrene	9549	11415	27815	10444; 15098	195	6970

Table C 3 The summary statistics for individual PAHs in the 2016 sediment cores are reported in µg/kg OC and compared to the USEPA Region 4's Ecological Screening Value (R4-ESV) and Refinement Screening Value (R4 – RSV) for freshwater sediments (United States Environmental Protection Agency, 2018). These value comparisons contextualize how the individual PAHs may contribute to sediment toxicity.

	Min	Median	Max	IQR
LMW PAHs				
Acenaphthene	20	383	6613	211; 721
Acenaphthylene	67	1343	109532	761; 3354
Anthracene	116	2613	127861	1345; 5849
Fluorene	36	414	9902	291; 878
Naphthalene	71	757	31311	449; 1762
Phenanthrene	423	4552	90997	2509; 12130
HMW PAHs				
Benzo(a)anthracene	384	5299	66918	3095; 10272
Benzo(b)fluoranthene	0	10217	154217	4173; 16160
Benzo(k)fluoranthene	61	2927	37688	1366; 6671
Benzo(g,h,i)perylene				
Benzo(a)pyrene	125	5827	62701	3451; 11723
Chrysene	191	7997	75275	4343; 15217
Dibenzo(a,h)anthracene	0	813	16774	455; 1325
Fluoranthene	1175	14289	210907	7398; 27991
Indeno(1,2,3-c,d)pyrene	0	4060	65306	2634; 8119
Perylene	0	4363	71220	2616; 7935
Pyrene	1037	12515	176033	7096; 26428

Table C 4 The individual EPA 16 PAHs and Perylene summary statistics for the 2017 soils are reported in µg/kg OC. There are no comparator screening values from the USEPA Region 4, aside (United States Environmental Protection Agency, 2018) from total LMW PAHs and HMW PAHs as reported in Table 2.